BioMed Research International

Advances of Techniques in Deep Regional Blocks

Lead Guest Editor: Jui-An Lin
Guest Editors: Rafael Blanco, Yasuyuki Shibata, and Tatsuo Nakamoto

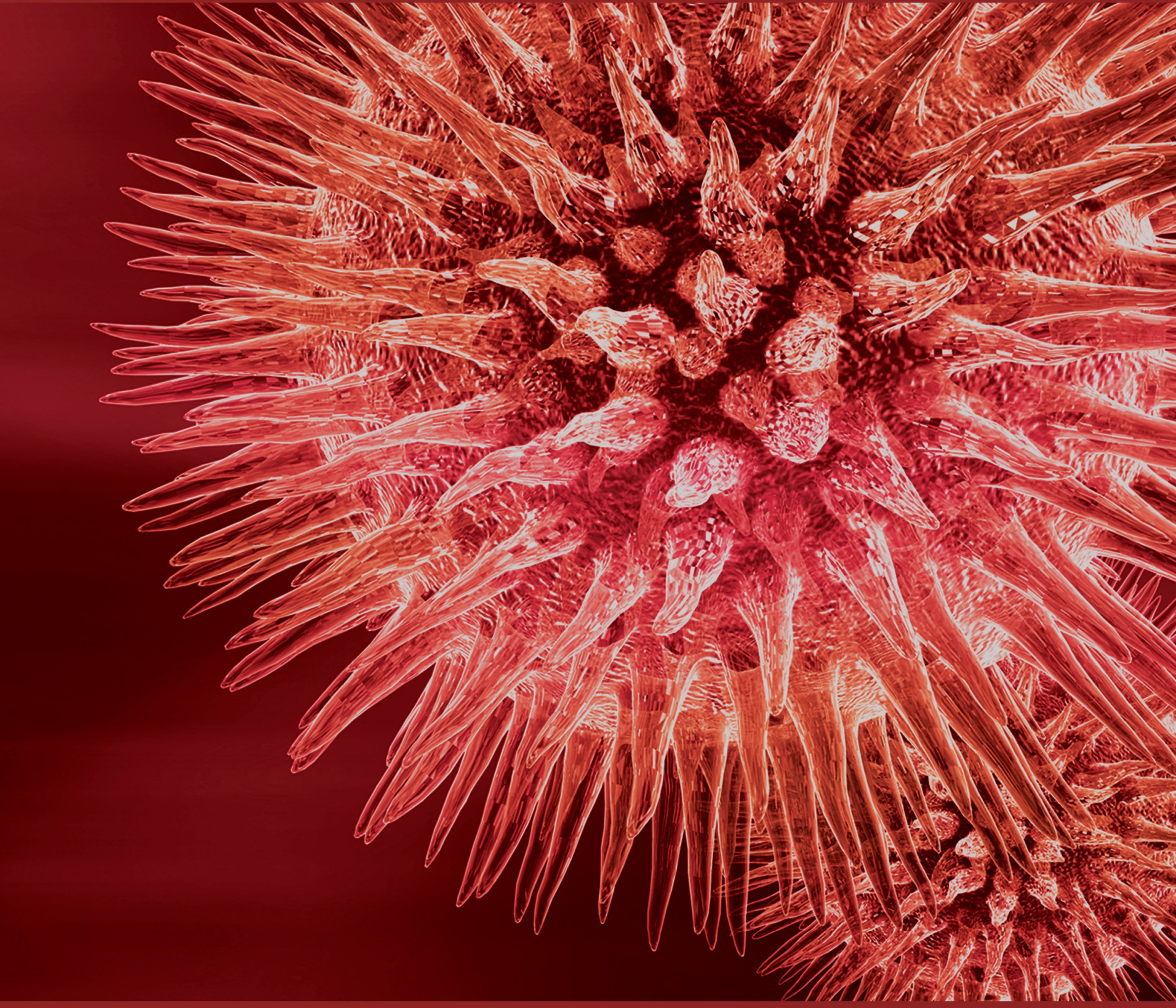

Advances of Techniques in Deep Regional Blocks

BioMed Research International

Advances of Techniques in Deep Regional Blocks

Lead Guest Editor: Jui-An Lin
Guest Editors: Rafael Blanco, Yasuyuki Shibata,
and Tatsuo Nakamoto

Contents

Hindawi
BioMed Research International
Volume 2017, Article ID 7268308, 4 pages
https://doi.org/10.1155/2017/7268308

Editorial

Advances of Techniques in Deep Regional Blocks

Jui-An Lin,[1,2] Rafael Blanco,[3] Yasuyuki Shibata,[4] and Tatsuo Nakamoto[5]

[1]*Department of Anesthesiology, Wan Fang Hospital, Taipei Medical University, Taipei, Taiwan*
[2]*Department of Anesthesiology, School of Medicine, College of Medicine, Taipei Medical University, Taipei, Taiwan*
[3]*Department of Anesthesia, Corniche Hospital, Abu Dhabi, UAE*
[4]*Department of Anesthesiology, Nagoya University Hospital, Nagoya, Japan*
[5]*Department of Anesthesiology, Kansai Medical University, Hirakata, Japan*

Correspondence should be addressed to Jui-An Lin; juian.lin@tmu.edu.tw

Received 1 October 2017; Accepted 2 October 2017; Published 4 December 2017

Advancing the techniques of deep regional blocks mainly relies on enhancing ergonomics and patient safety. As for ergonomics, efforts should be made to aid in decision-making process (cognitive ergonomics), to work with efficiency (e.g., shorter performance or onset time) and comfort (physical ergonomics), and to facilitate the operating room turnover by optimizing multidisciplinary cooperation (organizational ergonomics). Featured in this special issue is the updated reviews of several deep regional blocks on anatomy and techniques. Decision-making process (cognitive ergonomics) will be improved by the unified nomenclature system based on integrated applied anatomy and recommendation of suitable techniques for specific situations in these reviews. In the article reviewing obturator nerve block for this special issue, proximal approaches are recommended whenever possible, and the best patient position (supine or lithotomy) is yet to be determined. Although the authors worried about difficult alignment of the needle with the transducer in the supine position, needle visualization can be greatly facilitated by a true echogenic needle and meanwhile maintaining the eye, hand, needle, transducer, and ultrasound machine all in the same plane [1] according to recent advances in physical ergonomics [2, 3]. Furthermore, the supine position naturally keeps the leg straight and slightly externally rotated, which yields the best imaging on the obturator nerve [4]. To increase operating room efficiency (organizational ergonomics) for transurethral resection of bladder tumor, obturator nerve block is generally performed with the patient in the supine position immediately following spinal anesthesia, because preparation of lithotomy position (and subsequent surgical asepsis) following obturator nerve block could be viewed as a part of the interval for the deposited local anesthetic to take effect.

As for patient safety, ultrasound guidance for deep regional blocks is associated with significant limitations despite its popularity, which can be attributed to either the ultrasound machine (decreased ability to insonate deep neural structures) or the operator (errors in perception or interpretation in needle-nerve proximity during deep regional blocks) [5]. The inability of ultrasound to reliably insonate and locate deep neural structures could be circumvented with adjunctive neurostimulation. However, for some deep regional blocks (such as distal infraclavicular block [6, 7]), neurostimulation unnecessarily increases procedural time when there exist both a visible sonographic target and an identifiable sonographic endpoint. Thus, on the basis of ultrasound guidance as the gold standard, an important question has been raised regarding the definition of so-called "dual guidance" when choosing among ultrasound guidance, neurostimulation, and pressure monitoring for peripheral nerve blocks. Although ultrasound guidance indisputably leads to fewer needle passes for single-injection blocks, it seems to encourage small readjustment of needle tip position and multiple injections of local anesthetics [8, 9]. The ability of neurostimulation to predict relative needle-nerve proximity is not only limited by low sensitivity [10], but also attenuated by previous local anesthetic spread nearby [9, 11, 12]. Furthermore, current ultrasound technology may lack the resolution to differentiate epineurium from perineurium, and clinicians cannot always delineate cervical nerve roots clearly [12], let alone much deeper neural targets. These might explain, at least in part, the reason why the risk of neurological complications remains unchanged despite increased use of ultrasound guidance [13]. A 2015 consensus statement from the American Society of Regional Anesthesia and Pain Medicine expanded the recommendations to apply injection pressure monitoring for earlier detection of needle-nerve contact and avoidance of intrafascicular injection during peripheral nerve blocks [14]. Detection of needle-nerve contact on both oligofascicular [12] and multifascicular [11] neural targets can be greatly enhanced by monitoring opening injection pressure, which is the pressure level that must be overcome to initiate injection into the target place [15]. As for prevention of intrafascicular spread, pressure monitoring may prove to be most useful for its negative predictive value as no cases have been reported to suffer from functional neuropathy with low injection pressures [10, 16]. Because opening injection pressure of more than 20 psi is associated with intrafascicular spread, 15 psi has been chosen as the cut-off pressure to keep 5 psi lower than the lowest reported value that resulted in neurological injury [11, 12]. Clinically at this cut-off point, high opening injection pressure (>15 psi) can consistently detect needle-nerve contact [12], indicating that a typical perineural injection requires low opening pressure (<15 psi) [10]. This cut-off point (15 psi) was further supported by a fresh human cadaver model, where opening injection pressure for intraneural injection was ranging from 21.5 ± 4.9 psi to 25.8 ± 4.3 psi for common ultrasound-guided lower extremity blocks [17]. A volume of 5 mL injection into the brachial plexus root within 15 sec results in a much higher opening injection pressure (>30 psi) in 100% fresh cadavers [18]. A human study demonstrated cessation of injection when opening pressure more than 20 psi for popliteal sciatic block does not result in neurological dysfunction [19].

Although several means of monitoring injection pressure have been recommended [20, 21], its popularization is limited by the facilities required (e.g., the pump or the commercial kits) until the advent of a convenient alternative utilizing the half-the-air setting [9]. The half-the-air setting consists of a central stopcock with its male luer lock connecting an extension tube to the patient, a side female luer lock to the 5% dextrose water (D5W) syringe, and an end female luer lock to the local anesthetic syringe [9]. The concept of "half-the-air" to keep injection pressure below 15 psi derives from the reliability of compressed air injection technique [22, 23], and the facility-independent half-the-air setting helps popularize injection pressure monitoring in clinical practice by the advantages of low cost, easy assembling, and incorporating a test syringe (ensuring the total mass of local anesthetic to be delivered) and a long (200 cm) extension tube (facilitating the operation for the assistant, thus physical ergonomics) with a low dead space (1.4 mL) [9]. Thereafter, another improvised pressure gauge was proposed using the fluid meniscus level in the 1 ml syringe in place of D5W syringe as the passive indirect in-line manometer [24]. However, as with the drawback of the commercial in-line manometer, this improvised pressure gauge lacks a pop-off valve to limit the injection pressure and/or eliminate the initial high peak pressure [20, 24]. In other words, with the in-line manometer only as a monitor, "syringe feel" is still performed at the very beginning of injection. It would be safer to limit the initial pressure inherent to the act of half-the-air [9, 23] rather than only an in-line pressure gauge without a physical pressure limit. Theories behind the half-the-air setting are based on simple rules of physics. According to Pascal's law, pressure within the syringe, tubing, and needle is equal throughout the system until the opening pressure is reached (and flow begins to occur), regardless of the speed of injection, the lumen size, or the size of fluid passage [11, 12]. Consequently, the syringe pressure could accurately reflect the needle tip pressure in the closed system [15]. The flow through the needle tip will start upon reaching the opening pressure of the target tissue. In this dynamic phase, the needle tip pressure will be kept below the original exerted pressure within the syringe because of two reasons. First, as the fluid accelerates through a constriction of the needle, the pressure reduces owing to the Bernoulli effect [20]; second, according to the fact that, with the needle tip open to the atmosphere, the speed of the injectate coming out of the needle tip declines shortly after commencing the injection by the act of half-the-air, we can confirm that the injection pressure declines following air compression to a given volume during the same course of half-the-air technique. If flow stops during drug administration, it would reliably reflect syringe pressure in response to accumulated volume of the injectate within the tissue, because, again by Pascal's law, the injection pressure returns to a state in which the pressures transmitted are equally distributed throughout the closed system [15]. Expert opinion shows that as the evidence for the utility of injection pressure as a safety monitor continues to accumulate, injection pressure monitoring should be incorporated as the routine during peripheral nerve blocks as long as the setting is not expensive and easy to apply [25]. From what was described above, pressure monitoring in combination with ultrasound guidance should be regarded as what we called "dual guidance" for deep regional blocks. Otherwise, hydrodissection by D5W at all times towards deep neural targets helps push away nerve fibers and minimize discomfort during ultrasound-guided needle advancement, as proposed in a research article regarding chronic pain management in this special issue.

The importance of half-the-air setting in deep regional blocks needs to be stressed beyond neurological complications. Ultrasound guidance unequivocally decreases the incidence of local anesthetic systemic toxicity [26]. However, it seems that the benefit cannot apply to deep regional blocks because of the paradox inherent to ultrasound guidance for deeper targets [5]. A dose-finding study demonstrated that Shamrock method for lumbar plexus block, the archetype of deep regional blocks, "might improve but not eliminate all challenges related to a deep ultrasound-guided nerve block" [27], and complications encountered in their study include local anesthetic systemic toxicity and epidural spread. The authors claimed that systemic toxicity might result from a needle tip partially placed inside a blood vessel, although local anesthetic spread was observed during injection [27]. Probably before the spread is visible, significant amounts of local anesthetic have already been injected into the vessels [28]. This assumption urges, in addition to ultrasound guidance and neurostimulation, the need for incorporating the half-the-air setting to minimize local anesthetic systemic toxicity during lumbar plexus block [28, 29] because the volume consumed to hydrolocate the needle tip and to visualize the hypoechoic spread is D5W instead of local anesthetic [9]. As for epidural spread during lumbar plexus block, it is not the injection volume but the injection pressure that matters [28, 30]. Although the original half-the-air setting [9] can be used to check the initial pressure prior to injection of local anesthetic (ensuring opening injection pressure <15 psi), modification of the setting has been urged to avoid pressure fluctuation during local anesthetic injection [31]. In response to the request, performing the same half-the-air technique in the local anesthetic syringe after D5W spread may keep the injection pressure at (when the liquid level starts to decrease) or below (while liquid level is descending) 14.7 psi throughout. Our preliminary qualitative analysis demonstrated that, by using the pressure management system of Injectomat Agilia® pump (Fresenius Vial, Brezins, France) as an in-line manometer between the needle (the tip inserted 3 cm into the pork model) and the low-dead space extension tube, pushing pressure generated by the act of half-the-air was below 15 psi during injection (experiment was run in triplicate, and occlusion alarm did not occur after the flow had commenced in response to half-the-air pressure exerted in the 20 mL local anesthetic syringe with the syringe pump set to an infusion rate of 0.1 ml/h and a pressure limit of 750 mmHg). Therefore, to improve all aspects at the same time for lumbar plexus block [28, 29], the modified half-the-air setting (additionally adding the act of half-the-air in the local anesthetic syringe) might reduce epidural spread (half-the-air in both the D5W and local anesthetic syringes) and local anesthetic systemic toxicity (D5W test spread in response to half-the-air) as well as nerve injury (half-the-air in the D5W syringe) during lumbar plexus block. Utilizing a syringe with a larger capacity (such as 25 or 30 mL) for the modified half-the-air setting will increase the drug volume to be administered in a single syringe if the practitioner standardizes the air volume compressed (5 mL) in the local anesthetic syringe with 10 mL of air introduced above the fluid. To more easily administer the intended local anesthetic volume by maintaining a higher but no more than 15 psi pushing pressure, repeating the act of half-the-air could help empty the local anesthetic syringe without delay. As with the original one [28], D5W emptied in the low dead space (1.4 ml) extension tube before local anesthetic injection in the modified half-the-air setting will not result in a significant dilutional effect for lumbar plexus block.

Some deep regional blocks require precise hydrodissection of a specific fascial or interfascial plane. A test spread other than local anesthetic from the half-the-air setting [9] helps identify the correct target without consumption of local anesthetic in the wrong place or the need of adding total mass (thus toxicity) to achieve the desired effect, as mentioned in the review articles on transversus abdominis plane block and obturator nerve block for this special issue. Furthermore, a retrospective study from the same special issue indicates that D5W itself is a potential analgesic for hydrodissection. Compared with normal saline, D5W also preserves neurostimulation for deep regional blocks when needed. Therefore, D5W is the test solution of choice in the half-the-air setting. Compared to pure pressure monitors, the half-the-air setting is not only multifunctional but also a safer pressure limiter inherent to the act of half-the-air. In the absence of other advanced monitoring techniques, there is no reason to perform ultrasound-guided deep regional blocks without incorporating the half-the-air setting, complying with the recommendations from the review articles in this special issue.

Acknowledgments

This special issue was supported by a grant from Hualien Armed Forces General Hospital. Yueh-Tzeng Lin (Division of Psychiatry, Hualien Armed Forces General Hospital, Hualien, Taiwan) is acknowledged.

Jui-An Lin
Rafael Blanco
Yasuyuki Shibata
Tatsuo Nakamoto

References

[1] J.-A. Lin, T. Nakamoto, and S.-D. Yeh, "Ultrasound standard for obturator nerve block: the modified Taha's approach," *British Journal of Anaesthesia*, vol. 114, no. 2, pp. 337–339, 2015.

[2] M. Speer, N. McLennan, and C. Nixon, "Novice learner in-plane ultrasound imaging: which visualization technique?" *Regional Anesthesia and Pain Medicine*, vol. 38, no. 4, pp. 350–352, 2013.

[3] J. M. B. Wilson, G. Germain, H. Vaghadia, R. Tang, and A. Sawka, "In-plane ultrasound-guided needle insertion ALONG or ACROSS the visual axis hand positions," *British Journal of Anaesthesia*, vol. 113, no. 4, pp. 717-718, 2014.

[4] J. Soong, I. Schafhalter-Zoppoth, and A. T. Gray, "Sonographic imaging of the obturator nerve for regional block," *Regional Anesthesia and Pain Medicine*, vol. 32, no. 2, pp. 146–151, 2007.

[5] D. Q. Tran, A. P. Boezaart, and J. M. Neal, "Beyond ultrasound guidance for regional anesthesiology," *Regional Anesthesia and Pain Medicine*, vol. 42, no. 5, pp. 556–563, 2017.

[6] E. Dingemans, S. R. Williams, G. Arcand et al., "Neurostimulation in ultrasound-guided infraclavicular block: a prospective randomized trial," *Anesthesia & Analgesia*, vol. 104, no. 5, pp. 1275–1280, 2007.

[7] Y. Gürkan, M. Tekin, S. Acar, M. Solak, and K. Toker, "Is nerve stimulation needed during an ultrasound-guided lateral sagittal infraclavicular block?" *Acta Anaesthesiologica Scandinavica*, vol. 54, no. 4, pp. 403–407, 2010.

[8] A. Perlas, G. Lobo, N. Lo, R. Brull, V. W. S. Chan, and R. Karkhanis, "Ultrasound-guided supraclavicular block. Outcome of 510 consecutive cases," *Regional Anesthesia and Pain Medicine*, vol. 34, no. 2, pp. 171–176, 2009.

[9] J.-A. Lin and H.-T. Lu, "A convenient alternative for monitoring opening pressure during multiple needle redirection," *British Journal of Anaesthesia*, vol. 112, no. 4, pp. 771-772, 2014.

[10] R. Brull, A. Hadzic, M. A. Reina, and M. J. Barrington, "Pathophysiology and Etiology of Nerve Injury Following Peripheral Nerve Blockade," *Regional Anesthesia and Pain Medicine*, vol. 40, no. 5, pp. 479–490, 2015.

[11] J. Gadsden, M. Latmore, D. M. Levine, and A. Robinson, "High opening injection pressure is associated with needle-nerve and

needle-fascia contact during femoral nerve block," *Regional Anesthesia and Pain Medicine*, vol. 41, no. 1, pp. 50–55, 2016.

[12] J. C. Gadsden, J. J. Choi, E. Lin, and A. Robinson, "Opening injection pressure consistently detects needle-nerve contact during ultrasound-guided interscalene brachial plexus block," *Anesthesiology*, vol. 120, no. 5, pp. 1246–1253, 2014.

[13] J. M. Neal, "Ultrasound-guided regional anesthesia and patient safety: update of an evidence-based analysis," *Regional Anesthesia and Pain Medicine*, vol. 41, no. 2, pp. 195–204, 2016.

[14] J. M. Neal, M. J. Barrington, R. Brull et al., "The second ASRA practice advisory on neurologic complications associated with regional anesthesia and pain medicine: executive summary 2015," *Regional Anesthesia and Pain Medicine*, vol. 40, no. 5, pp. 401–430, 2015.

[15] A. Hadzic, F. Dilberovic, S. Shah et al., "Combination of intraneural injection and high injection pressure leads to fascicular injury and neurologic deficits in dogs," *Regional Anesthesia and Pain Medicine*, vol. 29, no. 5, pp. 417–423, 2004.

[16] A. J. R. MacFarlane, A. Bhatia, and R. Brull, "Needle to nerve proximity: what do the animal studies tell us?" *Regional Anesthesia and Pain Medicine*, vol. 36, no. 3, pp. 290–302, 2011.

[17] K. Vermeylen, M. Hermans, F. Soetens et al., "Opening injection pressure is higher in intraneural compared with perineural injections during simulated nerve blocks of the lower limb in fresh human cadavers," *Regional Anesthesia and Pain Medicine*, vol. 42, no. 3, pp. 362–367, 2017.

[18] S. L. Orebaugh, J. J. Mukalel, A. C. Krediet et al., "Brachial plexus root injection in a human cadaver model: injectate distribution and effects on the neuraxis," *Regional Anesthesia and Pain Medicine*, vol. 37, no. 5, pp. 525–529, 2012.

[19] C. Robards, A. Hadzic, L. Somasundaram et al., "Intraneural injection with low-current stimulation during popliteal sciatic nerve block," *Anesthesia & Analgesia*, vol. 109, no. 2, pp. 673–677, 2009.

[20] V. H. Y. Ip and B. C. H. Tsui, "Practical concepts in the monitoring of injection pressures during peripheral nerve blocks," *International Anesthesiology Clinics*, vol. 49, no. 4, pp. 67–80, 2011.

[21] C. Siegmueller and S. Ramessur, "A simple low-cost way of measuring injection pressure during peripheral nerve block," *Anaesthesia*, vol. 66, no. 10, p. 956, 2011.

[22] B. C. H. Tsui, L. X. Y. Li, and J. J. Pillay, "Compressed air injection technique to standardize block injection pressures," *Canadian Journal of Anesthesia*, vol. 53, no. 11, pp. 1098–1102, 2006.

[23] B. C. H. Tsui, M. P. Knezevich, and J. J. Pillay, "Reduced injection pressures using a compressed air injection technique (CAIT): an in vitro study," *Regional Anesthesia and Pain Medicine*, vol. 33, no. 2, pp. 168–173, 2008.

[24] J. Patil, H. Ankireddy, A. Wilkes, D. Williams, and M. Lim, "An improvised pressure gauge for regional nerve blockade/anesthesia injections: an initial study," *Journal of Clinical Monitoring and Computing*, vol. 29, no. 6, pp. 673–679, 2015.

[25] J. Gadsden, "Injection pressure monitoring: no more excuses," *Journal of Clinical Monitoring and Computing*, vol. 29, no. 6, pp. 671-672, 2015.

[26] M. J. Barrington and R. Kluger, "Ultrasound guidance reduces the risk of local anesthetic systemic toxicity following peripheral nerve blockade," *Regional Anesthesia and Pain Medicine*, vol. 38, no. 4, pp. 289–299, 2013.

[27] A. R. Sauter, K. Ullensvang, G. Niemi et al., "The Shamrock lumbar plexus block: a dose-finding study," *European Journal of Anaesthesiology*, vol. 32, no. 11, pp. 764–770, 2015.

[28] J. A. Lin, "Importance of half-the-air pressure test in Shamrock lumbar plexus block," *European Journal of Anaesthesiology*, vol. 33, no. 10, pp. 784–786, 2016.

[29] N. Mænchen, M. Dam, A. R. Sauter et al., "Reply to: importance of half-the-air pressure test in Shamrock lumbar plexus block," *European Journal of Anaesthesiology*, vol. 33, no. 10, pp. 784–786, 2016.

[30] J. C. Gadsden, D. M. Lindenmuth, A. Hadzic, D. Xu, L. Somasundarum, and K. A. Flisinski, "Lumbar plexus block using high-pressure injection leads to contralateral and epidural spread," *Anesthesiology*, vol. 109, no. 4, pp. 683–688, 2008.

[31] B. C. Tsui, "Compressed air injection technique for Shamrock lumbar plexus block," *European Journal of Anaesthesiology*, vol. 34, no. 9, pp. 629–631, 2017.

Hindawi
BioMed Research International
Volume 2017, Article ID 8284363, 12 pages
https://doi.org/10.1155/2017/8284363

Review Article

Transversus Abdominis Plane Block: An Updated Review of Anatomy and Techniques

Hsiao-Chien Tsai,[1] Takayuki Yoshida,[2] Tai-Yuan Chuang,[3,4] Sheng-Feng Yang,[5] Chuen-Chau Chang,[1,6,7] Han-Yun Yao,[5] Yu-Ting Tai,[5,7] Jui-An Lin,[5,7] and Kung-Yen Chen[5]

[1] *Department of Anesthesiology, Taipei Medical University Hospital, Taipei, Taiwan*
[2] *Department of Anesthesiology, Kansai Medical University Hospital, Osaka, Japan*
[3] *Department of Orthopedics, Wan Fang Hospital, Taipei Medical University, Taipei, Taiwan*
[4] *Department of Orthopedics, School of Medicine, College of Medicine, Taipei Medical University, Taipei, Taiwan*
[5] *Department of Anesthesiology, Wan Fang Hospital, Taipei Medical University, Taipei, Taiwan*
[6] *Health Policy Research Center, Taipei Medical University Hospital, Taipei, Taiwan*
[7] *Department of Anesthesiology, School of Medicine, College of Medicine, Taipei Medical University, Taipei, Taiwan*

Correspondence should be addressed to Kung-Yen Chen; araiza_popp@hotmail.com

Jui-An Lin and Kung-Yen Chen contributed equally to this work.

Received 29 December 2016; Revised 19 March 2017; Accepted 28 June 2017; Published 31 October 2017

Academic Editor: Ayhan Cömert

Purpose of Review. Transversus abdominis plane (TAP) block is a regional technique for analgesia of the anterolateral abdominal wall. This review highlights the nomenclature system and recent advances in TAP block techniques and proposes directions for future research. *Recent Findings*. Ultrasound guidance is now considered the gold standard in TAP blocks. It is easy to acquire ultrasound images; it can be used in many surgeries involving the anterolateral abdominal wall. However, the efficacy of ultrasound-guided TAP blocks is not consistent, which might be due to the use of different approaches. The choice of technique influences the involved area and block duration. To investigate the actual analgesic effects of TAP blocks, we unified the nomenclature system and clarified the definition of each technique. Although a single-shot TAP block is limited in duration, it is still the candidate of the analgesic standard for abdominal wall surgery because the use of the catheter technique and liposomal bupivacaine may overcome this limitation. *Summary*. Ultrasound-guided TAP blocks are commonly used. With the unified nomenclature and the development of catheter technique and/or liposomal local anesthetics, TAP blocks can be applied more appropriately to achieve better pain control.

1. Introduction

The transversus abdominis plane (TAP) block was first introduced by Rafi [1] in 2001 as a landmark-guided technique via the triangle of Petit to achieve a field block. It involves the injection of a local anesthetic solution into a plane between the internal oblique muscle and transversus abdominis muscle. Since the thoracolumbar nerves originating from the T6 to L1 spinal roots run into this plane and supply sensory nerves to the anterolateral abdominal wall [2], the local anesthetic spread in this plane can block the neural afferents and provide analgesia to the anterolateral abdominal wall.

With the advancement of ultrasound technology, TAP blocks become technically easier and safer to perform. Thus, there was a surge of interest in TAP blocks as therapeutic adjuncts for analgesia after abdominal surgeries. In the past decade, there has been growing evidence supporting the effectiveness of TAP blocks for a variety of abdominal surgeries, such as cesarean section, hysterectomy, cholecystectomy, colectomy, prostatectomy, and hernia repair [1, 3–9].

Although its analgesic effect covers only somatic pain with short duration [10], single-shot TAP block plays a valuable role in multimodal analgesia. With continuous infusion [11–17] or prolonged-release liposomal local anesthetics [18–22], TAP blocks could overcome the problem of short duration.

In this review, we will describe the relevant anatomy, formulate a nomenclature system to include various approaches, discuss recent advancements in techniques, and detail the possible complications.

2. Applied Anatomy

The relevant anatomy is shown in Figure 1. A thorough understanding of the anatomy may help clinicians to determine the site of injection, improve the success rate, and prevent complications.

2.1. The Sensory Nerves Innervating the Anterolateral Abdominal Wall. The thoracolumbar nerves are responsible for the segmental cutaneous supply of the abdominal wall. They divide into the anterior primary ramus and posterior primary ramus shortly after exiting from the intervertebral foramen. The posterior ramus travels backward, while the anterior ramus branches into lateral and anterior cutaneous nerves (Figure 1(b)). The anterolateral abdominal wall is mainly innervated by the anterior rami of the thoracolumbar spinal nerves (T6-L1), which become the intercostal (T6-T11), subcostal (T12), and ilioinguinal/iliohypogastric nerves (L1) (Figure 1(a)). These branches further communicate at multiple locations, including large branch communications on the anterolateral abdominal wall (intercostal/upper TAP plexus) and plexuses that run with the deep circumflex iliac artery (DCIA) (lower TAP plexus) and the deep inferior epigastric artery (DIEA) (rectus sheath plexus) [2]. Since these segmental nerves communicate just above the transversus abdominis muscle, the subfascial spread of local anesthetic can provide anterolateral abdominal wall analgesia [23].

2.2. Clinical Correlation of Cutaneous Branches. The anterior primary rami of T7-T12 spinal nerves pass between internal oblique and transversus abdominis and then perforate rectus abdominis and end as the anterior cutaneous branches, which innervate the anterior abdomen (from midline to midclavicular line). Among these anterior rami, the T12 crosses quadratus lumborum before entering the TAP, as shown in Figure 1(b) [24]. The lateral cutaneous branches depart near the angle of the rib posteriorly [15]. The lateral cutaneous branches of T7-T11 then divide into anterior and posterior branches: the anterior branches supply the abdominal wall toward the lateral margin of rectus abdominis; the posterior branches pass backward to supply the skin over latissimus dorsi. However, the lateral cutaneous branch of T12 does not further divide into anterior and posterior branches (Figure 1(b)). It supplies a part of the gluteal region, and some of its filaments extend as low as the greater trochanter (Figure 1(c)). The L1 spinal nerve divides into the iliohypogastric and ilioinguinal nerves, which innervate the skin of the gluteal region behind the lateral cutaneous branches of T12, the hypogastric region, the upper medial part of the thigh, and the genital area [25].

Since the lateral cutaneous branches leave the TAP posterior to the midaxillary line, posterior injection of local anesthetics is suggested if analgesia for both the anterior and lateral abdominal wall is required [26]. However, most of the lateral cutaneous branches arise before the main nerves enter the TAP, and only those of T11 and T12 have a short course within or through the TAP [15]. For the blockade of the lateral cutaneous branches, a TAP block can only cover the T11 and T12 lateral cutaneous branches even with a more posterior injection. Based on the distribution of the T9-T12 branches, the lateral approach performed at the midaxillary line between the costal margin and iliac crest could provide mainly periumbilical and infraumbilical analgesia, while the posterior approach performed posterior to the midaxillary line has the potential to provide some degree of lateral abdominal wall analgesia [10]. Paravertebral spread from T5 to L1 has been reported only with posterior TAP blocks [27]. The L1 branches, which become the ilioinguinal and iliohypogastric nerves, pass into the TAP near the anterior part of the iliac crest [15]. Thus, a TAP block at this level is similar to ilioinguinal and iliohypogastric nerve blocks. Direct ilioinguinal/iliohypogastric nerve block is a better choice than TAP block if only L1 analgesia is needed [28, 29].

The spread of injectate in TAP might be affected by anatomical variation [30], injected volume [31], and choice of approach [32–35]. To achieve the best quality of analgesia without increasing the volume and associated systemic toxicity, it is important to choose the most appropriate method by considering the distribution of segmental nerves.

2.3. The TAP Block-Related Muscles. There are four paired muscles in the anterolateral abdominal wall: rectus abdominis, transversus abdominis, internal oblique, and external oblique. Rectus abdominis runs parallel in the midline and is separated by the linea alba. The other three are laterally located muscles, transversus abdominis, internal oblique, and external oblique, sequentially from deep to superficial, and are mainly related to TAP blocks. The three muscles overlie one another in the lateral abdomen and terminate medially as an aponeurosis called the linea semilunaris, which is lateral to rectus abdominis [15] (Figure 2). The TAP plexuses lie on transversus abdominis. Therefore, intramuscular injection of local anesthetics might also have some analgesic effects [36].

3. New Nomenclature

The TAP is a potential anatomical space between transversus abdominis and internal oblique (or rectus abdominis) [37], and the field block by TAP infiltration is referred to as a TAP block. There are several different approaches for ultrasound-guided TAP block, such as lateral, posterior, and subcostal approaches. Unlike specific peripheral nerve blocks, TAP block is a nondermatomal "field block." This has led to a debate on whether there is a need for standardization of techniques or technique nomenclature [33]. Even with the same ultrasound-guided technique, the extent of spread of

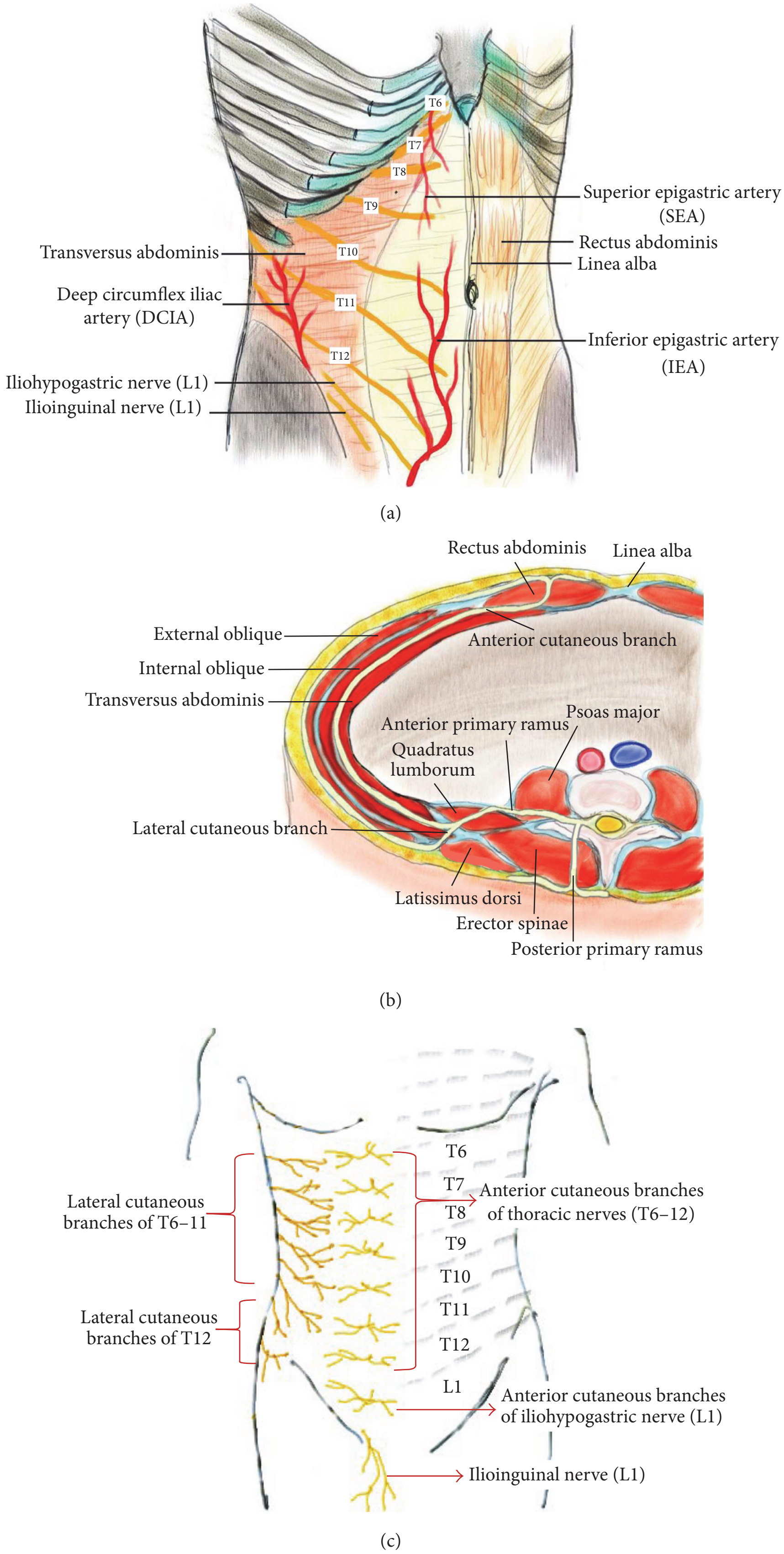

Figure 1: The thoracolumbar spinal nerves (T6~L1) innervating the anterolateral abdominal wall. (a) Distribution of neurovascular structure in the anterolateral abdominal wall. (b) The pathway of the thoracolumbar spinal nerves (T12). This is the cross-sectional view of the left abdomen. The anterior primary ramus of the segmental nerves divides into anterior and lateral cutaneous branches, which supply the anterolateral abdominal wall. (c) The segmental distribution of cutaneous nerve on the anterolateral trunk.

Table 1: The classification of ultrasound-guided TAP blocks and the corresponding supplied areas.

Approach	The main segmental thoracolumbar nerves [15]		Supplied area [15]
Subcostal [39–41]	T6-9	Anterior cutaneous branches	Upper abdomen just below the xiphoid and parallel to the costal margin
Lateral [10, 26]	T10-12	Anterior cutaneous branches	Anterior abdominal wall at the infraumbilical area, from midline to midclavicular line
Posterior [10, 42]	T9-12	Anterior cutaneous branches (possibly lateral cutaneous branches)	Anterior abdominal wall at the infraumbilical area and possibly lateral abdominal wall between costal margin and iliac crest
Oblique subcostal [11, 13, 15, 17, 43]	T6-L1	Anterior cutaneous branches	Upper and lower abdomen

TAP: transversus abdominis plane.

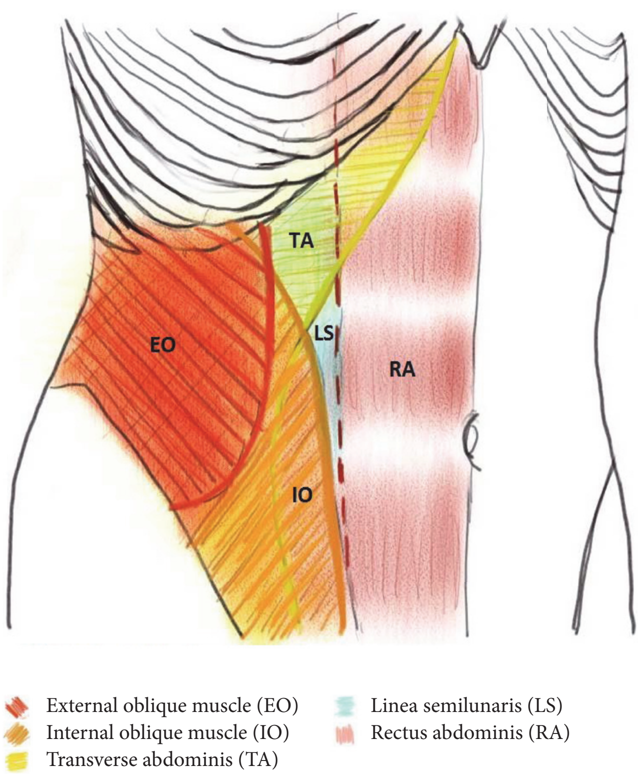

Figure 2: The muscular structure of the anterolateral abdominal wall. RA: rectus abdominis; TA: transversus abdominis; IO: internal oblique; EO: external oblique; LS: linea semilunaris. The red dotted line: the lateral border of rectus abdominis.

local anesthetics can be variable due to individual anatomical variations [30, 33]. However, there has been evidence supporting the idea that the nuances of various techniques can also affect the analgesic outcomes. For example, a meta-analysis showed that posterior approach appears to produce longer analgesia compared to that of the lateral approach [10]. Furthermore, based on cadaveric and radiologic evaluations, dye injected via different approaches demonstrated different nerve involvement [23, 32, 34, 38]. Therefore, it is important to classify the "TAP block" group according to a reasonable nomenclature system before comparing the analgesic effects among different approaches.

The nomenclature regarding TAP block is confusing, and there is still no consensus about its terminology after an explosive growth in numbers of studies about it. Therefore, we provided a nomenclature system to categorize the various approaches into four groups comprising subcostal, oblique subcostal, lateral, and posterior TAP blocks. The classification is based on the involved spinal nerves rather than the probe positions only. Although all anterior branches communicate on TAP, each segmental nerve supplies different areas (Figure 1(a)). The T6-8 supply the area below the xiphoid and parallel to the costal margin; T9-12 supply the periumbilical area and the lateral abdominal wall between the costal margin and iliac crest; L1 supplies the anterior abdomen near the inguinal area and thigh [15].

Classification of TAP blocks based on a unified nomenclature system is shown in Table 1. Many approaches have been suggested to provide analgesia over the upper abdomen, such as oblique subcostal, subcostal, or upper subcostal approaches [11, 13, 15, 17, 39, 40, 43]. However, they are quite similar in the area where local anesthetics deposit except for the oblique subcostal approach, which covers both the upper and lower abdomen using the hydrodissection technique. We suggest categorizing similar approaches as "subcostal" since it is easier to remember it by probe position and associated blocked plexus.

A midaxillary or lateral TAP block is performed by placing the probe at or anterior to the midaxillary line between the costal margin and iliac crest. It can provide lower abdominal wall analgesia from the midline to the midclavicular line [10, 26]. Compared to a lateral TAP block, a posterior TAP block approximates the double-pop TAP technique at the lumbar triangle of Petit [44] by injecting local anesthetic superficial to the transversus abdominis aponeurosis [45] and offers better and more prolonged analgesia than the lateral approach [10, 42]. While subcostal and lateral TAP injections do not always cover the lateral cutaneous branches of the segmental nerves [35], the posterior approach deposits the injectate posterior to the midaxillary line and may provide better analgesia to the lateral abdominal wall [26].

Dual TAP block, which technically combines subcostal with lateral/posterior TAP block, provides a wider coverage for both the upper and lower abdominal walls. By anesthetizing both the upper TAP plexus (the intercostal plexus, which

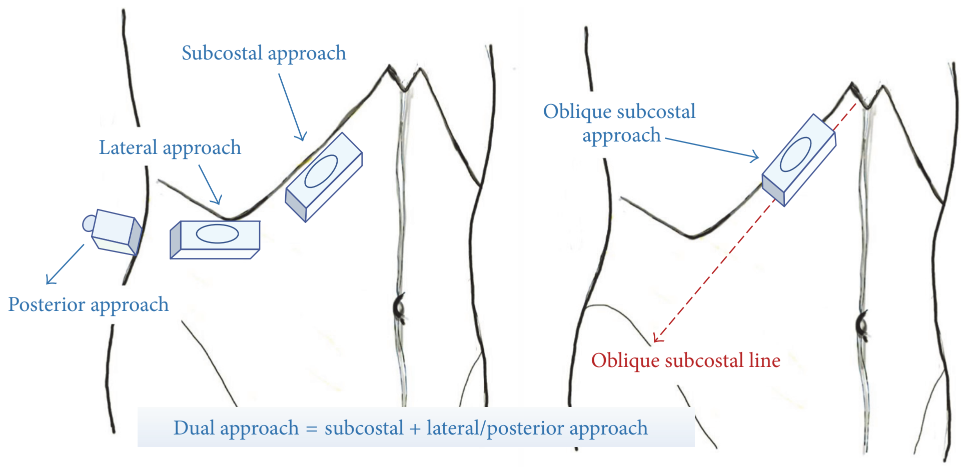

FIGURE 3: Four approaches of ultrasound-guided transversus abdominis plane (TAP) blocks. Red dashed line indicates the oblique subcostal line, from the xiphoid to the anterior part of the iliac crest.

consists of large branch communications anterolaterally) and the lower TAP plexus (the deep circumflex iliac artery plexus) (Figure 1(a)), a lateral-to-medial long-needle approach can cover T7/8 to L1. [35, 46]. If the dual TAP block is performed bilaterally, it is called bilateral dual TAP block, which was introduced by Borglum et al. [47, 48]. It is similar to the four-quadrant TAP block by Niraj et al. [12, 16]. As Borglum et al. described previously, "dual" stands for two extent areas of the anatomical TAP and expresses the anterior abdominal wall correctly rather than "four-quadrant" one [46]. A TAP block can be performed unilaterally or bilaterally. Therefore, "dual TAP block, unilateral or bilateral," is more precise and suitable for clinical communication.

As mentioned earlier, the oblique subcostal TAP block is a modified subcostal TAP block, which was first introduced by Hebbard et al. [15]. By hydrodissecting the TAP along the oblique subcostal line (from the xiphoid toward the anterior part of the iliac crest), the anesthetic solution spreads across the location of T6-L1 nerves and thus potentially covers both the upper and lower abdominal walls. Since it requires only a single penetration through the subcostal approach but covers both the upper and lower TAP plexuses like a dual TAP block, it cannot be classified into either one of these two groups appropriately. Thus, the oblique subcostal TAP block should be categorized as an independent, specific technique for TAP block (Table 1). This nomenclature is slightly different from the one proposed by Hebbard [49], which divided the subcostal TAP block to upper subcostal and lower subcostal TAP blocks. Since a lower subcostal TAP block covers the same area as a lateral TAP block and does not provide analgesia over the T7-8 dermatomes, we suggest categorizing the lower subcostal TAP block as a lateral TAP block to simplify the nomenclature. Furthermore, the upper and lower TAP blocks suggested by Borglum et al. correspond exactly to subcostal and lateral approaches, respectively [46].

In addition to the above dichotomy, a posterior TAP block has different manifestations compared to a lateral TAP block, including analgesic effectiveness and duration [10, 42]. Neither a lateral nor subcostal approach results in dye spread posterior to the midaxillary line and thus spares the lateral cutaneous nerve branches, which could possibly be circumvented by the posterior approach [35]. The L1 branches divide into the ilioinguinal and iliohypogastric nerves. If analgesia over the L1 dermatome is the major concern, it is recommended to target the L1 branches specifically. The ilioinguinal and iliohypogastric nerve block can provide more specific and better analgesia than a TAP block [28, 29]. The anterior quadratus lumborum block is also a promising alternative to block the L1 branches coursing over the surface of quadratus lumborum [45]. Ultrasound-guided transversalis fascia plane block also provides analgesia over the L1 dermatome [50]; however, the injection is deeper than TAP blocks and is at risk for unanticipated motor weakness due to central and proximal spread toward psoas major [51].

As described above, classification based on the logic of this nomenclature system is reasonable and clinically useful and can aid in discussion among clinicians. The detailed definition of different approaches will be described in the Techniques of TAP Block.

4. Techniques of TAP Block

In this review, we described the original landmark-guided technique in brief and four ultrasound-guided TAP blocks according to the unified nomenclature system: lateral, posterior, subcostal, and oblique subcostal TAP blocks (Table 1 and Figure 3). Furthermore, current advancement in continuous techniques to overcome the limitation of one-shot TAP blocks was discussed. The patient is placed in a supine position for all these approaches, except for slight lateralization for the posterior approach in some cases.

4.1. Landmark-Guided TAP Block. The blunt landmark-guided technique applies loss of resistance as the needle is advanced through the fascia layers of external oblique and internal oblique [1]. After locating the triangle of Petit, the TAP is identified using the subjective double-pop loss of resistance technique. McDonnell et al. suggested that the first pop

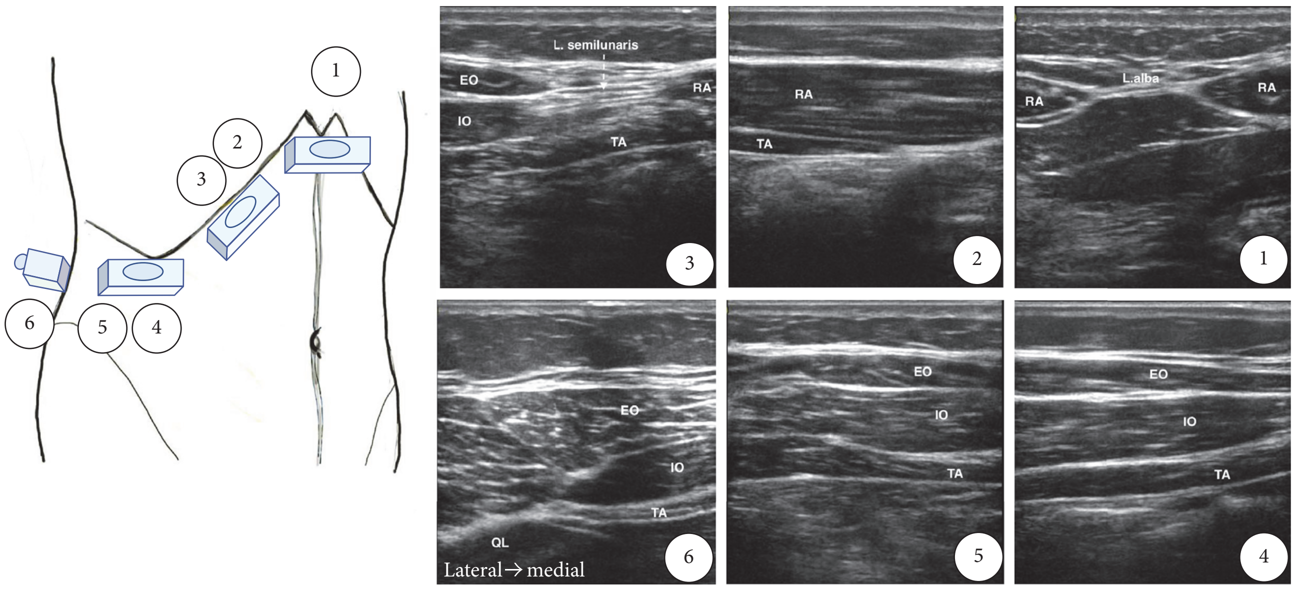

FIGURE 4: Ultrasound identification of the transversus abdominis plane. RA: rectus abdominis; TA: transversus abdominis; IO: internal oblique muscle; EO: external oblique muscle; QL: quadratus lumborum; L. alba: linea alba; L. semilunaris: linea semilunaris.

indicates penetration of the fascia of the external oblique muscle, and the second indicates piercing of the fascia of internal oblique and entry of the needle into the TAP [23, 33]. However, Rafi et al. suggested that the first pop indicates the needle has reached the plane between internal oblique and transversus abdominis, and the second pop indicates the needle has passed through transversus abdominis and thus the needle went too far [1, 37]. Debates continue regarding the adequacy of "single-pop" [1], "double-pop" [23], and the structures responsible for the "pop."

Currently, landmark-guided technique is no longer recommended because of ambiguity of the standard procedure sequence, small size and large variation of the lumbar triangle of Petit, and the risk of peritoneal perforation during the blind technique [37, 52].

4.2. Ultrasound-Guided TAP Blocks. Ultrasound guidance is now considered the gold standard for peripheral nerve block [53]. Usually, a linear probe is adequate for most TAP blocks. However, a convex probe is preferable for TAP blocks in markedly obese patients [54, 55].

4.2.1. Ultrasound Identification of TAP. To perform an ultrasound-guided TAP block, identification of the TAP is a priority. We suggest the scanning steps as follows: (1) Put the transducer transversely just below the xiphoid process and locate the paired rectus abdominis and the linea alba. (2) Rotate the transducer obliquely and move laterally, parallel to the costal margin. At this level, the TAP is between rectus abdominis and transversus abdominis, or the TAP is absent here because transversus abdominis ends at the lateral end of rectus abdominis in some patients. (3) Move the transducer along the costal margin more laterally until the aponeurosis of the linea semilunaris, which is lateral to the rectus abdominis, appears. Internal oblique and external oblique are located lateral to the linea semilunaris. We can start to identify the three muscle layers: transversus abdominis, internal oblique, and external oblique (from deep to superficial). The TAP is located just above transversus abdominis. (4) Move the transducer more laterally to the midaxillary line, and scan up and down between the costal margin and iliac crest. Typically, three muscle layers can be seen. The TAP is between internal oblique and transversus abdominis. (5) If the transducer is placed posteriorly, we find that internal oblique and transversus abdominis taper off into a common aponeurosis, also called the thoracolumbar fascia, which is connected to the lateral border of the quadratus lumborum. The TAP is between internal oblique and transversus abdominis and continuous with the aponeurosis [40, 56]. The probe position of each ultrasound-guided TAP block is shown in Figure 3, and the corresponding ultrasound images are shown in Figure 4.

4.2.2. Subcostal TAP Block. As shown in Figure 5(a) and described in steps (1) and (2), transversus abdominis is identified as the more hypoechoic muscle layer just beneath rectus abdominis. Deposition of the local anesthetic starts between transversus abdominis and rectus abdominis, medial to the linea semilunaris (Figure 5(b)). If transversus abdominis ends at the lateral end of rectus abdominis, the local anesthetic can be deposited between transversus abdominis and internal oblique lateral to the linea semilunaris, but it might be better to include the injection from beneath rectus abdominis toward the lateral side to achieve a higher success rate.

Shibata et al. suggested that only lower abdominal surgery should be an indication for lateral TAP block because of the limited level of sensory block [57]. Hebbard et al. also demonstrated that the lateral TAP block is suitable for surgery below the umbilicus, while the subcostal TAP block is more suitable for supraumbilical and periumbilical analgesia [15]. Lee et al. further proved that there was a difference in the

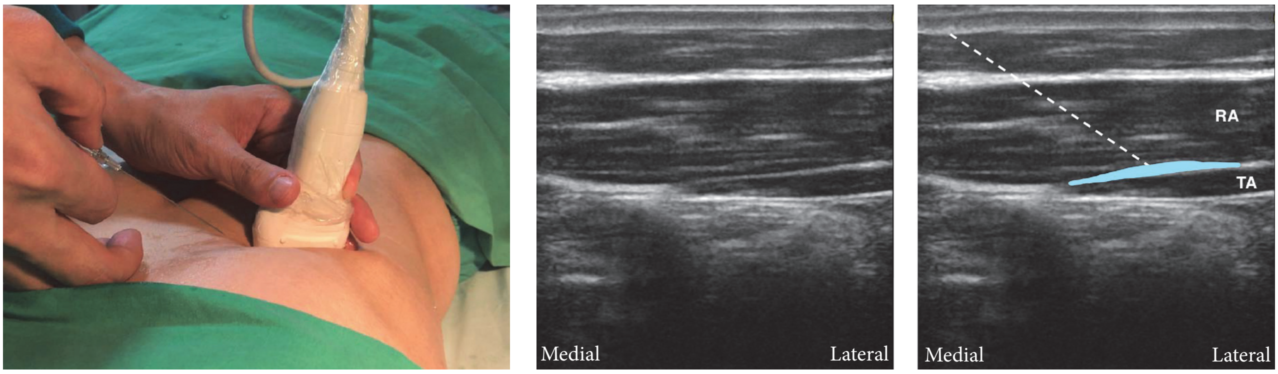

(a) (b)

Figure 5: Subcostal approach of transversus abdominis plane (TAP) block. (a) The probe position and needle direction. The probe is parallel to the costal margin near the xiphoid. The needle is inserted in plane. (b) The corresponding ultrasound images. The TAP is between rectus abdominis and transversus abdominis, and the local anesthetic is deposited in this plane to cover the upper TAP plexus. White dashed line: the needle trajectory. Light blue area: the deposition sites of local anesthetic. RA: rectus abdominis; TA: transversus abdominis.

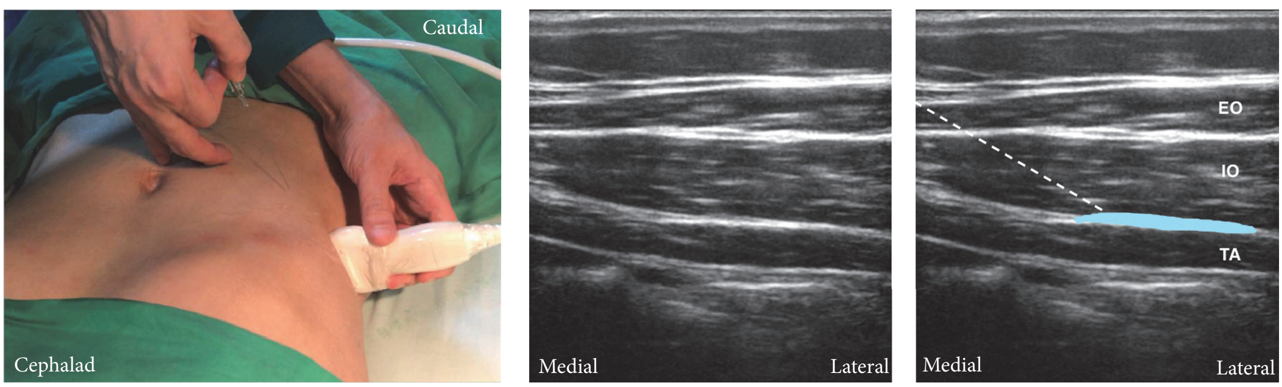

(a) (b)

Figure 6: Lateral approach of transversus abdominis plane (TAP) block. (a) The probe position and needle trajectory. The probe is near or at the midaxillary line between the costal margin and the iliac crest. The needle is inserted in plane. (b) Corresponding ultrasound images. The TAP is between internal oblique and transversus abdominis. The local anesthetic is deposited in this plane to cover the lower TAP plexus. White dashed line: needle trajectory. Light blue area: the deposition site of local anesthetic. TA: transversus abdominis; IO: internal oblique; EO: external oblique.

dermatomal spread between lateral and subcostal approaches [41]. The pattern of spread differs depending on the site of injection and it has important implications for the extent of analgesia produced with each approach [27]. Therefore, the subcostal approach should be considered for upper abdominal analgesia.

4.2.3. Lateral TAP Block. In step (4), we can identify the typical three muscles layers at the midaxillary line between the costal margin and iliac crest. After measuring the depth of the TAP, a needle is inserted away from the transducer at the same distance according to the principle to make the needle in plane for deep regional blocks [58] (Figure 6(a)). The needle is advanced into the transversus abdominis and pulled back incrementally with regular aspiration and then the plane is hydrodissected until the eye sign, an elliptical, hypoechoic spread of local anesthetic, is seen. Otherwise, it is also logical to deposit local anesthetic underneath the fascial layer to ensure optimal analgesia because the nerves are bound to the transversus abdominis [33]. If a patchy opacity appears within the internal oblique, indicating intramuscular injection, or the local anesthetic does not separate the fascia well, the needle tip should be repositioned. However, intramuscular injection of the transversus abdominis might still provide some analgesic effects [36]. Half-the-air setting can also help identify the correct fascial plane using test volume injection and prevent incidental neurologic injury [59, 60]. Figure 6(b) shows the ultrasound image of a lateral TAP block.

4.2.4. Posterior TAP Block. The posterior approach is similar to the lateral approach, but the ultrasound transducer is moved more posteriorly as shown in Figure 7(a). This is to view the point where transversus abdominis ends, as described in step (5). When scanning posteriorly, transversus abdominis tails off and turns into the aponeurosis. Quadratus

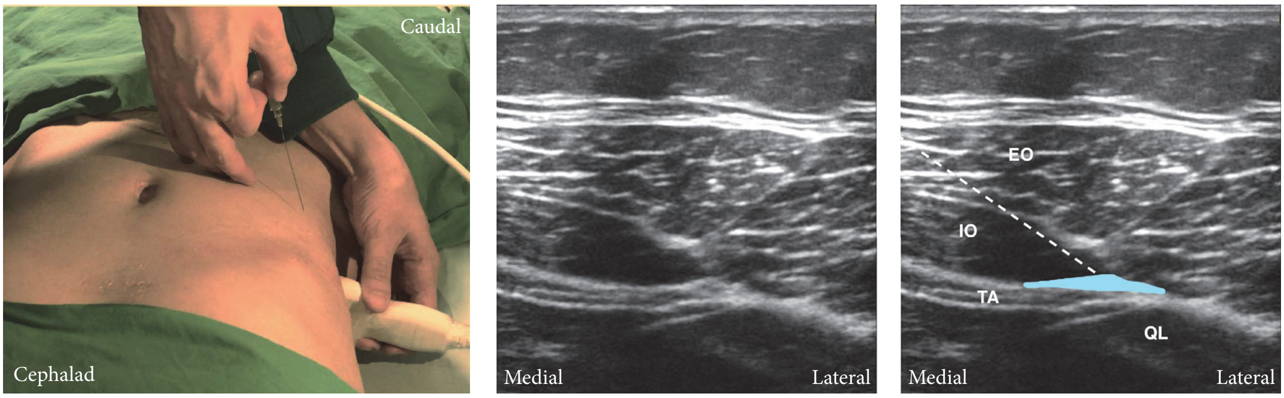

(a) (b)

Figure 7: Posterior approach of transversus abdominis plane (TAP) block. (a) The probe position and needle trajectory. The probe is placed posterior to the midaxillary line between the costal margin and the iliac crest. The needle is inserted in plane. (b) Corresponding ultrasound images. Posteriorly, transversus abdominis tails off and turns into the aponeurosis. The quadratus lumborum can be seen posteromedial to the aponeurosis. The injection site is at the TAP between internal oblique and transversus abdominis posterior to the midaxillary line and near the aponeurosis. White dashed line: needle trajectory. Light blue area: the deposition site of local anesthetic. TA: transversus abdominis; IO: internal oblique; EO: external oblique; QL: quadratus lumborum.

lumborum can be seen posteromedial to the aponeurosis (Figure 7(b)). The injection site is superficial to the aponeurosis near quadratus lumborum [27, 45]. There have been studies suggesting that a posterior TAP block provides more effective and prolonged analgesia than the lateral approach [10, 42]. Evidence showed the absence of posterior spread in the lateral approach [26] and a wider expansion of local anesthetics in the posterior approach [27].

4.2.5. Oblique Subcostal TAP Block. The oblique subcostal TAP block is modified from the subcostal TAP block, which was first introduced by Hebbard et al. [15]. Unlike other approaches, a much longer needle (15–20 cm) and a larger volume of anesthetics (40–80 ml) are required. The oblique subcostal line extends from the xiphoid toward the anterior part of the iliac crest and potentially covers the T6-L1 nerves in the TAP (Figure 3). Thus, local anesthetic injected in the TAP along this line provides both upper and lower abdominal wall analgesia, like a dual TAP block. Compared to a dual TAP block, the oblique subcostal TAP block more consistently covers L1 dermatome. Only single penetration is required for the oblique subcostal approach. A large volume of local anesthetics is required to hydrodissect the TAP along the whole ipsilateral oblique subcostal line. It can provide promising analgesia for abdominal surgeries [61–63] and might be better compared to the lateral approach [64]. However, the oblique subcostal TAP block is much more difficult. Bending the needle initially and then reinserting during the advancement of the needle might be helpful in performing the block [15].

5. Other Considerations

5.1. Dual TAP Block. If analgesia is needed for both the supraumbilical and infraumbilical abdomen, the dual TAP block could also be considered. Dual TAP block is the combination of the subcostal and the lateral/posterior TAP block. Compared to the oblique subcostal TAP block, the dual TAP block technically ensures more easily that local anesthetic is deposited throughout the plane and provides analgesia for both the upper (T6-T9) and lower (T10-T12) abdomen. The bilateral dual TAP block was first introduced by Borglum et al. as the four-point approach [47]. Niraj et al. once called it the "four-quadrant" TAP block [12]. After making the skin aseptic, we suggest performing the lateral/posterior approach first and then the subcostal approach, to keep the probe aseptic. In other words, the probe is placed in the gravity-dependent part as a general rule below the needle insertion site for single-shot peripheral nerve blocks [65, 66]. Jelly introduction into the central part of the body should be avoided whenever possible, even if it is aseptic [67], and ultrasound gel itself near peripheral nerves may cause inflammation [68]. Performing the dual TAP block in this sequence keeps the needle away from gravity-dependent gel contamination.

5.2. Continuous TAP Block. Petersen et al. [69] reported that anesthetized dermatomes produced by a continuous TAP block employing the lateral approach comprised only two segments (T10 and T11) in healthy volunteers. Nevertheless, two previous randomized controlled trials [11, 17] have reported that adding continuous TAP blocks to single-injection TAP blocks improves analgesia after laparotomy for gynecological cancer. Both studies employed an oblique subcostal approach for a continuous TAP block [15]. After incremental hydrodissection of the TAP along the oblique subcostal line, a catheter is threaded through the needle into the TAP. Yoshida et al. [17] proposed that this thorough hydrodissection of the TAP and the catheter passage might facilitate a wider spread of sensory block by providing a track for the local anesthetics along the catheter within the

TAP. However, this hypothesis should be validated in a future study. In the two above-mentioned studies regarding continuous oblique subcostal TAP blocks [11, 17], a point-source catheter, such as an epidural catheter, was used for providing a continuous TAP block. A continuous TAP block using a catheter with more extensive holes may produce a wider spread of sensory block and superior analgesia [13], although there has been no research evaluating the effectiveness of the multihole catheter compared to the point-source catheter.

6. Complications

Visceral damage due to inadvertent peritoneal puncture while performing blind TAP block has been reported [70]. Although the risk can be minimized with ultrasound guidance, the potential of iatrogenic injury still exists due to a failure to image the entire needle during its advancement [71]. Other reported complications of TAP block include seizure, ventricular arrhythmia, and transient femoral nerve palsy [72–75]. To limit local systemic toxicity, a low concentration of local anesthetic should be chosen when a high-volume regimen (e.g., 20 ml bilaterally) is necessary for a successful block [76]. Good communication between anesthesiologists and surgeons also helps prevent overdose by incidental repeated local anesthetics injection after a TAP block. The immediate availability of lipid emulsion along with other emergency therapeutics is recommended for TAP block [77]. Transient femoral palsy after TAP block is induced by incorrect local anesthetic deposition between transversus abdominis and the transversalis fascia [75]. Since the femoral nerve lies in the same tissue plane, as little as 1 ml of injectate flowing posteromedially can surround the femoral nerve [78]. This complication is usually self-limited but will delay patient discharge especially in day-case surgeries. Using a test solution to locate the needle tip under ultrasound guidance will help identify the TAP and avoid spread of the anesthetic toward the femoral nerve [78].

Since the role of a nerve stimulator during TAP block is elusive and the nervous structures might be too small to be identified by ultrasound, "half-the-air" setting should be considered to avoid intrafascicular spread by keeping the injection pressure below 15 psi [60]. Intrafascicular needle placement associated with high injection pressure can result in neurologic injury in animal models [79, 80]. Monitoring and limiting injection pressure to 15 psi reliably detects needle-nerve contact [81]. Since the TAP belongs to a vessel-rich plane [37], the test solution instead of local anesthetic should be injected first. By using the test solution to hydrolocate the needle tip and visualize the hypoechoic spread, the surrounding tissues, not only vessels but also nerves, are usually pushed away from the needle tip by the test spread [59].

In brief, half-the-air setting takes advantage of the test solution and pressure monitoring at the same time [59]. To avoid all complications mentioned above, it is recommended to inject the least volume of local anesthetic required under dual guidance with ultrasound and half-the-air setting.

7. Conclusion

With the advancement in ultrasound technology, the success rate and safety of TAP blocks have markedly improved. There are several different approaches for ultrasound-guided TAP block, and the nuances of various techniques can affect the analgesic outcomes. It is important to classify the "TAP block" group according to a reasonable nomenclature system before comparing the analgesic effects among different approaches. In this review, we provided a nomenclature system to categorize the various approaches into four groups comprising subcostal, lateral, posterior, and oblique subcostal TAP blocks. This new nomenclature system based on the involved spinal nerves is clinically useful and can aid in discussion among clinicians. A posterior TAP block offers a longer duration of analgesia than does a lateral TAP block for the infraumbilical abdominal wall. If analgesia over the supraumbilical wall is required, subcostal, oblique subcostal, or dual TAP blocks are recommended. Adding continuous TAP block to single-injection TAP block can further improve and prolong its analgesic effect. Based on the accumulating evidence, dual guidance with ultrasound and half-the-air setting should be considered for TAP blocks.

Conflicts of Interest

The authors declare that there are no conflicts of interest regarding the publication of this paper.

Authors' Contributions

Jui-An Lin and Kung-Yen Chen contributed equally to this work.

Acknowledgments

This work was supported by Grants from Taipei Medical University, Taiwan (TMU101-AE1-B66) and Ministry of Science and Technology, Taiwan (MOST 104-2314-B-038 -016 -MY2). The authors acknowledge Editage for providing editorial assistance.

References

[1] A. N. Rafi, "Abdominal field block: a new approach via the lumbar triangle," *Anaesthesia*, vol. 56, no. 10, pp. 1024–1026, 2001.

[2] W. M. Rozen, T. M. N. Tran, M. W. Ashton, M. J. Barrington, J. J. Ivanusic, and G. I. Taylor, "Refining the course of the thoracolumbar nerves: A new understanding of the innervation of the anterior abdominal wall," *Clinical Anatomy*, vol. 21, no. 4, pp. 325–333, 2008.

[3] E. Brogi, R. Kazan, S. Cyr, F. Giunta, and T. M. Hemmerling, "Transversus abdominal plane block for postoperative analgesia: a systematic review and meta-analysis of randomized-controlled trials," *Canadian Journal of Anesthesia*, vol. 63, no. 10, pp. 1184–1196, 2016.

[4] R. Champaneria, L. Shah, J. Geoghegan, J. K. Gupta, and J. P. Daniels, "Analgesic effectiveness of transversus abdominis plane

blocks after hysterectomy: A meta-analysis," *European Journal of Obstetrics & Gynecology and Reproductive Biology*, vol. 166, no. 1, pp. 1–9, 2013.

[5] N. Elkassabany, M. Ahmed, S. B. Malkowicz, D. F. Heitjan, J. A. Isserman, and E. A. Ochroch, "Comparison between the analgesic efficacy of transversus abdominis plane (TAP) block and placebo in open retropubic radical prostatectomy: A prospective, randomized, double-blinded study," *Journal of Clinical Anesthesia*, vol. 25, no. 6, pp. 459–465, 2013.

[6] K. Peng, F.-H. Ji, H.-Y. Liu, and S.-R. Wu, "Ultrasound-Guided Transversus Abdominis Plane Block for Analgesia in Laparoscopic Cholecystectomy: A Systematic Review and Meta-Analysis," *Medical Principles and Practice*, vol. 25, no. 3, pp. 237–246, 2016.

[7] B. M. Mishriky, R. B. George, and A. S. Habib, "Transversus abdominis plane block for analgesia after Cesarean delivery: a systematic review and meta-analysis," *Canadian Journal of Anesthesia*, vol. 59, no. 8, pp. 766–778, 2012.

[8] N. T. Ventham, S. O'Neill, N. Johns, R. R. Brady, and K. C. H. Fearon, "Evaluation of novel local anesthetic wound infiltration techniques for postoperative pain following colorectal resection surgery: A meta-analysis," *Diseases of the Colon & Rectum*, vol. 57, no. 2, pp. 237–250, 2014.

[9] T. Gao, J.-J. Zhang, F.-C. Xi et al., "Evaluation of Transversus Abdominis Plane (TAP) block in hernia surgery," *The Clinical Journal of Pain*, vol. 33, no. 4, pp. 369–375, 2017.

[10] F. W. Abdallah, J. G. Laffey, S. H. Halpern, and R. Brull, "Duration of analgesic effectiveness after the posterior and lateral transversus abdominis plane block techniques for transverse lower abdominal incisions: a meta-analysis," *British Journal of Anaesthesia*, vol. 111, no. 5, pp. 721–735, 2013.

[11] A. Maeda, S. C. Shibata, T. Kamibayashi, and Y. Fujino, "Continuous subcostal oblique transversus abdominis plane block provides more effective analgesia than single-shot block after gynaecological laparotomy," *European Journal of Anaesthesiology*, vol. 32, no. 7, pp. 514-515, 2015.

[12] G. Niraj, A. Kelkar, E. Hart, V. Kaushik, D. Fleet, and J. Jameson, "Four quadrant transversus abdominis plane block and continuous transversus abdominis plane analgesia: A 3-year prospective audit in 124 patients," *Journal of Clinical Anesthesia*, vol. 27, no. 7, pp. 579–584, 2015.

[13] A. Maeda, S. C. Shibata, H. Wada et al., "The efficacy of continuous subcostal transversus abdominis plane block for analgesia after living liver donation: a retrospective study," *Journal of Anesthesia*, vol. 30, no. 1, pp. 39–46, 2016.

[14] E. Farag, M. N. Guirguis, M. Helou et al., "Continuous transversus abdominis plane block catheter analgesia for postoperative pain control in renal transplant," *Journal of Anesthesia*, vol. 29, no. 1, pp. 4–8, 2014.

[15] P. D. Hebbard, M. J. Barrington, and C. Vasey, "Ultrasound-guided continuous oblique subcostal transversus abdominis plane blockade: Description of anatomy and clinical technique," *Regional Anesthesia and Pain Medicine*, vol. 35, no. 5, pp. 436–441, 2010.

[16] G. Niraj, A. Kelkar, E. Hart et al., "Comparison of analgesic efficacy of four-quadrant transversus abdominis plane (TAP) block and continuous posterior TAP analgesia with epidural analgesia in patients undergoing laparoscopic colorectal surgery: an open-label, randomised, non-inferiority trial," *Anaesthesia*, vol. 69, no. 4, pp. 348–355, 2014.

[17] T. Yoshida, K. Furutani, Y. Watanabe, N. Ohashi, and H. Baba, "Analgesic efficacy of bilateral continuous transversus abdominis plane blocks using an oblique subcostal approach in patients undergoing laparotomy for gynaecological cancer: a prospective, randomized, triple-blind, placebo-controlled study," *British Journal of Anaesthesia*, vol. 117, no. 6, pp. 812–820, 2016.

[18] J. L. Hutchins, R. Kesha, F. Blanco, T. Dunn, and R. Hochhalter, "Ultrasound-guided subcostal transversus abdominis plane blocks with liposomal bupivacaine vs. Non-liposomal bupivacaine for postoperative pain control after laparoscopic hand-assisted donor nephrectomy: A prospective randomised observer-blinded study," *Anaesthesia*, vol. 71, no. 8, pp. 930–937, 2016.

[19] M. Fayezizadeh, A. Majumder, R. Neupane, H. L. Elliott, and Y. W. Novitsky, "Efficacy of transversus abdominis plane block with liposomal bupivacaine during open abdominal wall reconstruction," *The American Journal of Surgery*, vol. 212, no. 3, pp. 399–405, 2016.

[20] A. Hadzic, J. A. Abikhaled, and W. J. Harmon, "Impact of volume expansion on the efficacy and pharmacokinetics of liposome bupivacaine," *Local and Regional Anesthesia*, vol. 8, pp. 105–111, 2015.

[21] J. Hutchins, D. Delaney, R. I. Vogel et al., "Ultrasound guided subcostal transversus abdominis plane (TAP) infiltration with liposomal bupivacaine for patients undergoing robotic assisted hysterectomy: A prospective randomized controlled study," *Gynecologic Oncology*, vol. 138, no. 3, pp. 609–613, 2015.

[22] S. Ayad, R. Babazade, H. Elsharkawy et al., "Comparison of transversus abdominis plane infiltration with liposomal bupivacaine versus continuous epidural analgesia versus intravenous opioid analgesia," *PLoS ONE*, vol. 11, no. 4, Article ID e0153675, 2016.

[23] J. G. McDonnell, B. D. O'Donnell, T. Farrell et al., "Transversus Abdominis Plane Block: A Cadaveric and Radiological Evaluation," *Regional Anesthesia and Pain Medicine*, vol. 32, no. 5, pp. 399–404, 2007.

[24] "Abdomen study guide," in *Atlas of Human Anatomy*, F. H. Netter, Ed., pp. e62–e81, Elsevier, 6th edition, 2014, New York, USA.

[25] "The thoracic nerves," in *Gray's Anatomy (Illustrated With 1247 Coloured Well Drawing Engrawings): [Autobiography & Book's History & Index Added]*, H. Gray, Ed., pp. 287–290, eKitap Projesi, Istanbul, Turkey, 2016.

[26] M. Desmet, D. Helsloot, E. Vereecke, C. Missant, and M. Van De Velde, "Pneumoperitoneum Does Not Influence Spread of Local Anesthetics in Midaxillary Approach Transversus Abdominis Plane Block: A Descriptive Cadaver Study," *Regional Anesthesia and Pain Medicine*, vol. 40, no. 4, pp. 349–354, 2015.

[27] J. Carney, O. Finnerty, J. Rauf, D. Bergin, J. G. Laffey, and J. G. Mc Donnell, "Studies on the spread of local anaesthetic solution in transversus abdominis plane blocks," *Anaesthesia*, vol. 66, no. 11, pp. 1023–1030, 2011.

[28] M. J. Fredrickson, C. Paine, and J. Hamill, "Improved analgesia with the ilioinguinal block compared to the transversus abdominis plane block after pediatric inguinal surgery: a prospective randomized trial," *Pediatric Anesthesia*, vol. 20, no. 11, pp. 1022–1027, 2010.

[29] A. Stav, L. Reytman, M. Stav et al., "Transversus Abdominis Plane Versus Ilioinguinal and Iliohypogastric Nerve Blocks for Analgesia Following Open Inguinal Herniorrhaphy," *Rambam Maimonides Medical Journal*, vol. 7, no. 3, p. e0021, 2016.

[30] K. Stoving, C. Rothe, C. V. Rosenstock, E. K. Aasvang, L. H. Lundstrom, and K. H. W. Lange, "Cutaneous sensory block area, muscle-relaxing effect, and block duration of the transversus abdominis plane block: a randomized, blinded, and placebo-controlled study in healthy volunteers," *Regional Anesthesia and Pain Medicine*, vol. 40, no. 4, pp. 355–362, 2015.

[31] S. M. Moeschler, N. S. Murthy, B. C. Hoelzer, H. M. Gazelka, R. H. Rho, and M. J. Pingree, "Ultrasound-guided transversus abdominis plane injection with computed tomography correlation: a cadaveric study," *Journal of Pain Research*, vol. 6, pp. 493–496, 2013.

[32] M. J. Barrington, J. J. Ivanusic, W. M. Rozen, and P. Hebbard, "Spread of injectate after ultrasound-guided subcostal transversus abdominis plane block: A cadaveric study," *Anaesthesia*, vol. 64, no. 7, pp. 745–750, 2009.

[33] J. Gadsden, S. Ayad, J. J. Gonzales, J. Mehta, J. Boublik, and J. Hutchins, "Evolution of transversus abdominis plane infiltration techniques for postsurgical analgesia following abdominal surgeries," *Local and Regional Anesthesia*, vol. 8, pp. 113–117, 2015.

[34] Z. Milan, D. Tabor, P. McConnell et al., "Three different approaches to Transversus abdominis planeblock: a cadaveric study," *Medicinski Glasnik*, vol. 8, no. 2, pp. 181–184, 2011.

[35] R. V. Sondekoppam, J. Brookes, L. Morris, M. Johnson, and S. Ganapathy, "Injectate spread following ultrasound-guided lateral to medial approach for dual transversus abdominis plane blocks," *Acta Anaesthesiologica Scandinavica*, vol. 59, no. 3, pp. 369–376, 2015.

[36] M. Weintraud, P. Marhofer, A. Bösenberg et al., "Ilioinguinal/iliohypogastric blocks in children: where do we administer the local anesthetic without direct visualization?" *Anesthesia & Analgesia*, vol. 106, no. 1, pp. 89–93, 2008.

[37] Z. B. Jankovic, F. M. Du Feu, and P. McConnell, "An anatomical study of the transversus abdominis plane block: Location of the lumbar triangle of petit and adjacent nerves," *Anesthesia & Analgesia*, vol. 109, no. 3, pp. 981–985, 2009.

[38] T. M. N. Tran, J. J. Ivanusic, P. Hebbard, and M. J. Barrington, "Determination of spread of injectate after ultrasound-guided transversus abdominis plane block: A cadaveric study," *British Journal of Anaesthesia*, vol. 102, no. 1, pp. 123–127, 2009.

[39] K. Takimoto, N. Sakai, and M. Ono, "The effects of adding upper and lower subcostal transversus abdominis plane blocks to a lateral transversus abdominis plane block after laparoscopic cholecystectomy: A randomised, double-blind clinical trial," *European Journal of Anaesthesiology*, vol. 32, no. 11, pp. 819-820, 2015.

[40] P. Hebbard, "Subcostal transversus abdominis plane block under ultrasound guidance," *Anesthesia & Analgesia*, vol. 106, no. 2, pp. 674-675, 2008.

[41] T. H. W. Lee, M. J. Barrington, T. M. N. Tran, D. Wong, and P. D. Hebbard, "Comparison of extent of sensory block following posterior and subcostal approaches to ultrasound-guided transversus abdominis plane block," *Anaesthesia and Intensive Care*, vol. 38, no. 3, pp. 452–460, 2010.

[42] S. Yoshiyama, H. Ueshima, R. Sakai, and H. Otake, "A posterior tap block provides more effective analgesia than a lateral tap block in patients undergoing laparoscopic gynecologic surgery: a retrospective study," *Anesthesiology Research and Practice*, vol. 2016, Article ID 4598583, 9 pages, 2016.

[43] G. Niraj, A. Kelkar, and A. J. Fox, "Oblique sub-costal transversus abdominis plane (TAP) catheters: An alternative to epidural analgesia after upper abdominal surgery," *Anaesthesia*, vol. 64, no. 10, pp. 1137–1140, 2009.

[44] M. Abrahams, R. Derby, and J.-L. Horn, "Update on ultrasound for truncal blocks: a review of the evidence," *Regional Anesthesia and Pain Medicine*, vol. 41, no. 2, pp. 275–288, 2016.

[45] H. Ueshima, H. Otake, and J.-A. Lin, "Ultrasound-guided quadratus lumborum block: an updated review of anatomy and techniques," *BioMed Research International*, vol. 2017, Article ID 2752876, 7 pages, 2017.

[46] J. Borglum, F. W. Abdallah, J. G. McDonnell, B. Moriggl, and T. F. Bendtsen, "TAP block terminology," *Anaesthesia*, vol. 69, no. 9, pp. 1055-1056, 2014.

[47] J. Borglum, C. Maschmann, B. Belhage, and K. Jensen, "Ultrasound-guided bilateral dual transversus abdominis plane block: A new four-point approach," *Acta Anaesthesiologica Scandinavica*, vol. 55, no. 6, pp. 658–663, 2011.

[48] J. Borglum, K. Jensen, A. F. Christensen et al., "Distribution patterns, dermatomal anesthesia, and ropivacaine serum concentrations after bilateral dual transversus abdominis plane block," *Regional Anesthesia and Pain Medicine*, vol. 37, no. 3, pp. 294–301, 2012.

[49] P. Hebbard, "TAP block nomenclature," *Anaesthesia*, vol. 70, no. 1, pp. 112-113, 2015.

[50] P. D. Hebbard, "Transversalis fascia plane block, a novel ultrasound-guided abdominal wall nerve block," *Canadian Journal of Anesthesia*, vol. 56, no. 8, pp. 618–620, 2009.

[51] S. Lee, T. Goetz, and A. Gharapetian, "Unanticipated Motor Weakness with Ultrasound-Guided Transversalis Fascia Plane Block," *A & A case reports*, vol. 5, no. 7, pp. 124-125, 2015.

[52] Z. Zietek, K. Starczewski, T. Sulikowski et al., "Useful points of geometry and topography of the lumbar triangle for transversus abdominis plane block," *Medical Science Monitor*, vol. 21, pp. 4096–4101, 2015.

[53] P. M. Hopkins, "Ultrasound guidance as a gold standard in regional anaesthesia," *British Journal of Anaesthesia*, vol. 98, no. 3, pp. 299–301, 2007.

[54] H. Ueshima, K. Kubo, S. Sakamoto et al., "A case of the transversus abdominis plane block in a super obese patient using a convex probe," *Masui (The Japanese Journal of Anesthesiology)*, vol. 62, no. 4, pp. 439–441, 2013.

[55] M. Wassef, D. Y. Lee, J. L. Levine et al., "Feasibility and analgesic efficacy of the transversus abdominis plane block after single-port laparoscopy in patients having bariatric surgery," *Journal of Pain Research*, vol. 6, pp. 837–841, 2013.

[56] P. Hebbard, Y. Fujiwara, Y. Shibata, and C. Royse, "Ultrasound-guided transversus abdominis plane (TAP) block," *Anaesthesia and Intensive Care*, vol. 35, no. 4, pp. 616-617, 2007.

[57] Y. Shibata, Y. Sato, Y. Fujiwara, and T. Komatsu, "Transversus abdominis plane block [15]," *Anesthesia & Analgesia*, vol. 105, no. 3, p. 883, 2007.

[58] J.-A. Lin and H.-T. Lu, "Solution to the challenging part of the Shamrock method during lumbar plexus block," *British Journal of Anaesthesia*, vol. 113, no. 3, pp. 516-517, 2014.

[59] J. A. Lin, "Importance of half-the-air pressure test in Shamrock lumbar plexus block," *European Journal of Anaesthesiology*, vol. 33, no. 10, p. 784, 2016.

[60] J.-A. Lin and H.-T. Lu, "A convenient alternative for monitoring opening pressure during multiple needle redirection," *British Journal of Anaesthesia*, vol. 112, no. 4, pp. 771-772, 2014.

[61] C. K. Chen, P. C. S. Tan, V. E. Phui, and S. C. Teo, "A comparison of analgesic efficacy between oblique subcostal

transversus abdominis plane block and intravenous morphine for laparascopic cholecystectomy. a prospective randomized controlled trial," *Korean Journal of Anesthesiology*, vol. 64, no. 6, pp. 511–516, 2013.

[62] A. Mukherjee, R. Guhabiswas, S. Kshirsagar, and E. Rupert, "Ultrasound guided oblique subcostal transversus abdominis plane block: An observational study on a new and promising analgesic technique," *Indian Journal of Anaesthesia*, vol. 60, no. 4, pp. 284–286, 2016.

[63] B. Basaran, A. Basaran, B. Kozanhan, E. Kasdogan, M. A. Eryilmaz, and S. Ozmen, "Analgesia and respiratory function after laparoscopic cholecystectomy in patients receiving ultrasound-guided bilateral oblique subcostal transversus abdominis plane block: A randomized double-blind study," *Medical Science Monitor*, vol. 21, pp. 1304–1312, 2015.

[64] H.-J. Shin, A.-Y. Oh, J.-S. Baik, J.-H. Kim, S.-H. Han, and J.-W. Hwang, "Ultrasound-guided oblique subcostal transversus abdominis plane block for analgesia after laparoscopic cholecystectomy: A randomized, controlled, observer-blinded study," *Minerva Anestesiologica*, vol. 80, no. 2, pp. 185–193, 2014.

[65] J.-A. Lin, T. Nakamoto, and S.-D. Yeh, "Ultrasound standard for obturator nerve block: the modified Taha's approach," *British Journal of Anaesthesia*, vol. 114, no. 2, pp. 337–339, 2015.

[66] J.-A. Lin, Y.-J. Lee, H.-T. Lu, and Y.-T. Lin, "Ultrasound standard for popliteal sciatic block: Circular expansion of the paraneural sheath with the needle in-plane fromlateral-to-medial in the 'reverse Sim's position'," *British Journal of Anaesthesia*, vol. 115, no. 6, pp. 938–940, 2015.

[67] J.-A. Lin, H.-T. Lu, and T.-L. Chen, "Ultrasound standard for lumbar plexus block," *British Journal of Anaesthesia*, vol. 113, no. 1, pp. 188-189, 2014.

[68] T. S. Pintaric, E. Cvetko, M. Strbenc et al., "Intraneural and perineural inflammatory changes in piglets after injection of ultrasound gel, endotoxin, 0.9% NaCl, or needle insertion without injection," *Anesthesia & Analgesia*, vol. 118, no. 4, pp. 869–873, 2014.

[69] P. L. Petersen, K. L. Hilsted, J. B. Dahl, and O. Mathiesen, "Bilateral transversus abdominis plane (TAP) block with 24 hours ropivacaine infusion via TAP catheters: A randomized trial in healthy volunteers," *BMC Anesthesiology*, vol. 13, article no. 30, 2013.

[70] M. Farooq and M. Carey, "A case of liver trauma with a blunt regional anesthesia needle while performing transversus abdominis plane block," *Regional Anesthesia and Pain Medicine*, vol. 33, no. 3, pp. 274-275, 2008.

[71] P. Lancaster and M. Chadwick, "Liver trauma secondary to ultrasound-guided transversus abdominis plane block," *British Journal of Anaesthesia*, vol. 104, no. 4, pp. 509-510, 2010.

[72] Z. Jankovic, N. Ahmad, N. Ravishankar, and F. Archer, "Transversus abdominis plane block: How safe is it?" *Anesthesia & Analgesia*, vol. 107, no. 5, pp. 1758-1759, 2008.

[73] V. Scherrer, V. Compere, C. Loisel, and B. Dureuil, "Cardiac arrest from local anesthetic toxicity after a field block and transversus abdominis plane block: a consequence of miscommunication between the anesthesiologist and surgeon," *A & A Case Reports*, vol. 1, no. 5, pp. 75-76, 2013.

[74] R. K. Naidu and P. Richebe, "Probable local anesthetic systemic toxicity in a postpartum patient with acute Fatty liver of pregnancy after a transversus abdominis plane block," *A & A Case Reports*, vol. 1, no. 5, pp. 72–74, 2013.

[75] D. K. Manatakis, N. Stamos, C. Agalianos, M. A. Karvelis, M. Gkiaourakis, and D. Davides, "Transient femoral nerve palsy complicating "blind" transversus abdominis plane block," *Case Reports in Anesthesiology*, vol. 2013, Article ID 874215, 3 pages, 2013.

[76] E. Weiss, C. Jolly, J.-L. Dumoulin et al., "Convulsions in 2 patients after bilateral ultrasound-guided transversus abdominis plane blocks for cesarean analgesia," *Regional Anesthesia and Pain Medicine*, vol. 39, no. 3, pp. 248–251, 2014.

[77] T. Sakai, W. Manabe, T. Kamitani, E. Takeyama, and S. Nakano, "Ropivacaine-induced late-onset systemic toxicity after transversus abdominis plane block under general anesthesia: successful reversal with 20% lipid emulsion," *Masui (The Japanese Journal of Anesthesiology)*, vol. 59, no. 12, pp. 1502–1505, 2010.

[78] G. Walker, "Transversus abdominis plane block: a note of caution!," *British Journal of Anaesthesia*, vol. 104, no. 2, p. 265, 2010.

[79] A. Hadzic, F. Dilberovic, S. Shah et al., "Combination of intraneural injection and high injection pressure leads to fascicular injury and neurologic deficits in dogs," *Regional Anesthesia and Pain Medicine*, vol. 29, no. 5, pp. 417–423, 2004.

[80] E. Kapur, I. Vuckovic, F. Dilberovic et al., "Neurologic and histologic outcome after intraneural injections of lidocaine in canine sciatic nerves," *Acta Anaesthesiologica Scandinavica*, vol. 51, no. 1, pp. 101–107, 2007.

[81] J. C. Gadsden, J. J. Choi, E. Lin, and A. Robinson, "Opening injection pressure consistently detects needle-nerve contact during ultrasound-guided interscalene brachial plexus block," *Anesthesiology*, vol. 120, no. 5, pp. 1246–1253, 2014.

Hindawi
BioMed Research International
Volume 2017, Article ID 7920438, 17 pages
https://doi.org/10.1155/2017/7920438

Research Article

Transition from Deep Regional Blocks toward Deep Nerve Hydrodissection in the Upper Body and Torso: Method Description and Results from a Retrospective Chart Review of the Analgesic Effect of 5% Dextrose Water as the Primary Hydrodissection Injectate to Enhance Safety

Stanley K. H. Lam,[1,2,3] Kenneth Dean Reeves,[4] and An-Lin Cheng[5]

[1]*Department of Family Medicine, Faculty of Medicine, The Chinese University of Hong Kong, Sha Tin, Hong Kong*
[2]*KH Lam Musculoskeletal Pain Management and Sports Injury Centre, Kowloon, Hong Kong*
[3]*The Hong Kong Institute of Musculoskeletal Medicine, Tsuen Wan, Hong Kong*
[4]*Private Practice PM&R and Pain Management, Roeland Park, KS, USA*
[5]*Department of Biomedical and Health Informatics, University of Missouri-Kansas City School of Medicine, Kansas City, MO, USA*

Correspondence should be addressed to Stanley K. H. Lam; drlamkh@gmail.com

Received 16 December 2016; Revised 19 March 2017; Accepted 24 July 2017; Published 1 October 2017

Academic Editor: Jui-An Lin

Deep nerve hydrodissection uses fluid injection under pressure to purposely separate nerves from areas of suspected fascial compression, which are increasingly viewed as potential perpetuating factors in recalcitrant neuropathic pain/complex regional pain. The usage of 5% dextrose water (D5W) as a primary injectate for hydrodissection, with or without low dose anesthetic, could limit anesthetic-related toxicity. An analgesic effect of 5% dextrose water (D5W) upon perineural injection in patients with chronic neuropathic pain has recently been described. Here we describe ultrasound-guided methods for hydrodissection of deep nerve structures in the upper torso, including the stellate ganglion, brachial plexus, cervical nerve roots, and paravertebral spaces. We retrospectively reviewed the outcomes of 100 hydrodissection treatments in 26 consecutive cases with a neuropathic pain duration of 16 ± 12.2 months and the mean Numeric Pain Rating Scale (NPRS) 0–10 pain level of 8.3 ± 1.3. The mean percentage of analgesia during each treatment session involving D5W injection without anesthetic was 88.1% $\pm$ 9.8%. The pretreatment Numeric Pain Rating Scale score of 8.3 ± 1.3 improved to 1.9 ± 0.9 at 2 months after the last treatment. Patients received 3.8 ± 2.6 treatments over 9.7 ± 7.8 months from the first treatment to the 2-month posttreatment follow-up. Pain improvement exceeded 50% in all cases and 75% in half. Our results confirm the analgesic effect of D5W injection and suggest that hydrodissection using D5W provides cumulative pain reduction.

1. Introduction

Deep regional blocks have been used for years to provide perioperative anesthesia for surgery and postoperative pain control [1]. In the management of patients with chronic pain, such as those with complex regional pain syndrome (CRPS) and postherpetic neuralgia, deep regional blocks, for example, stellate ganglion blocks (SGBs), serve as an alternative to other medical treatments. The mechanism of action of deep regional blocks or repeated peripheral focal nerve blocks for neuropathic pain remains unclear [2]. A benefit from repeated depolarization by a local anesthetic was originally proposed; however, the effects of this method with regard to the normalization of nerve physiology have not been confirmed [2]. More recently, the concept has emerged that fascial compression of nerves can occur in multiple locations and that part of the benefit of deep regional blocks may be through partial amelioration of fascial compression [3]. Nerve hydrodissection is a technique involving the use of fluid injection under pressure to purposely and more completely separate nerves from their surrounding tissue [4]. Ultrasound is used to guide the needles and fluid (hydro) is used to separate and release (dissect) the nerves from the surrounding soft tissue/fascia.

Potential safety concerns with any perineural injection method using an anesthetic include temporary muscular weakness and loss of protective sensation [5]. The rate of inadvertent intraneural injection under ultrasound guidance approximates 16%-17% [6, 7], although long-term sequelae appear to be quite rare [6, 7]. Furthermore, inadvertent intravascular injection may occur because of the frequent close proximity of nerves and vessels. Injection of a high volume of anesthetic for hydrodissection is associated with an increased risk of both dose-related systemic anesthetic toxicity and inadvertent intravascular injection. The use of 5% dextrose water (D5W) as the primary injectate for perineural injection during hydrodissection in the presence of chronic pain, particularly neuropathic pain, is receiving increasing attention [8–12]. D5W is also considered for use as a coadministration injectate along with noxious agents such as chemotherapeutics [13, 14] and microbiospheres [15] to decrease pain, as well as a means to separate nerves from fascia while decreasing the risk of anesthetic toxicity [16]. An independent-of-anesthetic analgesic potential of D5W has been demonstrated in a recent randomized controlled trial of epidural D5W injection versus saline injection for patients with back pain accompanied by either buttock or leg pain [17], with potential long-term efficacy suggested by long-term follow-up data in those patients [18].

2. Objectives

Although low-level studies have demonstrated the effectiveness of nerve hydrodissection, no high-level studies have been reported [4]. Performance of high-level studies will be facilitated by procedural methods that are reproducibly performed, consistent in clinical effect and safe. The objectives of this study were to illustrate reproducible methods of hydrodissection for deep nerve structures in the upper torso, including the stellate ganglion, brachial plexus, cervical nerve roots, and paravertebral spaces and gather preliminary data related to the analgesic effect and efficacy of D5W without lidocaine as the primary injectate during hydrodissection for patients with chronic neuropathic pain.

3. Materials and Methods

A formal letter of exemption allowing retrospective chart review was obtained from the International Cellular Medicine Society Institutional Review Board (ICMS-IRB). We reviewed consecutive outpatient charts for patients who underwent hydrodissection of the stellate ganglion, brachial plexus, cervical nerve roots, or paravertebral spaces for the management of pain with neuropathic characteristics. Videos and still photographs of these patients were all deidentified for use. Charts were consecutively reviewed to identify participants who received hydrodissection exclusively with D5W, with the use of lidocaine only for the placement of skin blebs. Chart selection continued until data from 100 treatments was available for analysis. Methods of hydrodissection utilized for these consecutively recruited patients were illustrated with the use of both anatomical diagrams and ultrasound images.

Neuropathic pain, for the purpose of this write-up, was defined in standard fashion as pain arising as a direct consequence of a lesion or disease affecting the somatosensory system either at the peripheral or at central level [19, 20]. Neuropathic pain is commonly characterized by allodynia, hyperalgesia, and/or changes in temperature sensation (e.g., burning or cold pain); the extent of the pain does not typically correspond to the extent of the nervous structure damage.

Ultrasound findings were not useful for the diagnosis of neuropathic pain unless the cervical nerve roots and brachial plexus were scanned. In case of unilateral lesions, a comparison of the cross-sectional area and echotextures of cervical nerve roots or the brachial plexus on the painful side with those on the contralateral side without pain generally showed that the painful side was larger in cross-sectional area [21].

The decision to hydrodissect was based on the following factors.

(1) A clinical diagnosis indicating that a neurogenic pain source is likely and knowledge of the corresponding involved deep nerve structures in patients with neuropathic pain, for example, dermatomes of the nerves involved in patients with postherpetic neuralgia

(2) Awareness of the effects of compression on the function of peripheral nerves

(3) Knowledge of all potential sites of compression of peripheral nerves, for example, the radial nerve at entry to and exit from the radial tunnel

(4) Experience regarding the appearance of peripheral nerves when they are encased in fascia, obtained by observing the "plumping up" of nerves upon freeing them from the surrounding fascial encasement

(5) Confidence to proceed with a higher volume of perineural injection in the absence of a risk of lidocaine toxicity, considering the lidocaine component is absent or negligible

Hydrodissection involved consistent fluid injection at all times during needle advancement, ostensibly to push away any small nerve fibers and avoid pain during advancement. This eliminated the need for anesthetic injection. Because fluid always leads needle advancement during hydrodissection and pushes away nerve structures, vessels, and other soft tissues, this technique, if performed properly, prevents soft tissue damage by the needle. Without inclusion of a local anesthetic, typical signs of motor blockade, such as Horner's syndrome, were not expected during stellate ganglion infiltration. Accordingly, the primary endpoint was pain reduction. Typically, 20–30 ml of fluid was utilized for each area of hydrodissection.

Adequacy of a particular hydrodissection procedure was based on patient symptoms, because visualization of fluid surrounding the nerve is only directly observable during hydrodissection of the brachial plexus and cervical nerve roots. In our experience, the analgesic effect of dextrose occurs within 5 min after deep regional hydrodissection for a variety of chronic neuropathic pain conditions. Accordingly, 5 min after completion of the initial procedure, the pain was rated on a 0–10 Numeric Pain Rating Scale (NPRS) using the question "how much pain do you have?" A score of 0 represented "no pain" and a score of 10 represented the "most severe pain imaginable." If the pain was rated as 3/10 or less, the reported score was considered to represent the postprocedural pain level. If residual pain was rated as 4/10 or more, another regional procedure that was reasonably expected to affect the region of pain was performed, and pain was rated again at 5 min after the procedure. This process was repeated for up to three pertinent procedures, and the final pain level was that following the last hydrodissection procedure. The same sequence was performed during follow-up visits.

The primary measure for a potential intraprocedural analgesic effect of D5W hydrodissection was the mean difference between pretreatment and immediate (5 min) posttreatment NPRS scores.

Routine follow-up procedure in the primary investigator's office was to contact patients at 2 months after treatment to inquire about any further need for treatment and verbally obtain a final NPRS score to monitor the treatment efficacy. Data were analyzed using PASW 18 (Predictive Analytics Software 18.0.0, IBM Corporation, 1 New Orchard Road, Armonk, New York 10504-1722). Descriptive statistics (means ± standard deviations) were reported at baseline and at each time point for NPRS scores.

The cumulative improvement in pain levels over time was determined by calculating the mean difference between pretreatment NPRS scores and those obtained at 2 months after the last treatment visit. The proportion of patients who achieved more than 50% and more than 75% pain reduction was calculated.

3.1. Description of Hydrodissection Procedures by Area

3.1.1. Stellate Ganglion Hydrodissection

Applications. The stellate ganglion is part of the sympathetic network formed by the inferior cervical and first thoracic ganglia. It lies anterolateral to the C7 vertebral body (Figure 1), receives input from the paravertebral sympathetic chain, and provides sympathetic efferents to the upper extremities, head, neck, and heart. During pain management for CRPSs, particularly type I reflex sympathetic dystrophy (RSD) [22, 23], postherpetic neuralgia [24, 25], and chronic pain of the head and neck [26, 27] or thorax, a local anesthetic solution is injected as a local block for the stellate ganglion. Posttraumatic stress disorder [28, 29] may also be seen in these patients [30, 31]. Accordingly, its presence or absence was recorded, although the symptomatology was not assessed in the present study. Other applications of SGBs, such as vascular insufficiency and hyperhidrosis, were not within the scope of this study.

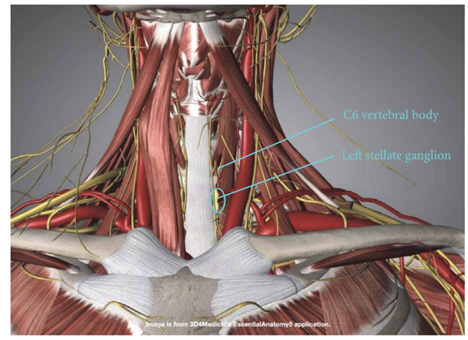

Figure 1: Longitudinal location of the stellate ganglion. The stellate ganglion is located at the level of the C7 vertebral body.

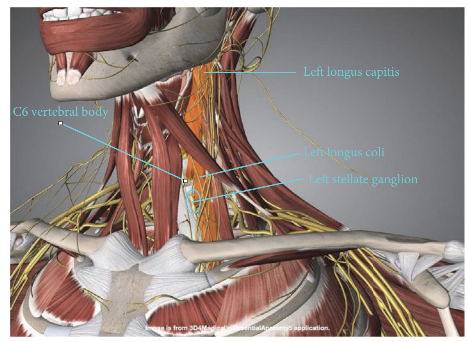

Figure 2: Relationship of the stellate ganglion to the longus colli. The stellate ganglion lies anterolateral to the C7 vertebral body and in the prevertebral fascia on the surface of the longus colli.

Nonhydrodissection Methods. A consecutive patient study described the efficacy and safety of using ultrasound to guide needles for SGB without the use of a high-volume technique [32]. Ultrasound guidance helps in the visualization of soft tissues to prevent complications and the subfascial deposition of the drug under direct vision [32, 33].

Primary Ultrasound Landmarks for Hydrodissection. The anterior tubercle of the C6 vertebral body, known as the Chassaignac tubercle or carotid tubercle, is an important landmark located superior to the stellate ganglion. C7 does not have an anterior tubercle, while the anterior tubercle of C5 is less prominent. Therefore, the anterior tubercle of C6 can be easily found. Identification of the longus colli is also key (Figure 2), as a cadaveric study using dye and clinical validation has shown adequate spread of the anesthetic solution to the stellate ganglion using a technique in which the needle tip is deep to the prevertebral fascia to avoid spread along the carotid sheath and superficial to the fascia investing the longus colli to avoid injection into the muscle substance [34].

Patient Position. The patient is supine, with a rolled towel underneath the neck for slight extension and another thin pillow or rolled towel beneath the ipsilateral shoulder for slight rotation of the head to the side contralateral to the point of needle entry (Figure 3).

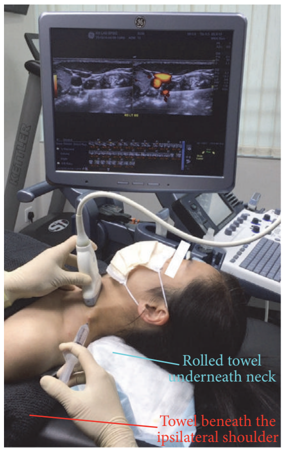

Figure 3: Procedure for stellate ganglion hydrodissection: patient positioning. Neck support, ipsilateral shoulder elevation, and probe and needle positions for stellate ganglion hydrodissection.

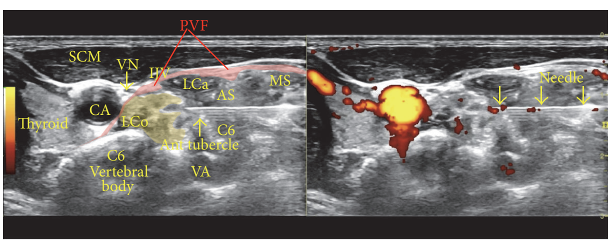

Figure 4: Procedure for stellate ganglion hydrodissection: sonoanatomy. The figure shows labeled structures, with the needle just past the anterior tubercle of C6. AS: anterior scalene, CA: carotid artery, IJV: internal jugular vein, LCa: Longus Capitis, LCo: longus colli, MS: middle scalene, PVF: prevertebral fascia, SCM: sternocleidomastoid, VN: vagus nerve, and VA: vertebral artery.

Probe Position. Probe placement is transverse to the neck. A lateral to medial in-plane approach is used, with the needle orientation slightly posterior to anterior (Figure 3).

Sonoanatomy. Figure 4 shows a dual sonographic image (left, B-mode; right, power Doppler) depicting the sonoanatomy and a sonographic view of the needle just past the anterior tubercle of the C6 vertebra (superior to the C6 nerve root and inferior to the C5 nerve root).

Needle Advancement/Injection. Visualize the hypoechoic nerve roots situated between the anterior and posterior tubercles of the transverse processes of the cervical vertebrae. Locate the longus colli and the anterior tubercle of C6 and the C6 nerve root. It is essential to follow the basic principle of hydrodissection; that is, the fluid opens the channel or space in front of the needle tip, and the needle just follows. Advance the needle (Figure 5(a)) and stop advancing when the tip reaches the prevertebral fascia superficial to the longus colli (Figure 5(b)). After reaching the prevertebral fascia, turn the bevel of the needle down so that the injectate will push down the soft tissues in front of and beneath the needle. The idea is to use the force of the injectate to open a potential space between the prevertebral fascia and the longus colli. The tracking of the fluid beneath the prevertebral fascial can be further observed by turning the probe 90 degrees to show a sagittal image. Upon continued hydrodissection the fluid will be seen tracking caudally to reach the stellate ganglion (Figure 5(c)). Video 1 (in Supplementary Material available online at https://doi.org/10.1155/2017/7920438) shows the procedure for stellate ganglion hydrodissection.

Treatment Frequency. The effects may last from one to a few weeks depending on the severity of the symptoms. Typically, after 3–6 repeated treatments at 4–6-week intervals, the patient's pain will be relieved to a satisfactory level.

3.1.2. Brachial Plexus Hydrodissection

Applications. Brachial plexus block is used for regional anesthesia during upper extremity surgery (arm, elbow, forearm, wrist, and hand) [35]. In chronic pain management, ultrasound-guided hydrodissection of the brachial plexus has been used to treat severe neck sprains (brachial plexus injury without rupture; it is only used to treat neuropraxia with or without axonotmesis) with radiating pain to the ipsilateral upper limb [36], CRPS [37] involving the ipsilateral upper limb, and thoracic outlet syndrome or other double/triple crush syndromes involving the ipsilateral upper limb [38].

General Approaches and Selection of the Right Approach. There are four different approaches/sites to perform brachial plexus hydrodissection: interscalene, supraclavicular [39], infraclavicular, and axillary [40]. Each approach has its own unique advantages and indications. Interscalene blocks are the most effective for anesthesia of the shoulder and proximal upper limb, while supraclavicular blocks are best suited for anesthesia from the mid-humerus to the fingers. Infraclavicular blocks are useful for procedures requiring continuous anesthesia, and axillary blocks provide effective anesthesia distal to the elbow. During brachial plexus hydrodissection for chronic pain management, the interscalene or supraclavicular approaches are typically used because these are two very common entrapment points for the brachial plexus [41]. The choice of approach depends on how proximal the cause of the neuropathic pain is. If the entrapment/neurological injuries are at the cervical root levels, interscalene brachial plexus hydrodissection is recommended. If the cause of the neuropathic pain is at the trunk or division level of the brachial plexus or if there is an excessive upward movement of the shaft of the first rib due to excessive pulling of the anterior and middle scalene, supraclavicular brachial plexus hydrodissection may provide better relief.

3.2. Interscalene Approach

Muscular Landmarks. The anterior, middle, and posterior scalenes are identified (Figure 6). The interscalene brachial plexus is generally formed by the C5, C6, C7, and C8 nerve roots. The needle is inserted in a direction posterior to anterior and lateral to medial, and it passes through the middle scalene to reach the interscalene brachial plexus.

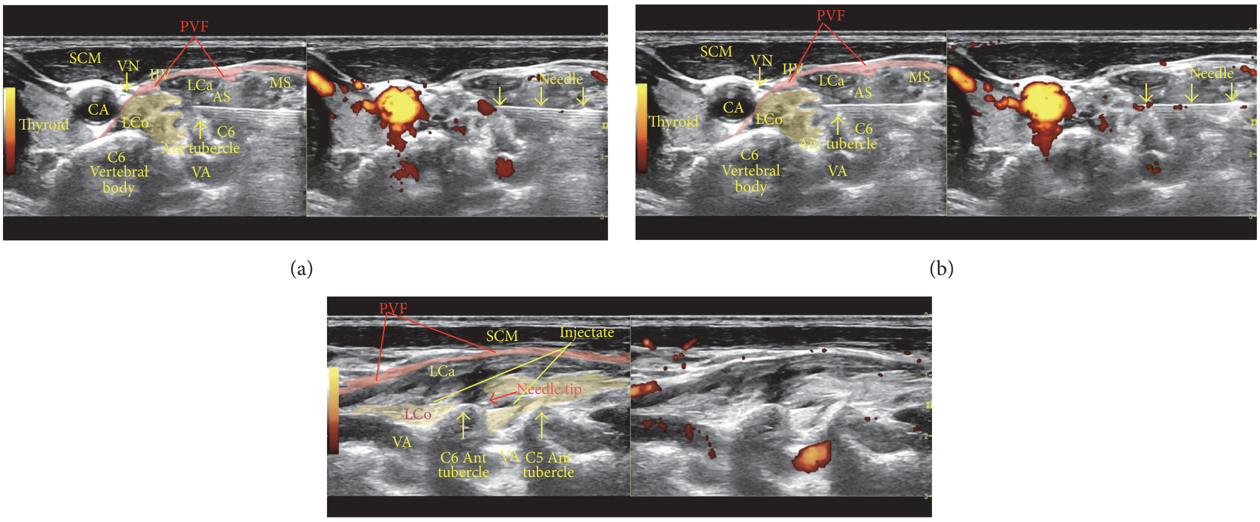

(a)

(b)

(c)

Figure 5: (a) Procedure for stellate ganglion hydrodissection: nearing the tip of the C6 anterior tubercle. Once the longus colli, anterior tubercle of C6, and the C6 nerve root are identified, advance the needle, with the bevel downwards, just ventral to the tip of the anterior tubercle of C6. AS: anterior scalene, CA: carotid artery, IJV: internal jugular vein, LCa: Longus Capitis, LCo: longus colli, MS: middle scalene, PVF: prevertebral fascia, SCM: sternocleidomastoid, VN: vagus nerve, and VA: vertebral artery. (b) Procedure for stellate ganglion hydrodissection: in the prevertebral fascia, superficial to the longus colli. Continue injecting (hydrodissecting) while advancing the needle to allow the fluid to open a channel for the needle when it is approaching in a direction from lateral to medial and posterior to anterior and passing through the middle scalene and in the space between the C5 and C6 nerve roots to approach the prevertebral fascia superficial to the longus colli. Stop advancing when the needle tip reaches the fascia, usually just anterior to the anterior tubercle of C6. (c) Procedure for stellate ganglion hydrodissection: observation of fluid tracking using sagittal images. The image shows the probe turned 90° to observe a sagittal image through the needle tip, which is next to the anterior tubercle of C6 at the insertion of the longus colli, for observation of fluid tracking in the prevertebral fascia superficial to the longus colli. The fluid will track down anterolaterally to the C7 vertebral body and reach the stellate ganglion.

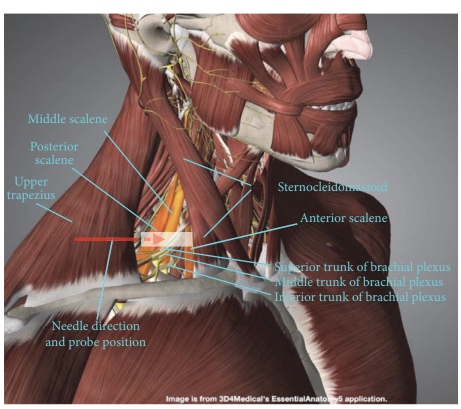

Figure 6: Procedure for interscalene brachial plexus hydrodissection: gross anatomy. Muscular landmarks, probe position, and needle orientation during interscalene brachial plexus hydrodissection.

Figure 7: Procedure for interscalene brachial plexus hydrodissection: patient positioning. Neck support, ipsilateral shoulder elevation, and probe and needle positions for interscalene brachial plexus hydrodissection.

Patient and Probe Positions. The patient is supine, with a rolled towel underneath the neck for slight extension and the head is straight up or slightly rotated to the side contralateral to the point of needle entry (Figure 7). The probe is transverse to the neck.

Sonoanatomy. Visualize the scalenes and the hypoechoic oval nerve roots of C5–C8, which are situated between the anterior and middle scalenes. The pertinent sonoanatomy is shown in Figure 8.

Needle Advancement/Injection (Figures 9(a)–9(c)). An in-plane approach is used, with the needle advancing in a

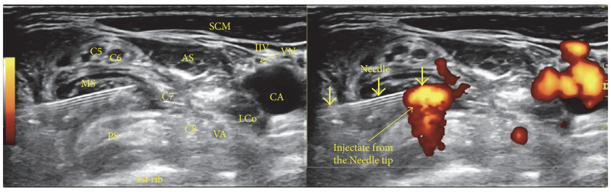

Figure 8: Procedure for interscalene brachial plexus hydrodissection: sonoanatomy. The image shows needle penetration through the middle scalene, with hydrodissection and fluid injection in the interscalene brachial plexus. AS: anterior scalene, CA: carotid artery, IJV: internal jugular vein, LCo: longus colli, MS: middle scalene, PS: posterior scalene, SCM: sternocleidomastoid, VA: vertebral artery, and VN: vagus nerve.

direction from posterior to anterior and lateral to medial (Figures 6 and 7). At the interscalene level, the cervical nerve roots start to form the superior trunk (C5/6), middle trunk (C7), and inferior trunk (C8/T1). The fascial sheath for these trunks is formed from the fascia of the surrounding scalenes. To perform interscalene brachial plexus hydrodissection, one needle entry point is typically used, and the needle should hydrodissect its way into the fascial sheath of each trunk. Once inside the fascial sheath, the injectate will surround the trunk effectively, although occasionally, hydrodissection above and below becomes necessary to separate the fascia from the trunk. Figure 9(d) shows visualization of the injectate during hydrodissection, and video 2 shows the procedure for interscalene brachial plexus hydrodissection.

3.3. Supraclavicular Approach. The anterior and middle scalenes may be traced to their insertions on the first rib, and the entire brachial plexus will gather on top of the first rib as the supraclavicular brachial plexus, lateral to the subclavian artery (Figures 10 and 11).

Patient and Probe Positions. The patient is supine, with a rolled towel underneath the neck for slight extension and another thin pillow or layers of towel beneath the ipsilateral shoulder for slight rotation of the entire trunk and neck to the side contralateral to the point of needle entry (Figure 11). The probe is transverse to the trunk and nearly parallel to the clavicle. An in-plane approach is used, with the needle advancing in a direction from posterior to anterior and lateral to medial.

Sonoanatomy. Visualize the brachial plexus gathered on top of the first rib, with the subclavian artery on the medial side (Figure 12).

Needle Advancement and Hydrodissection. Visualize the brachial plexus gathered on top of the first rib, with the subclavian artery on the medial side. Figures 13(a)–13(c) show sequential needle placement for hydrodissection below, above, and between portions of the supraclavicular brachial plexus. If the patient achieves good pain relief with hydrodissection below and above the brachial plexus, a third-needle placement does not appear to be necessary. Figure 13(d) shows the anechoic injectate during hydrodissection, and video 3 shows the procedure for supraclavicular brachial plexus hydrodissection.

3.3.1. Cervical Nerve Root Hydrodissection

Indications. Selective cervical nerve root blocks play an important role in the conservative treatment of patients with cervical radicular pain [42]. In chronic pain management, hydrodissection of selective cervical nerve roots has been used to treat patients with postherpetic neuropathic pain involving the dermatome of specific cervical nerve roots, patients with postradiation neuritis, and patients with nerve compression from fibrosis of the neck muscles.

Bony Landmarks. Bony landmarks include the hyperechoic anterior and posterior tubercles of the cervical vertebra, noting that C7 has no anterior tubercle and C8 has no anterior or posterior tubercle. Figure 14 shows the cross-sectional anatomy at the C6 level for C6 root hydrodissection.

Patient and Probe Positions. The patient is supine, with the neck straight or slightly tilted to the contralateral side. The probe is transverse to the neck (Figures 15 and 16). An in-plane approach is used, with the needle advancing in a direction from posterior to anterior and lateral to medial.

Sonoanatomy. Figure 17 is a snapshot showing the needle passing between the middle and posterior scalenes or, in some cases, only through the middle scalene. The needle tip is almost touching the posterior tubercle of the C6 transverse process.

Needle Advancement and Hydrodissection. Visualize the hypoechoic nerve roots situated between the anterior and posterior tubercles of the transverse processes of the cervical vertebrae. As illustrated in the representative image of C6 nerve root hydrodissection (Figure 18), the needle tip stops at the posterior tubercle to hydrodissect the soft tissue around the C6 nerve roots to the point where the injectate surrounds the entire nerve root. Typically, 20–30 ml of D5W is used to achieve satisfactory pain relief with fluid surrounding the nerve root. Exercise caution during C7 cervical nerve root hydrodissection, because C7 does not have an anterior tubercle. Ensure that power Doppler view is switched on to avoid mistaking the vertebral artery for the C7 nerve root. Figure 18(d) shows the anechoic injectate after hydrodissection of the C6 nerve root, and video 4 shows the procedure for C6 nerve root hydrodissection.

3.3.2. Paravertebral Hydrodissection

General Indications. Paravertebral block involves injection of a local anesthetic in a space immediately lateral to the point of emergence of the spinal nerves from the intervertebral foramina. This technique is increasingly being used for both intra- and postoperative analgesia and as a sole anesthetic technique for various procedures. Its popularity is mainly attributed to the ease of performance and lower complication rate when compared with techniques using catheters.

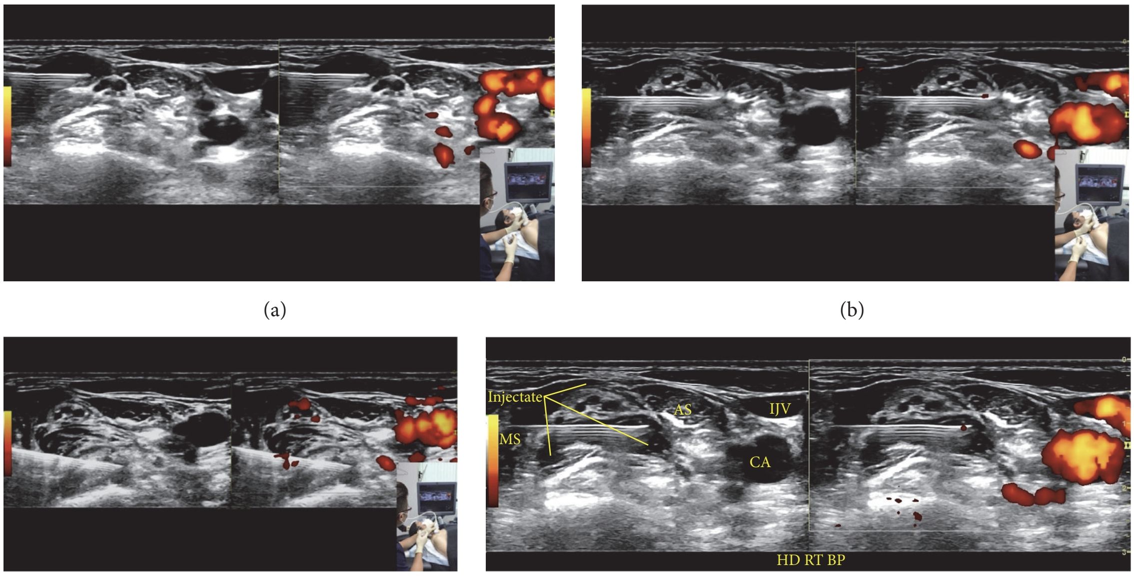

(a) (b) (c) (d)

Figure 9: (a) Procedure for interscalene brachial plexus hydrodissection: upper trunk. Needle positioning for hydrodissection of the C5 and C6 nerve roots/upper trunk. (b) Procedure for interscalene brachial plexus hydrodissection: middle trunk. Needle positioning for hydrodissection of the C7 nerve root/middle trunk. (c) Procedure for interscalene brachial plexus hydrodissection: lower trunk. Needle positioning for hydrodissection of the C8/T1 nerve root/lower trunk. (d) Procedure for interscalene brachial plexus hydrodissection: visualization of the injectate. Visualization of the injectate during hydrodissection of the middle trunk.

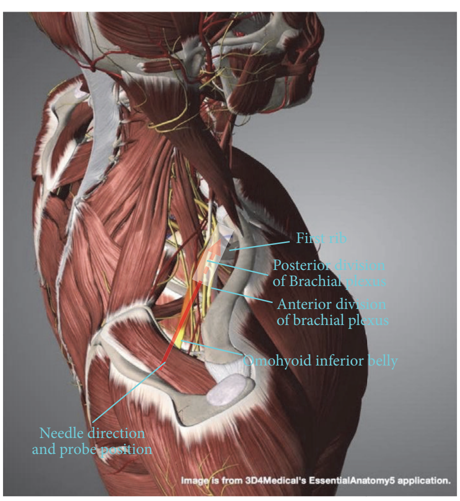

Figure 10: Procedure for supraclavicular brachial plexus hydrodissection: gross anatomy. Gross anatomy and needle direction for supraclavicular brachial plexus hydrodissection.

Figure 11: Procedure for supraclavicular brachial plexus hydrodissection: patient positioning. Neck support, ipsilateral shoulder elevation, and probe and needle positions for supraclavicular brachial plexus hydrodissection.

Hydrodissection Applications. In our experience, paravertebral hydrodissection has been observed to result in analgesia in patients who present with acute herpes zoster, prevent the development of postherpetic neuralgia, and benefit patients with established postherpetic neuralgia. This analgesic effect is consistently noted within 5 min of procedure completion and is often noted within seconds. It peaks within 30 min, maintains its peak for 2–4 h, and declines over 48 h, with a common residual effect of 10%–20% at 4 weeks.

Pictorial Anatomy. The target of this technique has been postulated to be the wedge-shaped paravertebral space whose boundaries were defined by Klein et al. [43] using a small (2.3 mm) fiber optic scope. These boundaries include the parietal pleura ventrolaterally; heads of the ribs, transverse process, and superior costotransverse ligament dorsally; and vertebra, intervertebral discs, and intervertebral foramina medially. There is a lateral extension in continuity with the intercostal space (Figure 19). A single injection into this

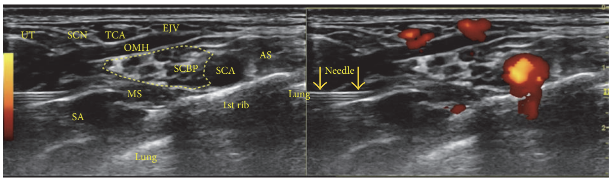

Figure 12: Procedure for supraclavicular brachial plexus hydrodissection: sonoanatomy. Sonographic view of the needle approaching the supraclavicular brachial plexus. AS: anterior scalene, EJV: external jugular vein, MS: middle scalene, OMH: omohyoid, SA: serratus anterior, SCA: subclavian artery, SCBP: supraclavicular brachial plexus, SCN: supraclavicular nerve, TCA: transverse cervical artery, and UT: upper trapezius.

space accesses not only the ventral and dorsal rami but also the sympathetic chain and gray rami communicantes. The advantage of using ultrasound guidance for injection into the paravertebral space has been described by Batra et al. [44].

Patient and Probe Positions. The patient is prone, with a rolled towel or pillow underneath the chest to increase the degree of thoracic kyphosis (Figure 20). The probe position is transverse to the trunk, parallel to the ribs above, and below the transverse process.

Pertinent Sonoanatomy. Figure 21(a) shows the surrounding structures when the transducer is placed immediately caudal to the costotransverse joint. Because the probe has a width and all the three-dimensional information scanned beneath the probe will be processed by the computer to be presented as a two-dimensional image on the monitor, the tip of the transverse process, which is not in the same plane of the needle and injection, will often appear as if it is in the same plane, providing additional information to confirm the costotransverse ligament position through visualization of its superomedial origin on the transverse process.

Needle Advancement and Hydrodissection. Hydrodissect while advancing the needle through the external and internal intercostals (Figure 21(a)). A 22-gauge needle is preferable to a 25-gauge needle, because a 22-gauge needle may provide a feeling of penetration. Stop advancing when penetration is felt or when the needle tip is observed to just pass through the costotransverse ligament (Figure 21(b)). With the needle tip beneath the lateral tip of the transverse process, further hydrodissection should be accompanied by visualization of the parietal pleura pushing away to confirm paravertebral space injection (Figure 21(c)). The fluid should then be able to access the nerve root and dorsal root ganglion, which are the targets for chronic pain control, considering the pleura forms the floor of the paravertebral space. Video 5 shows the procedure for paravertebral space hydrodissection.

Treatment of two to three levels of the paravertebral nerve roots is generally necessary for complete pain relief. To determine the thoracic spinal level by ultrasound, a paramedian sagittal view with the transducer in cross section to the transverse processes of the thoracic vertebrae and ribs is utilized to count down from the first rib or up from the twelfth rib. Video 6 explains how to use ultrasound to count the levels of the thoracic spinal nerves.

Empirically, one to two treatments are required for acute pain relief, with the second administered after rash subsidence to prevent the development of postherpetic neuralgia. In patients with established postherpetic neuralgia, pain scores will drop to 0–3/10 or to a tolerable level immediately after each injection and gradually increase thereafter, albeit with some cumulative effect. Four to six injections typically result in pain scores of 1-2/10.

4. Results

4.1. Retrospective Data Collection. Figure 22 depicts the flow chart for data selection in this retrospective study. In total, 30 consecutive patients who received D5W as the primary injectate during hydrodissection for neuropathic pain in the upper body were included. Of these, five patients requested the use of lidocaine in the injectate at some point during their treatment course because of injection discomfort. The remaining 25 patients (26 cases after considering two treatment sides in the patient with bilateral treatment) received lidocaine only for the placement of subcutaneous anesthetic blebs to numb the needle entry point. Data for 100 consecutive hydrodissection sessions performed in these 26 cases was collected by telephonic follow-up at 2 months after the last treatment session. Data capture was 100% up to the 2-month follow-up time point. All procedures were performed in Hong Kong at the office of the primary author between March 31, 2015, and December 29, 2016.

4.2. Demographics. Baseline demographics for the 26 cases are shown in Table 1. The sex distribution was even and the patients were middle-aged. The pain duration was 6 months or more except three with acute zoster pain (3 days, 3 days, and 1 week, resp.) and two with acute thoracic outlet symptoms (1 month each). Baseline pain was moderately severe to severe in this group. Only 1 patient rated their pain as less than 8.0.

4.3. Selection of Treatment Method according to the Primary Diagnosis and Area of Pain. Table 2 lists the number of cases with each primary diagnosis. Multiple diagnoses were frequent; diagnoses other than the primary diagnosis are mentioned in parentheses in the column titled "neuropathic pain areas." The hydrodissection method was selected on the basis of the area of neuropathic pain and the other diagnoses.

4.4. Intrasession Effects of D5W. The consistency of postprocedural analgesia was strong. The minimum degree of pain reduction for the 100 procedures was 69%, with 35 procedures resulting in 100% pain reduction. The mean degree of pain reduction at 5 min after the last injection was administered across all 100 treatment sessions for the 26 cases was $88.1 \pm 9.8\%$.

4.5. Cumulative Effects of D5W. From baseline to the 2-month posttreatment follow-up, a total of 3.8 ± 2.6 treatments were performed over 9.7 ± 7.8 months. Figure 23 is a graph

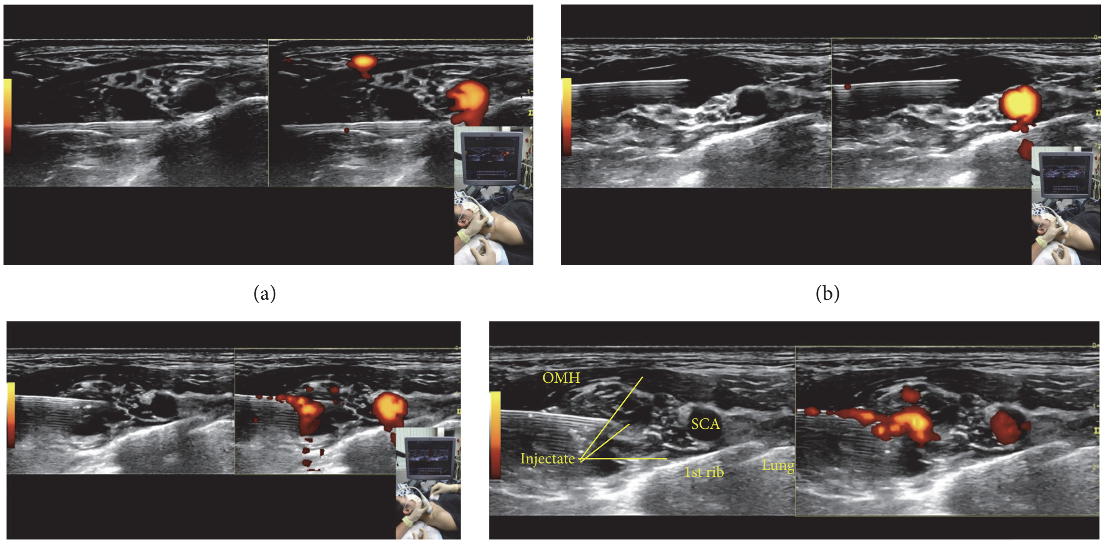

Figure 13: (a) Procedure for supraclavicular brachial plexus hydrodissection: first position. Needle positioning for hydrodissection of the bottom of the supraclavicular brachial plexus. (b) Procedure for supraclavicular brachial plexus hydrodissection: second position. Needle positioning for hydrodissection of the top of the supraclavicular brachial plexus. (c) Procedure for supraclavicular brachial plexus hydrodissection: third position. Needle positioning for hydrodissection of the middle of the supraclavicular brachial plexus. (d) Procedure for supraclavicular brachial plexus hydrodissection: visualization of the injectate. The image shows the anechoic injectate.

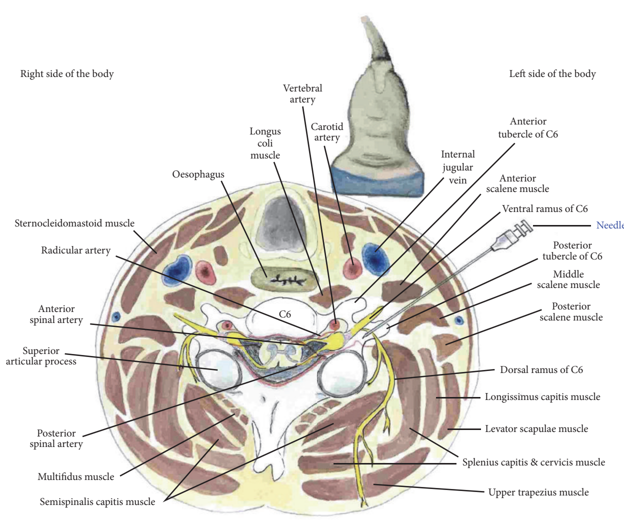

Figure 14: Procedure for cervical nerve root hydrodissection: cross-sectional anatomy. Cross-sectional anatomy at the C6 level.

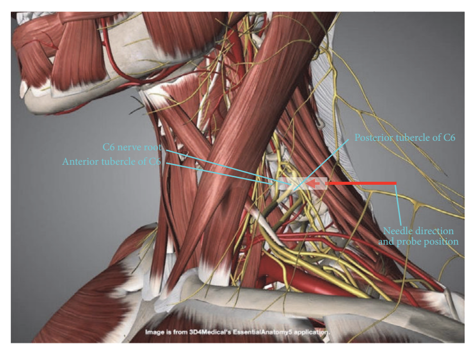

Figure 15: Procedure for cervical nerve root hydrodissection: gross anatomy. Gross anatomy and probe and needle directions for supraclavicular brachial plexus hydrodissection. The probe position is indicated by the white rectangle.

showing changes in pain levels over time for all 26 cases. Each line represents the changes in the mean NPRS over time for cases that received the same number of treatments. For example, the middle line shows the findings for two cases that received four treatments. When all 26 cases were combined for analysis, the mean NPRS improved from 8.3 ± 1.3 before treatment to 1.9 ± 09 after treatment, with an improvement of 6.4 ± 1.7 points. The degree of pain improvement exceeded 50% in all cases and 75% in 50% (13/26).

Table 1: Baseline demographics. These 26 cases (25 patients, with one receiving treatment bilaterally) represent 100 consecutive hydrodissection procedures.

Baseline demographics (n = 26)	
Female, n (% of procedures)	13 (50%)
Age years, mean (SD)	51 ± 14.7
Pain duration months, mean (SD)	16 ± 12.2
NRS pain prior to 1st injection, mean (SD)	8.3 ± 1.3

4.6. Effects of D5W Hydrodissection on Patients with Acute Pain. Of the 26 cases, 21 had pain for more than 6 months and five had pain for less than 2 months. Cases of acute

Figure 16: Procedure for cervical nerve root hydrodissection: patient positioning. Neck support, ipsilateral shoulder elevation, and probe and needle positions for cervical nerve root hydrodissection.

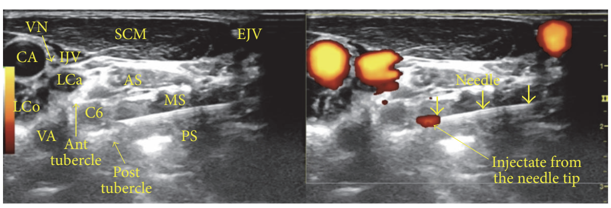

Figure 17: Procedure for cervical nerve root hydrodissection: sonoanatomy. Ant: anterior, Post: posterior, AS: anterior scalene, MS: middle scalene, PS: posterior scalene, CA: carotid artery, IJV: internal jugular vein, EJV: external jugular vein, VA: vertebral artery, SCM: sternocleidomastoid, VN: vagus nerve, LCa: Longus Capitis, and LCo: longus colli. The left side shows a B-mode image and the right side shows a power Doppler view.

pain received only one treatment, and the degree of pain reduction 5 minutes after the last injection was 97.0% ± 6.9% in cases of acute pain and 87.7% ± 9.8% in cases of chronic pain ($p = .04$). The mean improvement in NPRS at the 2-month posttreatment follow-up was 5.8 ± 1.9 points for cases of acute pain (8.0 ± 1.3 to 2.2 ± 0.7) and 6.5 ± 1.7 points for cases of chronic pain ($p = .385$).

5. Discussion

In the present study, we proposed and illustrated potentially reproducible methods of hydrodissection of the stellate ganglion, brachial plexus, cervical nerve roots, and paravertebral spaces. Salient methods common to all approaches included the following.

(1) One method is use of a skin bleb to eliminate pain at the point of needle entry.

(2) Another method is use of a 22- to 25-gauge needle, with minimization of the probe to needle angle and an emphasis on a needle in-plane approach to maximize needle visibility.

(3) Another one is constant hydrodissection, with marked reduction of any discomfort through dissection of soft tissue in front of the needle to lead the needle, rather than splitting of the soft tissue by the needle itself, as well as further improvement of needle tip visualization.

(4) Another method is an emphasis on D5W use without lidocaine to eliminate any possibility of intravascular anesthetic injection during the hydrodissection procedure.

If an anesthetic is preferred by a patient because of discomfort, a mixture of D5W and a low dose anesthetic, for example, 0.1%–0.2% lidocaine, can be injected along the needle track before the target area is reached, followed by a switch to D5W alone so that a higher volume can be instilled for the bulk of the hydrodissection procedure for the target nerve structures. However, although small doses of lidocaine may help in increasing patient comfort, the physician is advised to limit lidocaine application during stellate ganglion hydrodissection because of potential changes in vagal modulation and baroreceptor sensitivity [45] and during deep cervical plexus hydrodissection because of potential effects on the recurrent laryngeal nerve, particularly if the patient has an unrecognized baseline dysfunction of the contralateral recurrent laryngeal nerve or if bilateral hydrodissection is required [46].

(5) One of them is slow needle advancement, which allows the injectate to dissect the tissue layer by layer until the nerve/plexus is reached, with emphasis on precise visualization of the needle tip when the needle is approaching nerves and blood vessels.

(6) Another one is fluid delivery above and below the nerve for more complete hydrodissection.

This should preferably start just below the nerve, because if there is any air in the injectate, the acoustic shadow of the air will not block the view.

This retrospective data collection provides preliminary data which supports a consistent analgesic effect of D5W across a variety of neuropathic pain conditions and a cumulative benefit of repeated D5W hydrodissection. An important observation was that the onset speed of analgesia was fast enough that pain relief could be used to determine whether the procedure was sufficiently complete. The effect of D5W injection in patients with chronic neuropathic pain in the present study was similar, in both the speed of onset and magnitude of analgesic effect, to that in a recent randomized controlled trial of D5W versus saline injection in the epidural space of patients with chronic low back pain with various etiologies [17]. In that study, saline exhibited no analgesic effects. Moreover, the cumulative effect of repeated D5W hydrodissection was consistent with that in a prospective trial of epidural D5W injection [18]. However, the follow-up period in the present study was only 2 months after treatment completion. A prospective study with a long-term follow-up period and preferably including a control group is necessary to confirm our findings. The study should be of sufficient size to effectively compare treatment outcomes between patients with acute pain and those with chronic pain.

The mechanism of action of dextrose-induced analgesia is not clear, although research supports several hypotheses. First, dextrose may act at the level of pain receptors. Chronic neuropathic pain is associated with persistent upregulation of the transient receptor potential vanilloid receptor-1 (TRPV1)

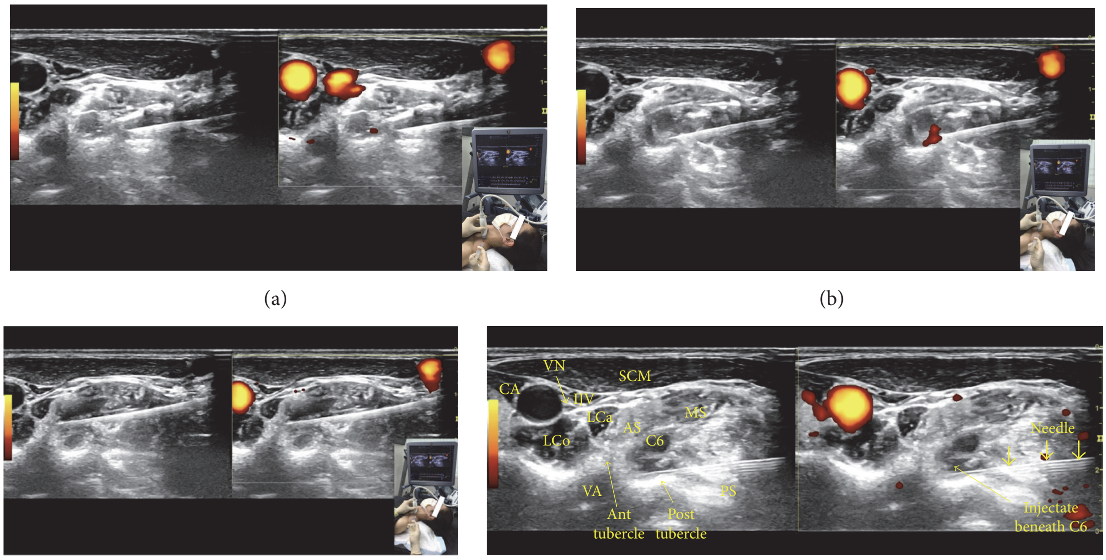

(a) (b) (c) (d)

FIGURE 18: (a) Procedure for C6 nerve root hydrodissection: position one. Hydrodissection while approaching the C6 nerve root. (b) Procedure for C6 nerve root hydrodissection: position two. Needle positioning for hydrodissection dorsal to the C6 nerve root. (c) Procedure for C6 nerve root hydrodissection: position three. Needle positioning for hydrodissection ventral to the C6 nerve root. (d) Procedure for C6 nerve root hydrodissection: visualization of the injectate. The image shows the anechoic injectate after C6 nerve root hydrodissection.

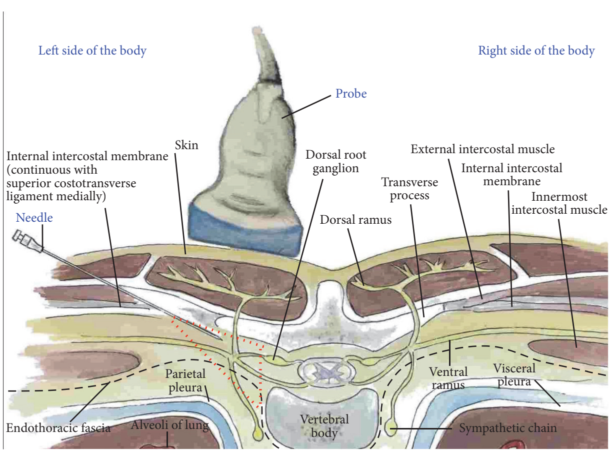

FIGURE 19: Procedure for paravertebral hydrodissection: cross-sectional anatomy. The red dashed triangle is an approximation of the paravertebral space.

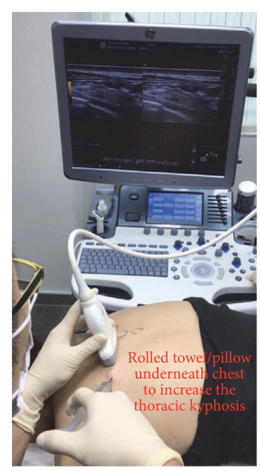

FIGURE 20: Procedure for paravertebral hydrodissection: patient positioning. Rounded back and needle and probe positions for thoracic paravertebral hydrodissection.

ion channel [47], which is upregulated by capsaicin. Mannitol (an analog of dextrose) application to the lip reduced the burning pain associated with capsaicin application in a lip pain model [48], and in our experience, dextrose has a similar effect. A class effect of sugars to indirectly reduce the effects of TRPV1 receptor activation is proposed, because neither dextrose nor mannitol has a known binding point to the TRPV1 receptor [49].

Second, extracellular dextrose elevation may hyperpolarize normoglycemic C fibers, lowering their firing rate. Dextrose elevation to 0.5% (from the normal blood level of 0.1) in the intestinal lumen rapidly results in hyperpolarization of enterocytic cell membranes to facilitate transport across the cell membrane by sodium glucose cotransporter (SGLT1) [50]. In peripheral nerves, the primary glucose transport is via glucose transporter one, not SGLT1 [51]. However, SGLT1 is still present on neuronal cell membranes [51]. The effect of a 50-fold increase in extracellular dextrose (D5W) on SGLT activity in normoglycemic C fibers has not been directly studied. However, recent reports on the coadministration of D5W to decrease the pain from infusion of chemotherapeutic

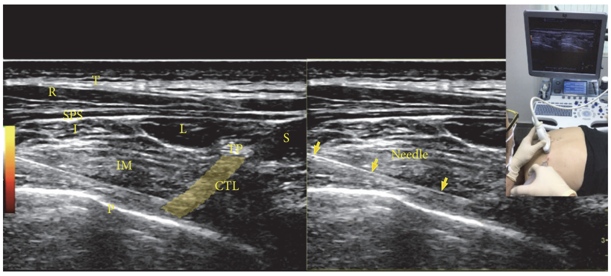

(a)

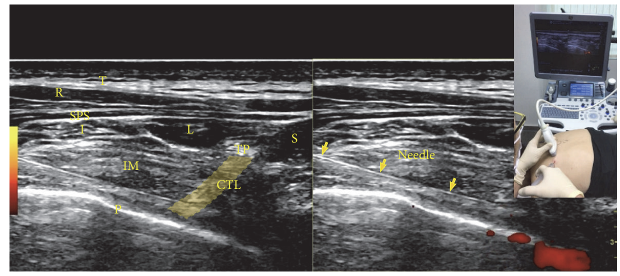

(b)

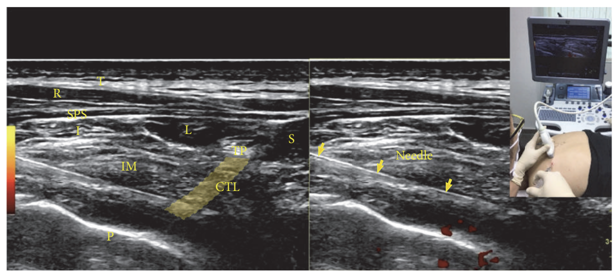

(c)

Figure 21: (a) Procedure for paravertebral hydrodissection: needle approaching the paravertebral space. CTL: costotransverse ligament, I: iliocostalis, IM: intercostal muscles, L: longissimus, P: pleura, R: rhomboid, S: spinalis, T: trapezius, SPS: serratus posterior superior, and TP: inferior edge of the transverse process as observed by volume averaging. The yellow band is centered over the costotransverse ligament. The yellow solid arrows show the needle. (b) Procedure for paravertebral hydrodissection: needle tip through the costotransverse ligament. Stop advancing the needle just as the tip passes the costotransverse ligament. (c) Procedure for paravertebral hydrodissection: visualization of the pleura. Pleura being pushed away by fluid.

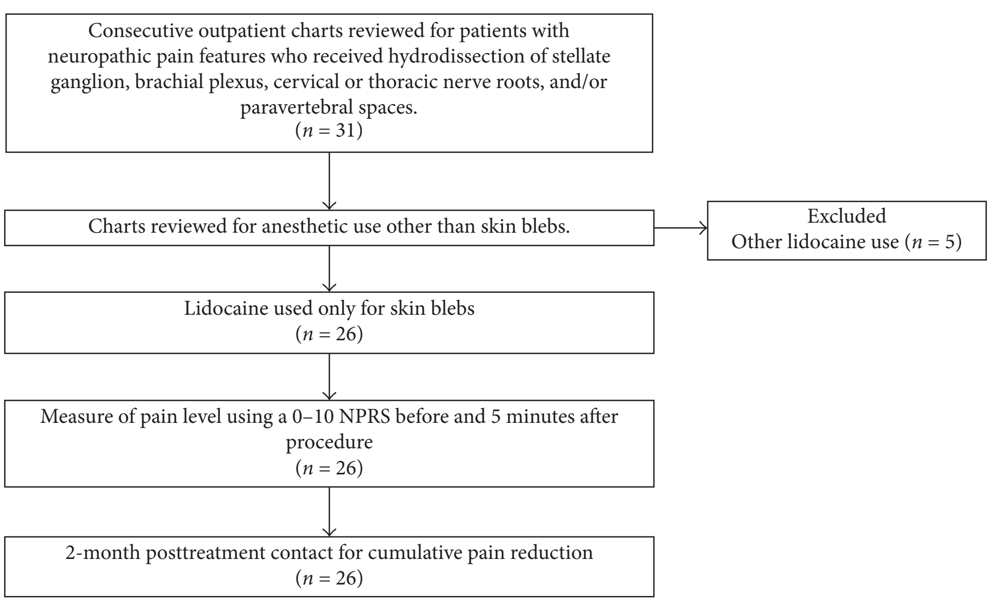

Figure 22: Flowchart for data collection. Retrospective data collection diagram.

agents [13, 14] or microspheres [15] point to a potential analgesic effect in normoglycemic subjects, although the mechanism remains to be confirmed.

Third, dextrose may reverse a proposed energy-deficient state of neuropathic nerves. A decrease in blood dextrose of only 25% (1.5 mM) from the normal fasting range in rats is reported to initiate histopathological changes in the peripheral nervous system [52] long before blood levels that will initiate brain damage in the rat [53] or brain dysfunction in humans [54] are reached. We propose that pain is an alarm signal produced by nociceptive C fibers which begins promptly upon development of intraneural hypoglycemia, prior to onset of histopathologic changes in the C fiber. Maclver and Tanelian [55] studied action potential changes

Table 2: Diagnoses, neuropathic pain regions, and hydrodissection performed for 26 cases in 25 patients.

n[a]	Primary diagnosis	Neuropathic pain areas (other diagnoses)	Regional hydrodissection[a]				
			PV[b]	SG[c]	SCBP[d]	ISBP[e]	CR[f]
3	Cervical root compression	Neck and arm			2	3	3
2	Cervical root compression	Neck					2
1	Postherpetic neuralgia	Neck					1
3	Postherpetic neuralgia	Chest	3				
3	Acute herpes zoster	Neck					1
3	Acute herpes zoster	Chest	2				
2	Thoracic outlet syndrome	Arm			2		
1	Thoracic outlet syndrome	Arm (panic attacks)[g]		1	1		
1	Thoracic outlet syndrome	Arm (triple crush syndrome)			1		
1	Thoracic outlet syndrome	Neck and arm (double crush syndrome) (cervical radiculopathy)			1		1
1	Neuropathic pain in the head and neck region	Head and neck (PTSD)[h]		1			
1	Neuropathic pain in the head and neck region	Head and neck (PTSD) (panic attacks)		1			
1	Cervicogenic headache	Head and neck (PTSD) (panic attacks)		1			
1	Stretch injury to the brachial plexus	Arm and hand (PTSD) (CRPS)		1	1		
1	Chronic regional pain syndrome (CRPS)	Arm and hand (double crush syndrome)		1	1		
1	Neuropathic pain in the thoracic region	Thorax (after rib fracture)	1				
1	Neuropathic pain in the thoracic region	Thorax (after electric shock)	1				
1	Neuropathic pain in the arm	Neck, arm, and hand			1	1	1
1	Cervical sprain	Neck and arm		1	1		

[a]n = number of cases with the same combination of diagnoses. Not all cases with the same diagnoses underwent hydrodissection in the same region. The number of cases receiving a given hydrodissection type is listed in each column under the main column titled "Regional hydrodissection." [b]PV = paravertebral hydrodissection, typically performed for neuropathic pain in the thoracic region. [c]SG = stellate ganglion hydrodissection, typically performed for CRPS and other chronic neuropathic pain conditions involving the head and neck region. [d]SCBP = supraclavicular brachial plexus hydrodissection, typically performed for CRPS, other chronic neuropathic pain conditions involving the ipsilateral upper limb, and double crush syndrome involving the ipsilateral upper limb. [e]ISCP = interscalene brachial plexus hydrodissection, typically performed for CRPS and other chronic neuropathic pain conditions involving the ipsilateral upper limb, particularly areas closer to the nerve roots. [f]CR = cervical root hydrodissection, typically performed for nerve root compression of any kind and neuropathic pain involving specific nerve roots. [g]Although panic attacks were not a primary diagnosis, they were recorded because of their frequent exacerbation by chronic pain and treatment by stellate ganglion hydrodissection. [h]PTSD = posttraumatic stress disorder, which was not the primary diagnosis but was recorded because of its frequent association with chronic pain and treatment by stellate ganglion hydrodissection.

in response to hypoglycemia in C fibers of the New Zealand White rabbit cornea in vitro and noted an increase in the C fiber discharge frequency of 653% ± 28% relative to that in a normoglycemic control within 15 min of hypoglycemia onset, followed by rapid return to normal firing levels after the administration of dextrose.

The theoretical basis for the clinical benefits of hydrodissection is compelling. Bennett and Wie developed an animal model of neuropathic pain caused by chronic constriction injury, which is widely utilized and involves the application of a ligature that is barely snug around the sciatic nerve [56]. Specific recommendations for the induction of neuropathic pain are as follows: use a high-power objective lens to observe the flow of red blood cells in the epineural vasculature and tie the ligature just tight enough for the flow to slow down without stopping or tighten the ligature so that it will

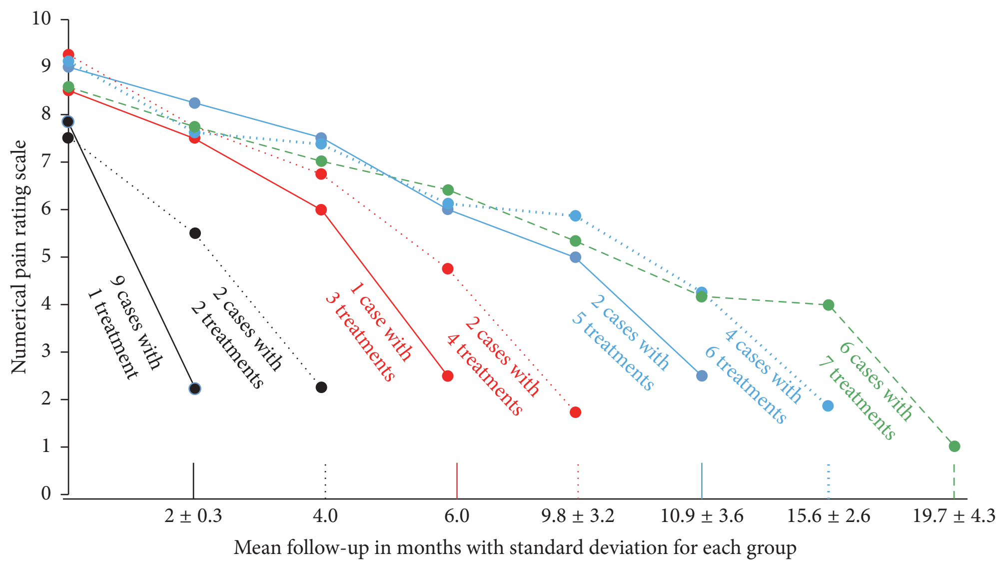

Figure 23: Graph showing the time course of changes in pain caused by hydrodissection with 5% dextrose water for chronic neuropathic pain. Time course of changes in 0–10 NPRS for all 26 cases (25 patients; one underwent bilateral treatment) grouped according to the number of treatment sessions. The last dot on each line represents the final pain score obtained by telephonic interview at 2 months after the last treatment session. The other dots at the beginning and along each line represent the mean pain scores for that group at each point during treatment.

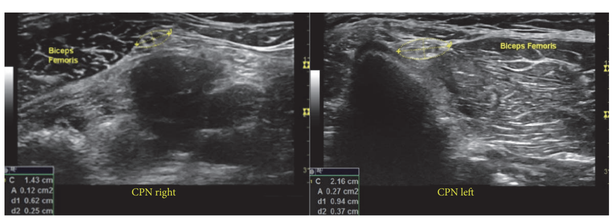

Figure 24: Illustration of a swollen nerve. The left image shows the left common fibular (peroneal) nerve at the level of the biceps femoris (knee). The larger right common fibular nerve is seen on the right side. The area was calculated using ultrasound measurement tools.

slide along the nerve, but not smoothly. The result is the development of a neural swelling, typically within 24 h, on both sides of the ligature, accompanied by classic findings of neuropathic pain such as hyperalgesia, allodynia, and, frequently, dysesthesia [56]. A similar swelling of nerves, accompanied by a graded compromise in the vascular nerve supply, is notable on high-resolution ultrasound examinations and is strongly associated with nerve compression, such as that occurring in carpal tunnel syndrome [57]. Ultrasound examination of peripheral nerves in the presence of neuropathic pain commonly demonstrates an increase in individual nerve fascicle size, an increase in neural volume, or, typically, both [21]. An example is shown in Figure 24, which depicts the smaller left and larger right common fibular (peroneal) nerve at the level of the knee in the same patient (symptomatic on the right side). Studies with large or formal data collection procedures showing changes in fascicular swelling in response to D5W injection have not yet been reported.

Future studies, particularly prospective studies are necessary to evaluate the frequency of intraneural edema in various neuropathic pain syndromes, long-term efficacy of hydrodissection in comparison to that of standard-volume anesthetic blocks, and use of injectates other than D5W, such as platelet-rich plasma, which may have a favorable effect on dysfunctional nerves by itself [58]. In addition, because the amount of compression necessary to create a chronic constriction effect appears to be minimal [56], it is important to consider all possible points of constriction on these predominantly small-fiber sympathetic nerves between their peripheral origin and central process entry into the neural foramina, without restriction to the classic entrapment locations.

The potential importance of the analgesic effect of dextrose in the absence of anesthetic should not be overlooked in clinical applications and research. Compared with a nerve block with anesthetic, injection of dextrose for diagnostic purposes may provide a more precise method for identifying which branch or portion of a peripheral nerve is the nociceptive source within the nerve tree because it does not depolarize the nerve [57].

6. Conclusions

In conclusion, we described and illustrated potentially reproducible methods of hydrodissection of the stellate ganglion, brachial plexus, cervical nerve roots, and paravertebral spaces, provided data supporting a consistent analgesic effect of D5W used as the primary injectate, and suggested a potentially sustainable clinical benefit in patients with chronic upper back/thoracic pain of neuropathic origin. The mechanism of analgesia may be related to an indirect (allosteric) effect on the TRPV1 cation channel, hyperpolarization of normoglycemic C fibers, correction of local neural hypoglycemia, or undiscovered, probably multiple, mechanisms. The well-developed chronic constriction injury model, which results in neuropathic pain and neural swelling, is the primary rationale behind hydrodissection to release the nerve from suspected local neural compression, particularly those nerves with fascicular swelling or an increase in the overall volume. The frequency of neural edema and the long-term efficacy for nerve hydrodissection in patients with neuropathic pain, as opposed to those for low-volume anesthetic nerve blocks, are important foci for future research on neuropathic pain conditions.

Conflicts of Interest

The authors declare that there are no conflicts of interest regarding the publication of this article.

Acknowledgments

Permission was obtained from Essential Anatomy Apps to use their anatomy illustrations as figures in this paper. This manuscript has been professionally edited by Editage.

References

[1] A. Wadhwa, S. K. Kandadai, S. Tongpresert, D. Obal, and R. E. Gebhard, "Ultrasound guidance for deep peripheral nerve blocks: a brief review," *Anesthesiology Research and Practice*, vol. 2011, Article ID 262070, 6 pages, 2011.

[2] F. Dach, Á. L. Éckeli, K. D. S. Ferreira, and J. G. Speciali, "Nerve block for the treatment of headaches and cranial neuralgias—a practical approach," *Headache*, vol. 55, no. 1, pp. 59–71, 2015.

[3] S. Clendenen, R. Greengrass, J. Whalen, and M. I. O'Connor, "Infrapatellar saphenous neuralgia after TKA can be improved with ultrasound-guided local treatments," *Clinical Orthopaedics and Related Research*, vol. 473, no. 1, pp. 119–125, 2015.

[4] S. P. Cass, "Ultrasound-guided nerve hydrodissection: what is it? a review of the literature," *Current Sports Medicine Reports*, vol. 15, no. 1, pp. 20–22, 2016.

[5] J. M. Neal, M. J. Barrington, R. Brull et al., "The second ASRA practice advisory on neurologic complications associated with regional anesthesia and pain medicine: executive summary 2015," *Regional Anesthesia and Pain Medicine*, vol. 40, no. 5, pp. 401–430, 2015.

[6] K. Hara, S. Sakura, N. Yokokawa, and S. Tadenuma, "Incidence and effects of unintentional intraneural injection during ultrasound-guided subgluteal sciatic nerve block," *Regional Anesthesia and Pain Medicine*, vol. 37, no. 3, pp. 289–293, 2012.

[7] S. S. Liu, J. T. Yadeau, P. M. Shaw, S. Wilfred, T. Shetty, and M. Gordon, "Incidence of unintentional intraneural injection and postoperative neurological complications with ultrasound-guided interscalene and supraclavicular nerve blocks," *Anaesthesia*, vol. 66, no. 3, pp. 168–174, 2011.

[8] J. Lyftogt, "Pain conundrums: which hypothesis? Central nervous system sensitization versus peripheral nervous system autonomy," *Australasian Musculoskeletal Medicine*, vol. 13, pp. 72–74, 2008.

[9] J. Lyftogt, "Subcutaneous prolotherapy for Achilles tendinopathy," *Australasian Musculoskeletal Medicine*, vol. 12, pp. 107–109, 2007.

[10] J. Lyftogt, "Subcutaneous prolotherapy treatment of refractory knee, shoulder and lateral elbow pain," *Australasian Musculoskeletal Medicine*, vol. 12, no. 2, pp. 110–112, 2007.

[11] J. Lyftogt, "Prolotherapy for recalcitrant lumbago," *Australasian Musculoskeletal Medicine*, vol. 13, pp. 18–20, 2008.

[12] M. J. Yelland, K. R. Sweeting, J. A. Lyftogt, S. K. Ng, P. A. Scuffham, and K. A. Evans, "Prolotherapy injections and eccentric loading exercises for painful Achilles tendinosis: a randomised trial," *British Journal of Sports Medicine*, vol. 45, no. 5, pp. 421–428, 2011.

[13] A. Hosokawa, T. Nakashima, Y. Ogawa, K. Kozawa, and T. Kiba, "Coadministration of 5% glucose solution relieves vascular pain in the patients administered gemcitabine immediately," *Journal of Oncology Pharmacy Practice*, vol. 19, no. 2, pp. 190–192, 2013.

[14] T. Nakashima, Y. Ogawa, A. Kimura et al., "Coadministration of 5% glucose solution has a decrease in bendamustine-related vascular pain grade," *Journal of Oncology Pharmacy Practice*, vol. 18, no. 4, pp. 445–447, 2012.

[15] K. J. Paprottka, S. Lehner, W. P. Fendler et al., "Reduced periprocedural analgesia after replacement of water for injection with glucose 5% solution as the infusion medium for 90Y-Resin microspheres," *Journal of Nuclear Medicine*, vol. 57, no. 11, pp. 1679–1684, 2016.

[16] E. Dufour, N. Donat, S. Jaziri et al., "Ultrasound-guided perineural circumferential median nerve block with and without prior dextrose 5% hydrodissection: a prospective randomized double-blinded noninferiority trial," *Anesthesia and Analgesia*, vol. 115, no. 3, pp. 728–733, 2012.

[17] L. Maniquis-Smigel, K. D. Reeves, H. J. Rosen et al., "Short term analgesic effects of 5% dextrose epidural injections for chronic low back pain: a randomized controlled trial," *Anesthesiology and Pain Medicine*, vol. 7, no. 1, Article ID e42550, 2017.

[18] L. Maniquis Smigel, K. D. Reeves, J. Lyftogt, A. L. Cheng, and D. Rabago, "Caudal epidural injections with 5% dextrose for chronic low back pain with accompanying buttock or leg pain: results of a consecutive participant open-label trial with long-term follow-up," *Archives of Physical Medicine and Rehabilitation*, vol. 2016, no. 8, 2016.

[19] T. S. Jensen, R. Baron, M. Haanpää et al., "A new definition of neuropathic pain," *Pain*, vol. 152, no. 10, pp. 2204-2205, 2011.

[20] R.-D. Treede, T. S. Jensen, J. N. Campbell et al., "Neuropathic pain: redefinition and a grading system for clinical and research purposes," *Neurology*, vol. 70, no. 18, pp. 1630–1635, 2008.

[21] H. Ebadi, H. Siddiqui, S. Ebadi, M. Ngo, A. Breiner, and V. Bril, "Peripheral nerve ultrasound in small fiber polyneuropathy," *Ultrasound in Medicine and Biology*, vol. 41, no. 11, pp. 2820–2826, 2015.

[22] W. E. Ackerman III and J.-M. Zhang, "Efficacy of stellate ganglion blockade for the management of type 1 complex regional pain syndrome," *Southern Medical Journal*, vol. 99, no. 10, pp. 1084–1088, 2006.

[23] I. Yucel, Y. Demiraran, K. Ozturan, and E. Degirmenci, "Complex regional pain syndrome type I: efficacy of stellate ganglion blockade," *Journal of Orthopaedics and Traumatology*, vol. 10, no. 4, pp. 179–183, 2009.

[24] A. Sinofsky, T. Sharma, and T. Wright, "Stellate ganglion block for debilitating photophobia secondary to trigeminal, postherpetic neuralgia," *Pain Practice*, vol. 16, no. 7, pp. E99–E102, 2016.

[25] M. Y. Makharita, Y. M. Amr, and Y. El-Bayoumy, "Effect of early stellate ganglion blockade for facial pain from acute Herpes Zoster and Incidence of postherpetic neuralgia," *Pain Physician*, vol. 15, no. 6, pp. 467–474, 2012.

[26] M. Melis, K. Zawawi, E. Al-Badawi, S. L. Lobo, and N. Mehta, "Complex regional pain syndrome in the head and neck: A review of the literature," *Journal of Orofacial Pain*, vol. 16, no. 2, pp. 93–104, 2002.

[27] R. L. Arden, S. J. Bahu, M. A. Zuazu, and R. Berguer, "Reflex sympathetic dystrophy of the face: current treatment recommendations," *Laryngoscope*, vol. 108, no. 3, pp. 437–442, 1998.

[28] S. W. Mulvaney, J. H. Lynch, and R. S. Kotwal, "Clinical guidelines for stellate ganglion block to treat anxiety associated with posttraumatic stress disorder," *Journal of Special Operations Medicine*, vol. 15, no. 2, pp. 79–85, 2015.

[29] J. H. Lynch, S. W. Mulvaney, E. H. Kim, J. B. de Leeuw, M. J. Schroeder, and S. F. Kane, "Effect of stellate ganglion block on specific symptom clusters for treatment of post-traumatic stress disorder," *Military Medicine*, vol. 181, no. 9, pp. 1135–1141, 2016.

[30] M. R. Summers and R. L. Nevin, "Stellate ganglion block in the treatment of post-traumatic stress disorder: a review of historical and recent literature," *Pain Practice*, vol. 17, no. 4, pp. 546–553, 2017.

[31] S. W. Mulvaney, J. H. Lynch, M. J. Hickey et al., "Stellate ganglion block used to treat symptoms associated with combat-related post-traumatic stress disorder: a case series of 166 patients," *Military Medicine*, vol. 179, no. 10, pp. 1133–1140, 2014.

[32] A. Ghai, T. Kaushik, Z. S. Kundu, S. Wadhera, and R. Wadhera, "Evaluation of new approach to ultrasound guided stellate ganglion block," *Saudi Journal of Anaesthesia*, vol. 10, no. 2, pp. 161–167, 2016.

[33] A. Ghai, T. Kaushik, R. Wadhera, and S. Wadhera, "Stellate ganglion blockade-techniques and modalities," *Acta Anaesthesiologica Belgica*, vol. 67, no. 1, pp. 1–5, 2016.

[34] M. Gofeld, A. Bhatia, S. Abbas, S. Ganapathy, and M. Johnson, "Development and validation of a new technique for ultrasound-guided stellate ganglion block," *Regional Anesthesia and Pain Medicine*, vol. 34, no. 5, pp. 475–479, 2009.

[35] Q. H. Tran, A. Clemente, J. Doan, and R. J. Finlayson, "Brachial plexus blocks: a review of approaches and techniques," *Canadian Journal of Anesthesia*, vol. 54, no. 8, pp. 662–674, 2007.

[36] Brachial Plexus Injury (BPI) at http://www.hopkinsmedicine.org/neurology_neurosurgery/centers_clinics/peripheral_nerve_surgery/conditions/brachial_plexus_injury_bpi.html.

[37] S. Fallatah, "Successful management of complex regional pain syndrome type 1 using single injection interscalene brachial plexus block," *Saudi Journal of Anaesthesia*, vol. 8, no. 4, pp. 559–561, 2014.

[38] V. Golovchinsky, *Double-Crush Syndrome*, Springer, Boston, Mass, USA, 2000.

[39] K. Vermeylen, S. Engelen, L. Sermeus, F. Soetens, and M. Van De Velde, "Supraclavicular brachial plexus blocks: review and current practice," *Acta Anaesthesiologica Belgica*, vol. 63, no. 1, pp. 15–21, 2012.

[40] A. Mian, I. Chaudhry, R. Huang, E. Rizk, R. S. Tubbs, and M. Loukas, "Brachial plexus anesthesia: a review of the relevant anatomy, complications, and anatomical variations," *Clinical Anatomy*, vol. 27, no. 2, pp. 210–221, 2014.

[41] N. Pratt, "Anatomy of nerve entrapment sites in the upper quarter," *Journal of Hand Therapy*, vol. 18, no. 2, pp. 216–229, 2005.

[42] J. Van Zundert, M. Huntoon, J. Patijn, A. Lataster, N. Mekhail, and M. Van Kleef, "Cervical radicular pain," *Pain Practice*, vol. 10, no. 1, pp. 1–17, 2010.

[43] S. M. Klein, K. C. Nielsen, N. Ahmed, C. C. Buckenmaier III, and S. M. Steele, "In situ images of the thoracic paravertebral space," *Regional Anesthesia and Pain Medicine*, vol. 29, no. 6, pp. 596–599, 2004.

[44] R. K. Batra, K. Krishnan, and A. Agarwal, "Paravertebral block," *Journal of Anaesthesiology Clinical Pharmacology*, vol. 27, no. 1, pp. 5–11, 2011.

[45] J.-G. Song, G.-S. Hwang, H. L. Eun et al., "Effects of bilateral stellate ganglion block on autonomic cardiovascular regulation," *Circulation Journal*, vol. 73, no. 10, pp. 1909–1913, 2009.

[46] A. Weiss, C. Isselhorst, J. Gahlen et al., "Acute respiratory failure after deep cervical plexus block for carotid endarterectomy as a result of bilateral recurrent laryngeal nerve paralysis," *Acta Anaesthesiologica Scandinavica*, vol. 49, no. 5, pp. 715–719, 2005.

[47] N. Malek, A. Pajak, N. Kolosowska, M. Kucharczyk, and K. Starowicz, "The importance of TRPV1-sensitisation factors for the development of neuropathic pain," *Molecular and Cellular Neuroscience*, vol. 65, pp. 1–10, 2015.

[48] H. Bertrand, M. Kyriazis, K. D. Reeves, J. Lyftogt, and D. Rabago, "Topical mannitol reduces capsaicin-induced pain: results of a pilot-level, double-blind, randomized controlled trial," *PM and R*, vol. 7, no. 11, pp. 1111–1117, 2015.

[49] M. Cui, V. Gosu, S. Basith, S. Hong, and S. Choi, "Polymodal transient receptor potential vanilloid type 1 nocisensor: structure, modulators, and therapeutic applications," *Advances in Protein Chemistry and Structural Biology*, vol. 104, pp. 81–125, 2016.

[50] L. Chen, B. Tuo, and H. Dong, "Regulation of intestinal glucose absorption by ion channels and transporters," *Nutrients*, vol. 8, no. 1, 2016.

[51] S. G. Patching, "Glucose transporters at the blood-brain barrier: function, regulation and gateways for drug delivery," *Molecular Neurobiology*, vol. 54, no. 2, pp. 1046–1077, 2017.

[52] V. F. H. Jensen, A.-M. Mølck, I. B. Bøgh, and J. Lykkesfeldt, "Effect of insulin-induced hypoglycaemia on the peripheral nervous system: focus on adaptive mechanisms, pathogenesis and histopathological changes," *Journal of Neuroendocrinology*, vol. 26, no. 8, pp. 482–496, 2014.

[53] V. F. H. Jensen, I. B. Bøgh, and J. Lykkesfeldt, "Effect of insulin-induced hypoglycaemia on the central nervous system: evidence from experimental studies," *Journal of Neuroendocrinology*, vol. 26, no. 3, pp. 123–150, 2014.

[54] S. Pramming, B. Thorsteinsson, B. Stigsby, and C. Binder, "Glycaemic threshold for changes in electroencephalograms during hypoglycaemia in patients with insulin dependent diabetes," *British Medical Journal*, vol. 296, no. 6623, pp. 665–667, 1988.

[55] M. B. MacIver and D. L. Tanelian, "Activation of C fibers by metabolic perturbations associated with tourniquet ischemia," *Anesthesiology*, vol. 76, no. 4, pp. 617–623, 1992.

[56] G. J. Bennett, J. M. Chung, M. Honore, and Z. Seltzer, "Models of neuropathic pain in the rat," *Current Protocols in Neuroscience*, 2003.

[57] C. Dejaco, M. Stradner, D. Zauner et al., "Ultrasound for diagnosis of carpal tunnel syndrome: comparison of different methods to determine median nerve volume and value of power

Doppler sonography," *Annals of the Rheumatic Diseases*, vol. 72, no. 12, pp. 1934–1939, 2013.

[58] S. Anjayani, Y. W. Wirohadidjojo, A. M. Adam, D. Suwandi, A. Seweng, and M. D. Amiruddin, "Sensory improvement of leprosy peripheral neuropathy in patients treated with perineural injection of platelet-rich plasma," *International Journal of Dermatology*, vol. 53, no. 1, pp. 109–113, 2014.

Hindawi
BioMed Research International
Volume 2017, Article ID 1873209, 12 pages
https://doi.org/10.1155/2017/1873209

Clinical Study

Real-Time Ultrasound/MRI Fusion for Suprasacral Parallel Shift Approach to Lumbosacral Plexus Blockade and Analysis of Injectate Spread: An Exploratory Randomized Controlled Trial

Jennie Maria Christin Strid,[1] Erik Morre Pedersen,[2] Sinan Naseer Hussain Al-Karradi,[3] Mathias Alrø Fichtner Bendtsen,[4] Siska Bjørn,[1,4] Mette Dam,[5] Morten Daugaard,[6] Martin Sejr Hansen,[4] Katrine Danker Linnet,[7] Jens Børglum,[5] Kjeld Søballe,[8] and Thomas Fichtner Bendtsen[1]

[1]*Department of Anesthesiology and Intensive Care, Aarhus University Hospital, Nørrebrogade 44, 8000 Aarhus C, Denmark*
[2]*Department of Radiology, Aarhus University Hospital, Nørrebrogade 44, 8000 Aarhus C, Denmark*
[3]*Department of Biomedicine, Faculty of Health, Aarhus University, Vennelyst Boulevard 4, 8000 Aarhus C, Denmark*
[4]*Medical Science, Faculty of Health, Aarhus University, Nordre Ringgade 1, 8000 Aarhus C, Denmark*
[5]*Department of Anesthesiology and Intensive Care Medicine, Zealand University Hospital, University of Copenhagen, Sygehusvej 10, 4000 Roskilde, Denmark*
[6]*Department of Anesthesiology, Regional Hospital of Viborg, Heibergs Alle 4, 8800 Viborg, Denmark*
[7]*Department of Anesthesiology and Intensive Care Medicine, Slagelse Hospital, Ingemannsvej 18, 4200 Slagelse, Denmark*
[8]*Department of Orthopedic Surgery, Aarhus University Hospital, Tage-Hansens Gade 2, 8000 Aarhus C, Denmark*

Correspondence should be addressed to Thomas Fichtner Bendtsen; tfb@dadlnet.dk

Received 11 November 2016; Accepted 29 January 2017; Published 15 March 2017

Academic Editor: Tatsuo Nakamoto

Fused real-time ultrasound and magnetic resonance imaging (MRI) may be used to improve the accuracy of advanced image guided procedures. However, its use in regional anesthesia is practically nonexistent. In this randomized controlled crossover trial, we aim to explore effectiveness, procedure-related outcomes, injectate spread analyzed by MRI, and safety of ultrasound/MRI fusion versus ultrasound guided Suprasacral Parallel Shift (SSPS) technique for lumbosacral plexus blockade. Twenty-six healthy subjects aged 21–36 years received two SSPS blocks (20 mL 2% lidocaine-epinephrine [1 : 200,000] added 1 mL diluted contrast) guided by ultrasound/MRI fusion versus ultrasound. Number (proportion) of subjects with motor blockade of the femoral and obturator nerves and the lumbosacral trunk was equal (ultrasound/MRI, 23/26 [88%]; ultrasound, 23/26 [88%]; $p = 1.00$). Median (interquartile range) preparation and procedure times (s) were longer for the ultrasound/MRI fusion guided technique (686 [552–1023] versus 196 [167–228], $p < 0.001$ and 333 [254–439] versus 216 [176–294], $p = 0.001$). Both techniques produced perineural spread and corresponding sensory analgesia from L2 to S1. Epidural spread and lidocaine pharmacokinetics were similar. Different compartmentalized patterns of injectate spread were observed. Ultrasound/MRI fusion guided SSPS was equally effective and safe but required prolonged time, compared to ultrasound guided SSPS. This trial is registered with EudraCT (2013-004013-41) and ClinicalTrials.gov (NCT02593370).

1. Introduction

An effective, safe, and easy-to-perform peripheral nerve block technique for surgical anesthesia of the hip joint and concurrent postoperative analgesia would be advantageous, because many of the patients admitted for hip fracture are elderly, fragile, and sometimes impaired by severe cardiovascular comorbidity [1].

General and spinal anesthesia is associated with increased hemodynamic instability, anesthesia related mortality, and complications in old and multimorbid patients [2].

Compared to general and spinal anesthesia, more stable hemodynamics, fewer complications, and superior postoperative pain relief are achieved with peripheral regional anesthesia with a minimal use of opioids [3–6].

The femoral and obturator nerves are the terminal nerves of the lumbar plexus that innervate the hip joint together with the lumbosacral trunk of the sacral plexus. All these nerves can be anesthetized with a single injection paravertebrally between the transverse process of the fifth lumbar (L5) vertebra and the cranial border of the sacral ala [7, 8]. However, the accuracy of targeting the nerves with an ultrasound guided injection may be impaired due to the deep location of the target nerves as well as the lumbosacral bony structures generating acoustic shadows impeding the visibility of the needle trajectory [9], especially in old, fragile, comorbid, or obese patients [10–13]. Consequently, the efficiency and safety of the blockade may be undesirably affected and epidural spread of the injectate [9] as well as vascular, neural, or muscular injury may occur.

The accuracy of image guided procedures may be improved by fusing real-time ultrasound with magnetic resonance imaging (MRI) thus defeating the limitations of ultrasonography as a stand-alone technique [14, 15]. Furthermore, the image fusion technology includes electromagnetic needle tip tracking, which allows the operator to continuously assess the best needle insertion point, the needle trajectory, and the target of the injection. Finally, image fusion can be used to better the understanding of (ultrasonographic) anatomy and needle guidance and to refine existing ultrasound guided needle techniques [16]. Fusion of real-time ultrasound and computer tomography (CT) or MRI has been used successfully especially in interventional radiology [14, 15]. In regional anesthesia, an application of fused ultrasound/CT or MRI of the lumbar spine has been briefly described in a phantom and in volunteers, respectively, but no injections were performed [17]. In chronic pain therapy, only a few cadaver and case reports have assessed ultrasound/CT or MRI fusion guided injections primarily of the sacroiliac joint, hand, and wrist [18–21].

In this exploratory randomized controlled crossover trial, we aim to investigate real-time ultrasound/MRI fusion versus ultrasound guidance applied on the Suprasacral Parallel Shift (SSPS) technique for lumbosacral plexus blockade [22]. Primary outcome is the proportion of study subjects with motor blockade of the femoral and obturator nerves as well as the lumbosacral trunk. Secondary outcomes are procedure-related, perineural spread of injectate analyzed by MRI, epidural spread, sensory blockade, lidocaine pharmacokinetics, and cost-effectiveness. In addition, we aim to explore compartmentalized patterns of injectate spread by MRI.

2. Methods and Materials

2.1. Ethics. The Regional Research Ethics Committee (MJ: 1-10-72-179-13), the Danish Medicines Agency (2013-004013-13), and the Danish Data Protection Agency (1-16-02-160-14) approved this randomized controlled crossover trial. The study was registered in EudraCT (2013-004013-41) and in ClinicalTrials.gov (NCT02593370), monitored by the Good Clinical Practice unit at Aalborg and Aarhus University Hospitals, and complied with the Helsinki Declaration. Written informed consent was obtained from all subjects.

2.2. Recruitment. ASA I subjects aged ≥18 years were recruited through a Danish website for research volunteers. Subjects who were non-Danish speakers or unable to cooperate, had a history of allergy to local anesthetics or contrast agents, daily consumption of analgesics, abuse of medicine or alcohol, contraindication to MRI or infection or prior surgery of the paravertebral lumbosacral region, or who were legally incompetent were excluded.

The study was conducted at the Department of Radiology, Aarhus University Hospital, in Denmark during two three-day sessions with a one-week interim period in October to November 2015. The volunteers received payment for participation.

2.3. MRI for Fusion with Ultrasound. An experienced radiographer recorded supine MRI scans of all subjects with a 1.5 T Philips Ingenia MRI scanner (Koninklijke Philips Electronics NV, Eindhoven, Netherlands) upon arrival on the first session. The subjects were scanned with a pillow under their knees to minimise lumbar lordosis and a dS flex coverage anterior coil for signal reception. The recordings of the lumbar spine were coronal 3D T2-TSE sequences with an scanning resolution of $1.00 \times 1.00 \times 2.00\,\mathrm{mm}^3$ (overlapping 2.40 mm slices, 1.20 spacing), TE 60 ms, and TR 1200 ms. A feet-head phase encoding was applied to minimise artifacts due to respiration and peristalsis. All sequences were reconstructed to $0.78 \times 0.78 \times 1.00\,\mathrm{mm}^3$ resolution and converted to axial orientation using OsiriX v6.5.2 64-bit (Pixmeo SARL, Bernex, Switzerland) prior to upload to the ultrasound system with image fusion software (Epiq 7 1.4; Koninklijke Philips Electronics NV, Eindhoven, Netherlands), because the system only accepts axially oriented datasets for fusion.

2.4. Lumbosacral Plexus Block Procedure. The subjects were monitored with three-lead ECG, noninvasive blood pressure measurement, and pulse oximetry. Peripheral intravenous access was established for blood sampling and safety.

All blocks were performed with the Epiq 7 1.4 ultrasound system. The regional anesthetist (TFB) who performed all blocks has extensive clinical experience with ultrasound and electrical nerve stimulation guided nerve blocks and experimental experience with ultrasound/MRI fusion guided lumbosacral procedures.

While performing all blocks, the field generator (Koninklijke Philips Electronics NV, Eindhoven, Netherlands) was positioned over the lumbosacral region to generate the electromagnetic field necessary for fusion or to strengthen blinding of the subjects. After prescanning and any coregistration of ultrasound and MRI, the skin was swapped with chlorhexidine in isopropyl alcohol and covered with a sterile fenestrated drape. The curved array ultrasound probe (C5-1;

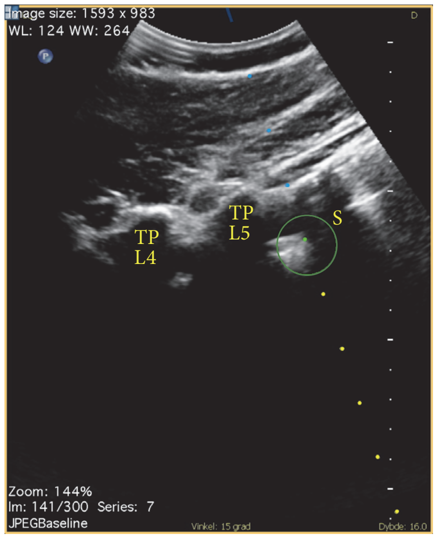

(a)

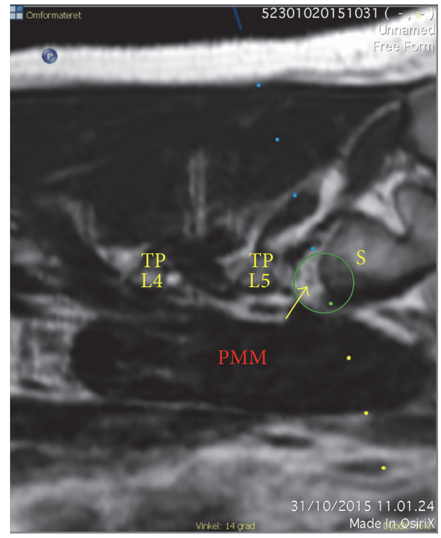

(b)

Figure 1: The ultrasonographic (a) and MR (b) images are fused and displayed side-by-side. The blue line in the top is the projection of the block needle and the large green circle marks the anticipated intersection of the block needle tip and the ultrasound beam, here coinciding with the rami of spinal nerve L5 (yellow arrow) displayed on the MR image. The line of small blue and yellow dots marks the anticipated trajectory of the block needle prior to and after the intersection with the ultrasound beam, respectively. PMM, major psoas muscle; S, sacral ala; TP L4-5, transverse processes of the fourth and fifth lumbar vertebral bodies.

Koninklijke Philips Electronics NV, Eindhoven, Netherlands) with the attached sensor was draped with a sterile cover. The skin and subcutaneous tissue were infiltrated with 2 mL 2% lidocaine prior to insertion of a 22 Gauge, 100 mm nerve block needle (Stimuplex Ultra; B. Braun, Melsungen, Germany). The injectate of each nerve block was 20 mL 2% lidocaine-epinephrine [1 : 200,000] with 1 mL diluted MRI contrast (0.13 mL 27.9% gadoterate meglumine [Dotarem®; Guerbet, Roissy CdG Cedex, France] and 0.87 mL 0.9% isotonic saline) added.

Ultrasound/MRI Fusion Guided SSPS. The subject was placed supine. The patient tracker, serving as a reference for the sensors mounted on the probe and the block needle, was affixed to the subject's iliac crest with adhesive tape on the side to be anesthetized. The probe was oriented axially on the abdomen. An identical reference point in the axial plane at the bifurcation of the common iliac arteries was used for coregistration of the real-time ultrasound and the MRI dataset. After coregistration, the ultrasonographic and MR images moved synchronically with any movement of the probe. The images were aligned using the iliac arteries, the aortic bifurcation, and the anterior margin of the lumbar vertebral body at the same level. Next, the subject was turned to the lateral decubitus position with the side to be anesthetized facing upwards. In order to take account for any misalignment due to the position change, the alignment of the fused datasets was fine adjusted using the borders of the L5 transverse process and vertebral body as well as the positions of the psoas major, quadratus lumborum, and erector spinae muscles. The probe was placed in the sagittal plane across the caudal border of the transverse process of L5 and the cranial border of the sacral ala, visualizing the interspace (osteofibrotic tunnel) in-between the bony structures on both images. Based on ultrasound/MRI visualization of the intertransverse ligament (posteriorly) and the lumbosacral ligament (anteriorly) marking out the osteofibrotic tunnel, the tip of the block needle was placed in the anticipated position for needle insertion caudad to the intercristal line. Using needle navigation, the position and angle of the insertion were adjusted until the anticipated intersection of the needle tip and the ultrasound beam coincided with the target compartment posterior to the psoas major muscle [8, 9] displayed on the MR image (Figure 1). Guided by real-time ultrasound/MRI fusion and needle navigation, the needle was advanced with an out-of-plane technique until a "loss of resistance" confirmed the visualized penetration through the lumbosacral ligament and the needle tip position anterior to the ligament on MRI.

Ultrasound Guided SSPS. This technique was performed in the lateral decubitus position and has been described in-depth previously [9]. The endpoint of injection was "loss of resistance" confirming the needle penetration of the lumbosacral ligament, sonographically visualized if possible.

An electrical nerve stimulator (0.1 ms, 2 Hz, 0.2 mA) was connected to the block needle during both procedures in order to decrease the risk of intraneural injection of local anesthetics. Prior to injection, any response to electrical nerve stimulation with 0.3 to 0.5 mA was registered [23]. The electrical nerve stimulation was use for safety only, not needle guidance. The local anesthetic with contrast was injected with intermittent aspiration.

Time zero (T_0) min was the time of withdrawal of the block needle from the skin after completed injection. All subjects were followed up until T_{90} for data sampling and were observed for adverse effects until the sensorimotor blockade had worn off.

2.5. Outcomes and Assessment. The primary outcome was the proportion of subjects with motor blockade of the femoral and obturator nerves as well as the lumbosacral trunk. Motor blockade was defined as ≥1 N reduction in muscle force (N) of the knee extensors, hip adductors, and hip abductors, respectively, at T_{40} compared to baseline. Muscle force was estimated in the supine position with a dynamometer (Commander Muscle Testing; JTECH Medical, Midvale, USA) maintained immobile by a steady grip of an observer. The observer instructed the subject to exert maximal pressure against the dynamometer during knee extension (with 90° flexion of the hip and knee joints), hip adduction (with extended and 45° abducted lower limb), and hip abduction (with extended lower limb). The highest value of three tests with 20 s intermittent intervals was recorded for each motion.

The secondary outcomes were (a) preparation time (s) from positioning of the subject on the bed until end of prescanning and coregistration, if any; (b) block procedure time (s) from placement of the probe on the skin until withdrawal of the block needle after completed injection; (c) number of needle insertions defined as each withdrawal of the needle followed by an advancement regardless the number of skin penetrations; (d) needle insertion point defined as the horizontal distance (cm) from the median to the skin penetration; (e) depth of needle tip gauged by reading the distance (cm) marked on the needle shaft at the endpoint of the injection; (f) minimal electrical nerve stimulation (mA) required to trigger any sensorimotor response immediately prior to injection; (g) type of response to electrical nerve stimulation ("Quadriceps," "Adductor," "Other motor," "Paresthesia," and "None"); (h) maximum procedural discomfort assessed by the subject on a numeric rating scale (NRS, 0 = "no discomfort", 10 = "worst possible discomfort") at T_0; (i) change in mean arterial blood pressure (ΔMAP) from baseline to T_5; (j) perineural injectate spread; (k) epidural injectate spread; (l) sensory blockade; (m) maximum plasma concentration of lidocaine ($C_{\max}$ of p-lidocaine, μg/mL); (n) time to $C_{\max}$ (T_{omc}) of p-lidocaine (min); (o) p-lidocaine concentration-time area under the curve; and (p) cost-effectiveness.

Injectate spread was analyzed on axial 3D T1-weighted MRI sequences (mDixonAll generating in-phase, out-of-phase, water and fat images as well as diffusion weighted images) sampled with a Philips Achieva 3.0 T dstream scanner (Koninklijke Philips Electronics, Eindhoven, Netherlands) at T_{15}. Perineural spread was assessed for the anterior rami of spinal nerves L2-S1, the femoral, obturator, and lateral femoral cutaneous nerves as well as the lumbosacral trunk. Perineural spread was considered "present" when direct contact between the injectate and the target nerve was visualized.

As an exploratory analysis, we observed different patterns of confinement of injectate inside the fascial compartments medial, posterior, and lateral to the psoas major muscle, respectively, as well as associated spread of injectate around compartment-specific nerves.

Epidural spread was considered "present" when there was circumferential epidural distribution of the injectate on any axial MRI level and concomitant bilateral blockade of cold in at least one pair of dermatomes.

Sensory blockade of cold, warmth, touch, and pain of the dermatomes Th12-S3 [24] and the skin innervated by the lateral femoral cutaneous nerve was tested with standardized stimuli (25° and 40° thermo test [Rolltemp II; Somedic, Hörby, Sweden], brush [SENSELab™ Brush-05; Somedic AB, Hörby, Sweden], and punctuated pin prick [PinPrick 512 mN; MRC Systems GmbH, Heidelberg, Germany]) at T_{50}. Sensation for each stimulus was assessed as "present" or "reduced/absent," where "reduced/absent" was considered a successful sensory blockade. The dermatomes Th12, L1, S2, and S3 were included in order to assess the effect of any epidural spread.

For the analysis of p-lidocaine, blood samples were collected at $T_{0,5,10,20,40,60,\text{ and }90}$ and centrifuged at $1,800g$ for 9 min. The plasma was transferred to 1.5 mL cryotubes and stored at −80°C until analysis with liquid chromatography tandem mass spectrometry [25].

The difference in mean marginal cost of the interventions was calculated as a measure of cost-effectiveness (extra price per patient) [26]. Unit costs were collected in Danish Kroner (DKK) in July 2016 and converted into US dollars (GBP/euros) in October 2016 (100 DKK = $14.86 [£12.08/€13.44]). Average annual total wages were used to calculate unit costs for time spent by medical staff. Because of the complexity of calculating the expense for the 1.5 T MRI scanner use, this cost is given as a time unit.

2.6. Randomization and Blinding. JMCS enrolled all subjects. Two study-independent assistants randomly allocated 26 consecutive subject identification numbers to sequences of interventions (Ultrasound/MRI fusion guided SSPS on day one and ultrasound guided SSPS on day two or vice versa) and side (right on day one and left on day two or vice versa). Twenty-six sheets with the sequences preprinted were put in 26 identical opaque and sealed envelopes marked 1 to 26. TFB and SB double-checked the allocated intervention and side immediately prior to each procedure without revealing it to others. The sheet was reenveloped and resealed. The procedure was repeated prior to the second intervention.

All sampling and analyses of data were blinded to the intervention. All interventions were performed with identical trial setup and equipment in order to blind the subjects. The MRI records of injectate spread were anonymised by a radiographer and hereafter analyzed in a random order by TFB.

2.7. Statistics. The primary outcome was proportion of subjects with motor blockade of the femoral and obturator nerves as well as the lumbosacral trunk. We hypothesized an increase in the proportion from 75% with ultrasound guidance to 100% with ultrasound/MRI fusion guidance. Detection of a 25% increase with 80% power ($1-\beta$) and $\alpha = 0.05$ would require a sample size of 24 subjects in a two-sided crossover analysis [27]. To avoid decreased power due to dropouts, we included 26 subjects.

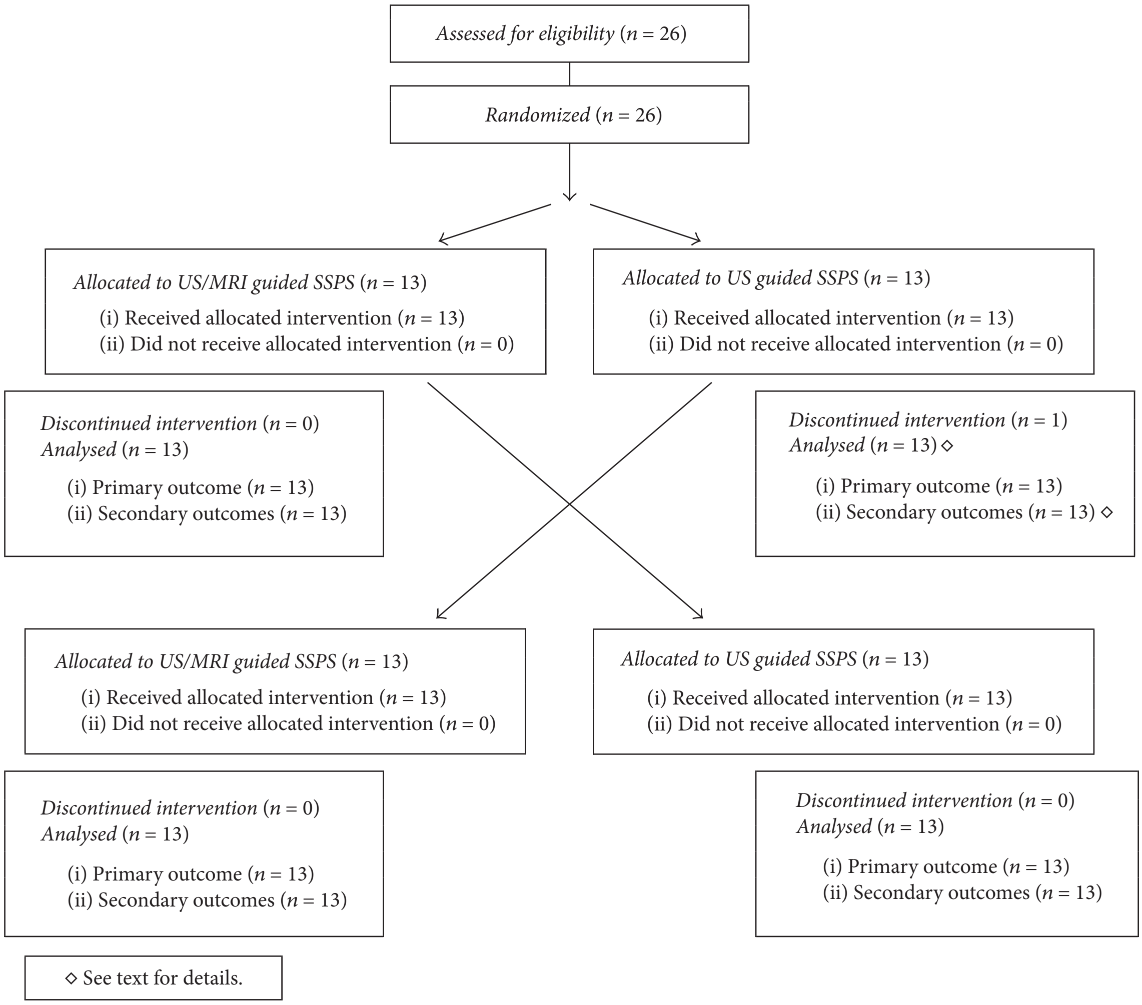

Figure 2: Modified CONSORT 2010 flow diagram of the study subjects receiving ultrasound (US)/magnetic resonance imaging (MRI) fusion versus US guided lumbosacral plexus blockade with the Suprasacral Parallel Shift (SSPS) technique.

Statistics were analyzed with Stata IC 14 (StataCorp LP, College Station, USA). Normality of distribution was assessed visually with the normal Q-Q-plot. Normally distributed differences between paired continuous variables were analyzed with one-sample Student's t-test. Nonnormally distributed differences between paired continuous variables and differences between paired ordinal variables were analyzed with Wilcoxon matched-pairs signed rank test. Differences between paired categorical variables were analyzed with McNemar's test. The level of significance was 0.05. Data are presented as mean (standard deviation [SD]) for continuous variables with normal distribution, as median (interquartile range [IQR] [range]) for continuous variables with nonnormal distribution and ordinal variables, and as number (proportion) for categorical variables.

3. Results

Twenty-six subjects (14/26 [54%] males) were enrolled during October 3 to 24, 2015 (Figure 2). Twenty-five subjects completed both interventions and follow-up per protocol. One ultrasound guided SSPS intervention was aborted due to aspiration of blood, but the subject completed the follow-up and contributed with his data per protocol.

The median (IQR [range]) age for all 26 subjects was 22 (22–24 [21–36]) years, mean (SD) weight was 73.2 (11.7) kg, mean (SD) height was 178 (8.1) cm, and mean (SD) BMI was 23.4 (2.7) $kg{\cdot}m^{-2}$.

The number (proportion) of subjects with motor blockade of the femoral and obturator nerves as well as the lumbosacral trunk was equal (ultrasound/MRI, 23/26 [88%]; ultrasound, 23/26 [88%]; $p = 1.00$). Table 1 displays the underlying data on muscle force and the number (proportion) of motor blockade of the femoral nerve, obturator nerve, and lumbosacral trunk, respectively.

Table 2 displays the values of the procedure-related outcomes.

There was no evidence for any difference in perineural spread to the anterior rami of spinal nerves L2 (ultrasound/MRI, 14/26 [54%]; ultrasound, 11/26 [42%]; $p = 0.58$), L3 (ultrasound/MRI, 21/26 [81%]; ultrasound, 21/26 [81%]; $p = 1.00$), L4 (ultrasound/MRI, 22/26 [85%];

Table 1: Baseline and postblock muscle force as well as number of subjects with motor blockade of the femoral nerve, obturator nerve, and the lumbosacral trunk for ultrasound/MRI fusion guided versus ultrasound guided lumbosacral plexus blockade with the Suprasacral Parallel Shift technique. Values are displayed as median (IQR [range]) or number (proportion).

	US*/MRI† (n = 26)	US† (n = 26)
Femoral nerve (knee extension)		
Baseline muscle force; N	244 (204–266 [176–343])	229 (215–253 [136–374])
Postblock muscle force; N	75 (0–121 [0–244])	72 (0–134 [0–255])
Motor blockade	25 (96%)	24 (92%)
Obturator nerve (hip adduction)		
Baseline muscle force; N	138 (114–176 [105–255])	134 (114–176 [101–237])
Postblock muscle force; N	0 (0–70 [0–149])	0 (0–31 [0–209])
Motor blockade	25 (96%)	24 (92%)
Lumbosacral trunk (hip abduction)		
Baseline muscle force; N	147 (114–160 [79-204])	144 (114–167 [79–233])
Postblock muscle force; N	79 (35–105 [0–173])	54 (41–79 [0–169])
Motor blockade	24 (92%)	24 (92%)

Motor blockade was defined as a decrease in postblock muscle force compared to baseline.
*US: ultrasound.
†MRI: magnetic resonance imaging.

Table 2: Procedure-related outcomes for ultrasound/MRI fusion guided versus ultrasound guided lumbosacral plexus blockade with the Suprasacral Parallel Shift technique. Values are displayed as median (IQR [range]), number (proportion), or mean (SD).

	US*/MRI† (n = 26)	US (n = 26)	p
Preparation time; s	686 (552–1023 [393–2501])	196 (167–228 [105–351])	<0.001
Block procedure time; s	333 (254–439 [201–1421])	216 (176–294 [117–458])	0.001
Number of needle insertions	4.5 (3.0–7.0 [2.0–24.0])	5.0 (3.0–7.0 [2.0–15.0])	0.87
Needle insertion point from midline; cm	4.0 (4.0–5.0 [2.0–6.0])	6.0 (5.0–6.0 [4.0–8.0])	<0.001
Needle depth; cm	8.0 (7.0–9.0 [5.0–10.0])	8.0 (7.0–8.5 [4.0–10.0])	0.37
Minimal nerve stimulation; mA	0.50 (0.50–0.50 [0.20–0.60])	0.50 (0.40–0.50 [0.30–0.50])	0.075
Electrical nerve stimulation response			0.37
1 Quadriceps femoris	4 (15%)	4 (15%)	1.00
2 Adductor	0 (0%)	1 (4%)	1.00
3 Other motor	0 (0%)	0 (0%)	1.00
4 Paresthesia	2 (8%)	0 (0%)	0.50
0 None	20 (77%)	21 (81%)	1.00
Procedural discomfort; NRS 0–10‡	2 (1–3 [0–7])	3 (2–4 [0–5])	0.036
ΔMAP; mmHg§	0.23 (12.77)	−4.50 (10.44)	0.070

*US: ultrasound.
†MRI: magnetic resonance imaging.
‡NRS: numeric rating scale.
§ΔMAP: change in mean arterial pressure from baseline to 5 min after completed injection of local anesthetic.

ultrasound, 25/26 [96%]; p = 0.38), L5 (ultrasound/MRI, 10/26 [38%]; ultrasound, 18/26 [69%]; p = 0.057), and S1 (ultrasound/MRI, 5/26 [19%]; ultrasound, 8/26 [31%]; p = 0.55), the femoral (ultrasound/MRI, 16/26 [62%]; ultrasound, 13/26 [50%]; p = 0.61), obturator (ultrasound/MRI, 14/26 [73%]; ultrasound, 11/26 [85%]; p = 0.58), and lateral femoral cutaneous (ultrasound/MRI, 16/26 [62%]; ultrasound, 11/26 [42%]; p = 0.58) nerves, or the lumbosacral trunk (ultrasound/MRI, 10/26 [38%]; ultrasound, 15/26 [58%]; p = 0.58).

We identified characteristic patterns of compartmentalized injectate spread inside three compartments (Figures 3, 4 and 5).

No difference in compartmentalized spread of injectate was observed between the two study groups. The frequencies of compartmentalized spread of injectate in the entire population of volunteers were 27% into the *parapsoas compartment (PPC)* and *retropsoas subcompartment (RPSC)*, 27% into the PPC, 37% into the RPSC, and 9% into the *retroperitoneal*

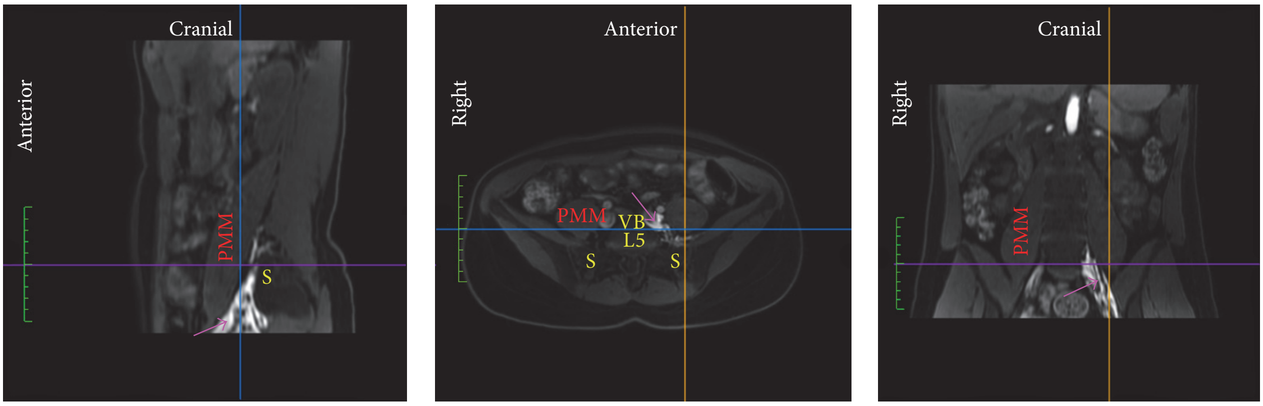

(a) (b) (c)

FIGURE 3: MRI of one subject visualizing spread of lidocaine-epinephrine added diluted contrast (magenta arrow) primarily medial to the psoas major muscle (PMM), that is, in the *parapsoas compartment*. (a) Sagittal plane. (b) Axial plane. (c) Coronal plane. Line (blue), position of coronal plane; Line (orange), position of sagittal plane; Line (purple), position of axial plane; S, sacral ala; VB L5, fifth lumbar vertebral body.

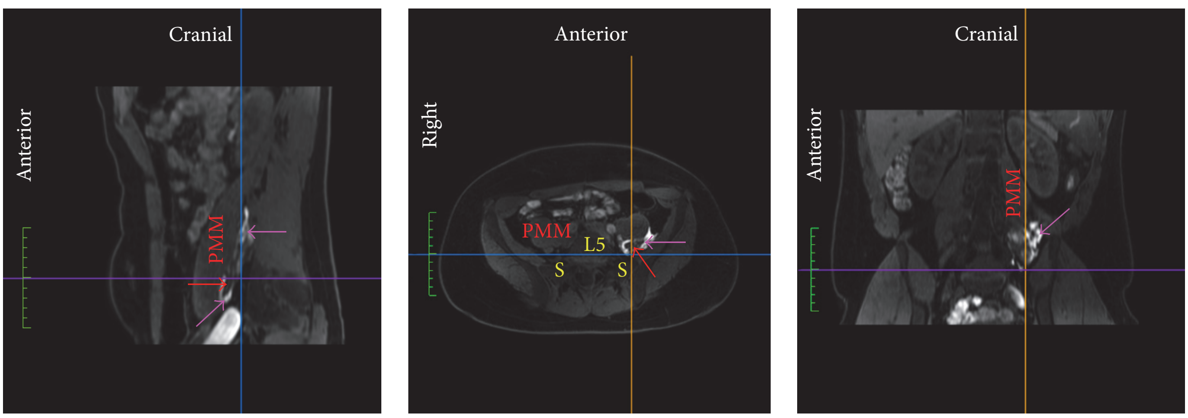

(a) (b) (c)

FIGURE 4: MRI of one subject visualizing spread of lidocaine-epinephrine added diluted contrast (magenta arrow) primarily posterior to the psoas major muscle (PPM), that is, in the *retropsoas subcompartment*, with minor seeping into the fascial plane between the anterior and posterior (red arrow) lamina of the PMM that contains the lumbar plexus. (a) Sagittal plane. (b) Axial plane. (c) Coronal plane. L5, fifth lumbar vertebral body; Line (blue), position of coronal plane; Line (orange), position of sagittal plane; Line (purple), position of axial plane; S, sacral ala.

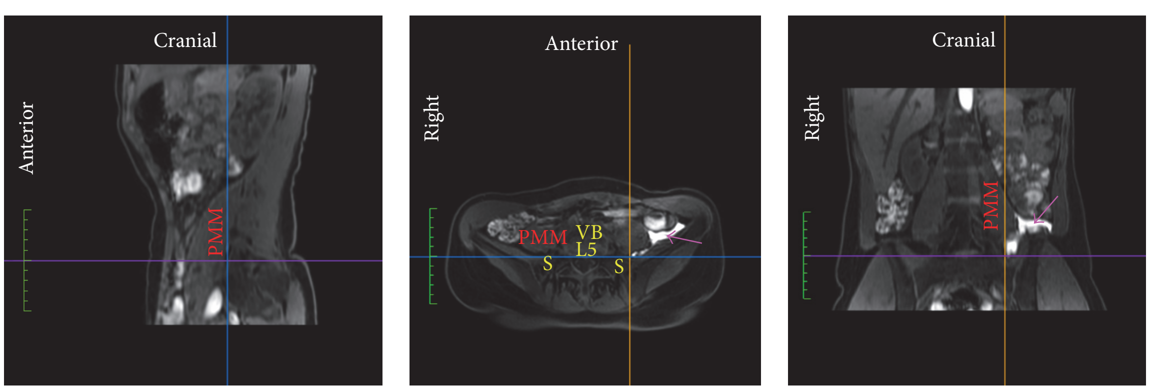

(a) (b) (c)

FIGURE 5: MRI of one subject visualizing spread of lidocaine-epinephrine added diluted contrast (magenta arrow) primarily lateral to the psoas major muscle (PMM), that is, in the *retroperitoneal compartment*, with minor seeping into the retropsoas subcompartment. (a) Sagittal plane. (b) Axial plane. (c) Coronal plane. Line (blue), position of coronal plane; Line (orange), position of sagittal plane; Line (purple), position of axial plane; S, sacral ala; VB L5, fifth lumbar vertebral body.

Table 3: Number of subjects with sensory blockade of the dermatomes Th12-S3 and the skin area innervated by the lateral femoral cutaneous nerve after ultrasound/MRI fusion guided ($n = 26$) versus ultrasound guided ($n = 26$) lumbosacral plexus blockade with the Suprasacral Parallel Shift technique. Values are displayed as number (proportion).

	Cold			Warmth			Touch			Pain		
	US*/MRI†	US	p	US/MRI	US	p	US/MRI	US	p	US/MRI	US	p
Th12	2 (8%)	0 (0%)	0.50	1 (4%)	1 (4%)	1.00	4 (15%)	1 (4%)	0.38	7 (8%)	2 (8%)	1.00
L1	4 (15%)	3 (12%)	1.00	2 (12%)	4 (15%)	1.00	9 (35%)	6 (23%)	0.55	7 (27%)	4 (15%)	0.51
L2	8 (31%)	10 (38%)	0.79	9 (35%)	10 (38%)	1.00	9 (35%)	11 (42%)	0.80	12 (46%)	11 (42%)	1.00
L3	18 (69%)	16 (62%)	0.75	13 (50%)	16 (42%)	0.58	7 (27%)	9 (35%)	0.75	15 (58%)	9 (35%)	0.18
L4	18 (69%)	15 (58%)	0.61	17 (65%)	14 (54%)	0.61	13 (50%)	13 (50%)	1.00	13 (50%)	14 (54%)	1.00
L5	10 (38%)	11 (42%)	1.00	9 (35%)	12 (46%)	0.55	8 (31%)	10 (38%)	0.75	8 (31%)	10 (38%)	0.75
S1	16 (62%)	14 (54%)	0.63	16 (52%)	18 (69%)	0.69	3 (12%)	10 (38%)	0.016	8 (31%)	12 (46%)	0.39
S2	5 (19%)	7 (27%)	0.75	7 (27%)	10 (38%)	0.55	8 (31%)	7 (27%)	1.00	7 (27%)	6 (23%)	1.00
S3	5 (19%)	8 (27%)	0.75	5 (19%)	7 (27%)	0.75	7 (27%)	9 (25%)	0.77	7 (27%)	8 (31%)	1.00
LFCN‡	13 (50%)	9 (35%)	0.39	14 (54%)	10 (38%)	0.34	16 (62%)	10 (38%)	0.18	17 (65%)	10 (38%)	0.092

*US: ultrasound.

†MRI: magnetic resonance imaging.

‡LFCN: lateral femoral cutaneous nerve.

compartment (RC). Seeping of injectate into the intrapsoas compartment, that is, the compartment between the anterior and posterior lamina of the psoas major muscle, and to the L2–L4 part of the lumbar plexus occurred in 89% of RPSC injection, 50% of PPC injection, and 40% of RC injection.

Table 3 displays the values of sensory blockade of the dermatomes Th12-S3 and the lateral femoral cutaneous nerve.

There was no evidence for any difference in epidural spread (ultrasound/MRI 3/26 (12%) subjects; ultrasound, 5/26 (19%) subjects; $p = 0.73$). The sensory effect was observed in the dermatomes L1 to S3 with individual variation.

Figure 6 illustrates the mean (SD) $C_{\max}$ of p-lidocaine. There was no evidence for any difference in mean (SD) $C_{\max}$, median (IQR [range]) T_{omc}, or mean (SD) concentration-time area under the curve (Figure 6). One subject in the ultrasound group was excluded from the analysis due to insufficient blood sampling.

The mean marginal cost of a SSPS block was Δ/\$28.19 (£22.91/€23.60) and 6 min and 34 s in the 1.5 T MRI scanner for the ultrasound/MRI fusion guided procedure compared to the ultrasound guided.

No serious adverse events were observed. One subject experienced a transitory hot flush prior to the intervention due to vasovagal needle phobia. Four subjects had two incidents of vasovagal syncope and three incidents of dizziness; two were related to reinsertion of an intravenous catheter or blood sampling during the follow-up; and one was related to previously diagnosed orthostatic hypotension.

4. Discussion

This is the first randomized controlled trial investigating ultrasound/MRI fusion guided lumbosacral plexus blockade. We found that the ultrasound/MRI fusion guided technique was equally effective and safe, but required longer preparation and block procedure time compared to the ultrasound guided technique.

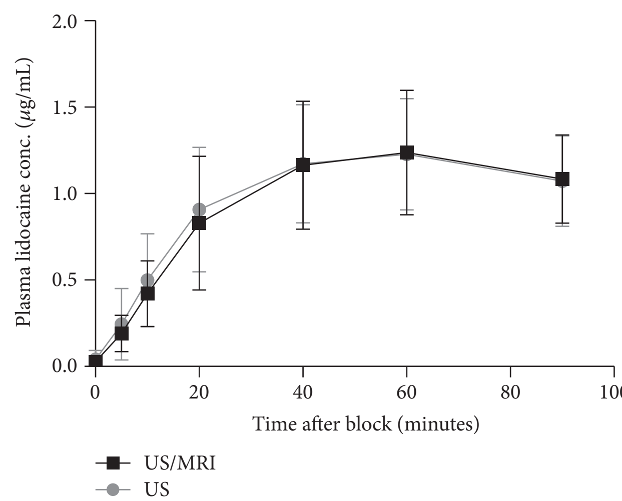

Figure 6: Plasma concentration of lidocaine 0 to 90 min after injection with the ultrasound/MRI fusion guided (US/MRI) versus the ultrasound guided (US) Suprasacral Parallel Shift technique for lumbosacral plexus blockade ($n = 25$). Values are presented as mean (SD).

4.1. Block Success. The initial hypothesis of a higher proportion of subjects with motor blockade of the femoral and obturator nerves as well as the lumbosacral trunk with ultrasound/MRI fusion guidance compared to ultrasound guidance was falsified. This may be explained by the demographics of the study subjects. That is, the target clinical group would be elderly and fragile patients, in whom the ultrasonoanatomical image quality may be impaired and in whom additional MRI visualization and needle navigation with fusion might improve the efficiency of needle guidance. In young healthy normal-weighted volunteers, however, adequate ultrasonographic quality is achieved with a higher frequency thus making the MRI scan, image fusion, and needle navigation redundant. Nonetheless, we assessed the fusion guided technique in healthy volunteers instead of clinical patients, because only ultrasound/MRI fusion of the lumbar spine, and not fusion guided lumbar needle insertions, has been briefly described in phantoms and volunteers before [17]. Furthermore, the body position of the subjects was different during the MRI sampling and the ultrasound/MRI fusion guided needle procedure. This may have affected the topography and dimensional stability of the anatomical structures under study, and hence the accuracy of the ultrasound/MRI fusion guided injection [15, 19]. However, we sampled the MRI dataset supine because this is technically and clinically most optimal. Moreover, any misalignment can be manually adjusted and a pilot study revealed no evidence that the target nerves, situated paravertebral to the rigid lumbar spine, moved significantly during change from supine to lateral decubitus. Yet, we cannot fully rule out such an effect.

4.2. Block Procedure-Related Outcomes. The prolonged time for the ultrasound/MRI fusion guided technique is in keeping with previous studies concerning real-time fusion [14]. It is explained by the extra time spent on coregistration and alignment of the datasets and on needle navigation. It is also reflected by the higher mean marginal cost and prolonged 1.5 T MRI time use of the fusion guided technique. Notably, both success rate and procedure time of a new technique follow a learning curve and technical perfection requires practice [14].

4.3. MRI Analysis of Injectate Spread versus Sensorimotor Blockade. We observed spread of injectate inside three fascial compartments. The first compartment is medial to the psoas major muscle and the iliopsoas compartment [28] (Figure 3). We therefore suggest referring to this as the *parapsoas compartment (PPC)*. We observed that the PPC extends from the level of the neural foramen of vertebra L4 cranially to the neural foramen of S1 caudally. Caudal to the transverse process of L5, the iliopsoas fascia is tied down to the sacral ala and separates the PPC from the iliopsoas compartment [28]. The PPC contains the anterior rami of spinal nerves L4-S1, the lumbosacral trunk, and the obturator nerve. The second compartment is a triangular groove that extends from the transverse process of L5 and the iliolumbar ligament cranially and between the psoas major and iliac muscles until they become fused as the iliopsoas muscle caudally (Figure 4). The compartment is bounded by the iliopsoas fascia, which medially separates it from the PPC and laterally covers the groove between the psoas major and iliacus muscles. It has been described previously [29], however, as it is a subcompartment of the iliopsoas compartment, we suggest referring to this as the *retropsoas subcompartment (RPSC)*. The RPSC contains the femoral and lateral femoral cutaneous nerves, as they emerge from the posterolateral border of the psoas major muscle caudal to the level of the iliac crest. The third compartment is the retroperitoneal fat-pad compartment between the peritoneum and the transversalis fascia and lateral to the iliopsoas compartment (Figure 5). We suggest referring to this as the *retroperitoneal compartment (RC)*. The RC contains none of the major terminal lumbar plexus nerves.

In all subjects, the injectate spread primarily into one or two of the three identified compartments. Hence the injectate primarily spread perineurally around the anterior rami of spinal nerves L4-S1, the lumbosacral trunk and the obturator nerve inside the PPC, around the femoral and lateral femoral cutaneous nerves inside the RPSC, or around no nerves inside the RC. Injectate spread inside the PPC therefore resulted in increased sensorimotor blockade of primarily the anterior rami of spinal nerves L4-S1, the lumbosacral trunk (superior gluteal nerves), and the obturator nerve, while injectate spread inside the RPSC resulted in increased sensorimotor blockade of primarily the femoral and lateral femoral cutaneous nerves. Injectate spread inside the RC had no sensorimotor effect since the compartment contains no major terminal nerves of the lumbosacral plexus.

Few previous studies have compared ultrasonography and MRI of the lumbosacral anatomy [30] and analyzed injectate spread with MRI [9, 31, 32]. The sensory mapping demonstrated segmental anesthesia from L2 to S1 in accordance with the perineural spread analyzed by MRI. A cadaver study on lumbosacral plexus blockade guided by anatomical landmarks showed weak staining of spinal nerve S1 in only 3/20 (15%) cadavers [7]. In contrast, our study demonstrates that an injection at the neuraxial level of L5/S1 may indeed block the cranial part of the sacral plexus.

Nonetheless, sensory mapping of dermatomes should be interpreted with caution because it may be unreliable due to anatomical variation and overlapping of innervation of adjacent cutaneous segments and terminal nerves territories [33]. We used motor blockade as a surrogate of sensory blockade of the femoral nerve, obturator nerve, and the lumbosacral trunk. However, the motor blockade definition does not take account for bi- and triple nerve innervation of specific muscle groups or measurement error of the method to estimate muscle force. Because knowledge concerning the correlation between reduced muscle force in healthy volunteers and sufficient motor blockade in clinical patients is sparse, the values of block success should be considered as a measure of comparison of the techniques, not as a clinically applicable measure. Due to this complexity, we recommend inclusion of an objective analysis such as MRI recordings of injectate spread when validating new techniques in healthy volunteers.

4.4. Compartmentalized Injectate Spread and a Theoretical Ultrasound/MRI Fusion Guided Anterior Approach. The MRI recordings allow analysis of patterns of injectate spread, which together with high-resolution MRI for fusion with real-time ultrasound offer the potential of improved understanding of the (ultrasonographic) anatomy [16]. In the present study, we identified characteristic patterns of injectate spread in the different fascial compartments. The observed patterns of spread imply that local anesthetic has to be injected into the PPC as well as the RPSC for sufficient spread to all target nerves relevant for anesthesia of the hip joint with a high clinical success rate. However, the visualization of the PPC and RPSC is impeded by bony structures when the ultrasound guided SSPS technique is employed. Furthermore, in the lateral decubitus position with the side to be

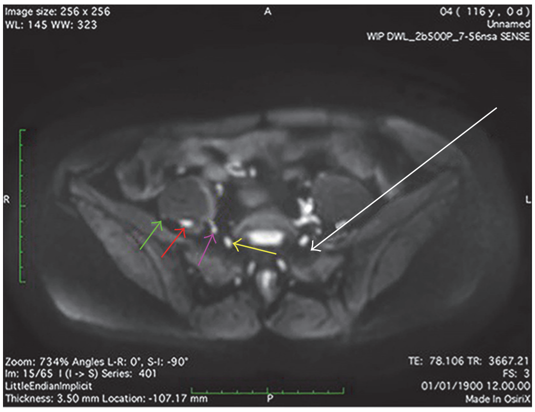

Figure 7: Axial diffusion weighted MRI at the level of the cranial border of the sacral ala, demonstrating a possible anterior approach to the lumbosacral plexus in the supine position. A needle (white arrow) can be inserted close to the anterior superior iliac spine and advanced between the psoas major and iliacus muscles. A first injection of local anesthetic into the *retropsoas subcompartment* will spread to the femoral nerve (red arrow) and the lateral femoral cutaneous nerve (green arrow). A second injection of local anesthetic into the *parapsoas compartment* will spread to the anterior rami of spinal nerves L4 and L5, the lumbosacral trunk (yellow arrow) and the obturator nerve (pink arrow).

anesthetized facing upwards, gravity may facilitate medial spread of the local anesthetic to the epidural space [34]. An ultrasound/MRI fusion guided anterior technique in the supine position may overcome these limitations and supply a safe, efficient, and easy needle path from the skin surface to the target nerves inside the PPC as well as the RPSC (Figures 7 and 8).

4.5. Pharmacokinetics of p-Lidocaine. The mean C_{max} of p-lidocaine was similar for the techniques and peaked approximately one hour after injection. This is in keeping with previous studies investigating plasma concentration of local anesthetics in regional anesthesia [9, 32, 35]. No dose-finding studies have been conducted for the SSPS technique, but the minimal effective anesthetic volume of 0.5% ropivacaine to accomplish a successful Shamrock lumbar plexus blockade in 95% of patients (ED_{95}) is 36.0 mL (95% CI 19.7 to 52.2) [36]. Because the aim of this study was to compare two techniques in a standardized setting, and not to achieve maximum block success, and the subjects were discharged on the same day, we chose a comparatively low dose of 20 mL 2% lidocaine-epinephrine corresponding approximately to the ED_{50} of 0.5% ropivacaine [36] and allowing fast discharge. However, injection of more clinical relevant local anesthetic volumes in excess of 20 mL would result in increased C_{max}. Also, pharmacokinetics of local anesthetic changes with age [37]. The present results might therefore not be directly applicable in elderly patients.

4.6. Limitations. Apart from the external limitations above, the expert anesthetist performing all blocks could not be blinded, as is the case with all procedure-related studies. In

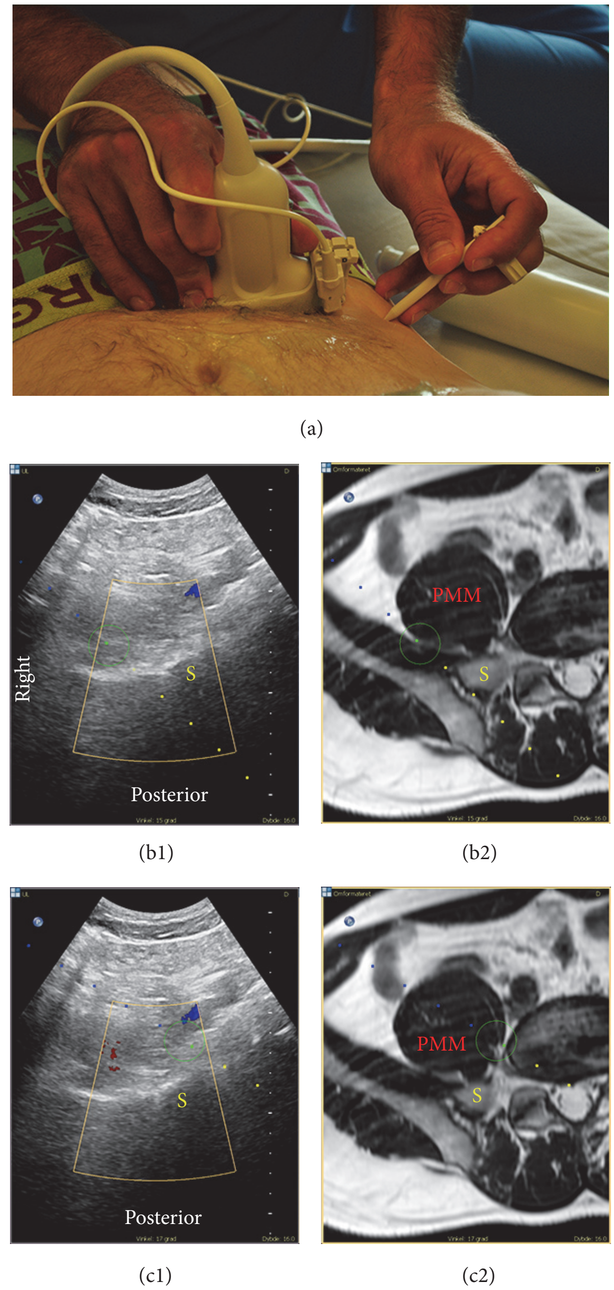

Figure 8: The anterior lumbosacral plexus approach guided by real-time ultrasound/MRI fusion in an anticipated experimental setting. (a) The probe is axially oriented, slightly rotated clockwise, and medial to the anterior superior iliac spine where the phantom needle is oriented in-plane with the US/MR image planes. (b) Fused real-time ultrasound (b1) and MRI (b2) depicting the needle trajectory into the *retropsoas subcompartment*. (c) Fused real-time ultrasound (c1) and MRI (c2) depicting the needle trajectory through the psoas major muscle (PMM) into the *parapsoas compartment*. Guided by real-time ultrasound/MRI fusion and needle navigation, the "insertion point" and angulation of the phantom needle are adjusted until the anticipated intersection between the needle tip and the ultrasound beam (green circle) coincides with the target lumbosacral plexus nerves in the retropsoas compartment (b) and in the parapsoas subcompartment (c) anterior to the border of the sacral ala (S). The line of small blue and yellow dots marks the anticipated trajectory of the block needle prior to and after the intersection with the ultrasound beam, respectively.

order to limit this source of bias, we adhered to a strict double-controlled protocol.

4.7. Perspectives. Ultrasound/MRI fusion for needle guidance in the lumbosacral region is an evolving technique and is proven to be neither more inaccurate nor more unsafe compared to ultrasound guidance. Future studies of real-time ultrasound/MRI needle guidance may include automatic coregistration based on image recognition or MRI-compatible external fiducials, or techniques that minimise the effect of position change and thereby improving the accuracy, time-efficiency, and ease-of-performance.

4.8. Conclusion. The ultrasound/MRI fusion guided SSPS technique was equally effective and safe but required longer time, compared to the ultrasound guided SSPS technique. Three patterns of compartmentalized injectate spread indicate that local anesthetic has to be injected into the parapsoas compartment as well as the retropsoas subcompartment to block the lumbosacral nerves innervating the hip joint.

Disclosure

A preliminary protocol of the study was presented at the 33rd Annual ESRA Congress 2014 in Seville, Spain, on 3–6 September 2014.

Competing Interests

None of the authors have any potential conflicts of interests to declare.

Acknowledgments

The A. P. Møller and Chastine Mc-Kinney Møller Foundation for General Purposes supported this study.

References

[1] C. de Luise, M. Brimacombe, L. Pedersen, and H. T. Sørensen, "Comorbidity and mortality following hip fracture: a population-based cohort study," *Aging Clinical and Experimental Research*, vol. 20, no. 5, pp. 412–418, 2008.

[2] A. Gottschalk, H. Van Aken, M. Zenz, and T. Standl, "Is anesthesia dangerous?" *Deutsches Arzteblatt International*, vol. 108, no. 27, pp. 469–474, 2011.

[3] S. G. Memtsoudis, R. Rasul, S. Suzuki et al., "Does the impact of the type of anesthesia on outcomes differ by patient age and comorbidity burden?" *Regional Anesthesia and Pain Medicine*, vol. 39, no. 2, pp. 112–119, 2014.

[4] V. De Visme, F. Picart, R. Le Jouan, A. Legrand, C. Savry, and V. Morin, "Combined lumbar and sacral plexus block compared with plain bupivacaine spinal anesthesia for hip fractures in the elderly," *Regional Anesthesia and Pain Medicine*, vol. 25, no. 2, pp. 158–162, 2000.

[5] T. F. Bendtsen, S. Haskins, J. A. Kølsen Petersen, and J. Børglum, "Do ultrasound-guided regional blocks signify a new paradigm in high-risk patients?" *Best Practice & Research. Clinical Anaesthesiology*, vol. 30, no. 2, pp. 191–200, 2016.

[6] P. S. Whiting, C. S. Molina, S. E. Greenberg, R. V. Thakore, W. T. Obremskey, and M. K. Sethi, "Regional anaesthesia for hip fracture surgery is associated with significantly more peri-operative complications compared with general anaesthesia," *International Orthopaedics*, vol. 39, no. 7, pp. 1321–1327, 2015.

[7] M. A. Huntoon and R. A. Yeasting, "Analysis of contrast spread of a modified posterior approach to lumbosacral plexus blockade in a cadaver model," *Regional Anesthesia and Pain Medicine*, vol. 23, no. 3, p. 16, 1998.

[8] T. F. Bendtsen, K. Søballe, E. M. Petersen et al., "Ultrasound guided single injection lumbosacral plexus blockade for hip surgery anaesthesia," *British Journal of Anaesthesia*, vol. 111, 2013.

[9] T. F. Bendtsen, E. M. Pedersen, S. Haroutounian et al., "The suprasacral parallel shift vs lumbar plexus blockade with ultrasound guidance in healthy volunteers—a randomised controlled trial," *Anaesthesia*, vol. 69, no. 11, pp. 1227–1240, 2014.

[10] H. S. Amonoo-Kuofi, "Changes in the lumbosacral angle, sacral inclination and the curvature of the lumbar spine during aging," *Acta Anatomica*, vol. 145, no. 4, pp. 373–377, 1992.

[11] Z. Shao, G. Rompe, and M. Schiltenwolf, "Radiographic changes in the lumbar intervertebral discs and lumbar vertebrae with age," *Spine*, vol. 27, no. 3, pp. 263–268, 2002.

[12] O. Sevinc, C. Barut, M. Is, N. Eryoruk, and A. A. Safak, "Influence of age and sex on lumbar vertebral morphometry determined using sagittal magnetic resonance imaging," *Annals of Anatomy*, vol. 190, no. 3, pp. 277–283, 2008.

[13] L. Kirchmair, T. Entner, J. Wissel, B. Moriggl, S. Kapral, and G. Mitterschiffthaler, "A study of the paravertebral anatomy for ultrasound-guided posterior lumbar plexus block," *Anesthesia and Analgesia*, vol. 93, no. 2, pp. 477–481, 2001.

[14] M. Zacchino and F. Calliada, "Ultrasound image fusion: a new strategy to reduce x-ray exposure during image guided pain therapies," in *Current Topics in Ionizing Radiation Research*, M. Nenoi, Ed., pp. 395–406, InTech, Rijeka, Croatia, 2012.

[15] C. Ewertsen, A. Săftoiu, L. G. Gruionu, S. Karstrup, and M. B. Nielsen, "Real-time image fusion involving diagnostic ultrasound," *American Journal of Roentgenology*, vol. 200, no. 3, pp. W249–W255, 2013.

[16] K. Galiano, A. A. Obwegeser, R. Bale et al., "Ultrasound-Guided and CT-navigation-assisted periradicular and facet joint injections in the lumbar and cervical spine: a new teaching tool to recognize the sonoanatomic pattern," *Regional Anesthesia and Pain Medicine*, vol. 32, no. 3, pp. 254–257, 2007.

[17] W. H. Kwok and M. K. Karmakar, "Fusion imaging: ultrasound and CT or ultrasound and MRI image fusion for spinal sonography," in *Musculoskeletal Ultrasound for Regional Anaesthesia and Pain Medicine*, M. K. Karmakar, Ed., pp. 503–508, Department of Anaesthesia and Intensive Care, The Chinese University of Hong Kong, Hong Kong, 2016.

[18] A. S. Klauser, T. De Zordo, G. M. Feuchtner et al., "Fusion of real-time US with CT images to guide sacroiliac joint injection in vitro and in vivo," *Radiology*, vol. 256, no. 2, pp. 547–553, 2010.

[19] M. Zacchino, J. Almolla, E. Canepari, V. Merico, and F. Calliada, "Use of ultrasound-magnetic resonance image fusion to guide sacroiliac joint injections: a preliminary assessment," *Journal of Ultrasound*, vol. 16, no. 3, pp. 111–118, 2013.

[20] A. Iagnocco, C. Perella, M. A. D'Agostino, E. Sabatini, G. Valesini, and P. G. Conaghan, "Magnetic resonance and ultrasonography real-time fusion imaging of the hand and wrist in osteoarthritis and rheumatoid arthritis," *Rheumatology*, vol. 50, no. 8, pp. 1409–1413, 2011.

[21] M. Zacchino, M. Allegri, M. Canepari et al., "Feasibility of pudendal nerve anesthetic block using fusion imaging technique in chronic pelvic pain," *European Journal of Pain Supplements*, vol. 4, no. 4, pp. 329–333, 2010.

[22] J. M. Strid, E. M. Pedersen, K. Søballe, and T. F. Bendtsen, "'Ultrasound/magnetic resonance image fusion guided lumbosacral plexus block—a clinical study', in 'Abstracts and Highlight Papers of 33rd Annual European Society of Regional Anaesthesia & Pain Therapy (ESRA) Congress 2014'," *Regional Anesthesia and Pain Medicine*, vol. 39, no. 5, supplement 1, p. e316, 2014.

[23] J. De Andrés, J. M. Alonso-Iñigo, X. Sala-Blanch, and M. A. Reina, "Nerve stimulation in regional anaesthesia: theory and practice," *Best Practice & Research. Clinical Anaesthesiology*, vol. 19, no. 2, pp. 153–174, 2005.

[24] M. W. L. Lee, R. W. McPhee, and M. D. Stringer, "An evidence-based approach to human dermatomes," *Clinical Anatomy*, vol. 21, no. 5, pp. 363–373, 2008.

[25] L. K. Sørensen and J. B. Hasselstrøm, "A high-throughput multi-class liquid chromatography tandem mass spectrometry method for quantitative determination of licit and illicit drugs in whole blood," *Analytical Methods*, vol. 5, no. 13, pp. 3185–3193, 2013.

[26] L. Ehlers, J. M. Jensen, and T. F. Bendtsen, "Cost-effectiveness of ultrasound vs nerve stimulation guidance for continuous sciatic nerve block," *British Journal of Anaesthesia*, vol. 109, no. 5, pp. 804–808, 2012.

[27] Sealed Envelope Ltd, *Power Calculator for Binary Outcome Superiority Trial*, 2012, http://www.sealedenvelope.com/power/binary-superiority.

[28] J. A. Van Dyke, H. C. Holley, and S. D. Anderson, "Review of iliopsoas anatomy and pathology," *Radiographics*, vol. 7, no. 1, pp. 53–84, 1987.

[29] D. Chayen, H. Nathan, and M. Chayen, "The psoas compartment block," *Anesthesiology*, vol. 45, no. 1, pp. 95–99, 1976.

[30] M. K. Karmakar, J. W. Li, W. H. Kwok, E. Soh, and A. Hadzic, "Sonoanatomy relevant for lumbar plexus block in volunteers correlated with cross-sectional anatomic and magnetic resonance images," *Regional Anesthesia and Pain Medicine*, vol. 38, no. 5, pp. 391–397, 2013.

[31] S. Mannion, J. Barrett, D. Kelly, D. B. Murphy, and G. D. Shorten, "A description of the spread of injectate after psoas compartment block using magnetic resonance imaging," *Regional Anesthesia and Pain Medicine*, vol. 30, no. 6, pp. 567–571, 2005.

[32] J. M. Strid, A. Sauter, K. Ullensvang et al., "Ultrasound-guided lumbar plexus block in volunteers; a randomized controlled trial," *British Journal of Anaesthesia*, vol. 118, no. 3, pp. 430–438, 2017.

[33] M. B. Downs and C. Laporte, "Conflicting dermatome maps: educational and clinical implications," *The Journal of Orthopaedic and Sports Physical Therapy*, vol. 41, no. 6, pp. 427–434, 2011.

[34] P. Di Benedetto, G. Pinto, R. Arcioni et al., "Anatomy and imaging of lumbar plexus," *Minerva Anestesiologica*, vol. 71, no. 9, pp. 549–554, 2005.

[35] J. Børglum, K. Jensen, A. F. Christensen et al., "Distribution patterns, dermatomal anesthesia, and ropivacaine serum concentrations after bilateral dual transversus abdominis plane block," *Regional Anesthesia and Pain Medicine*, vol. 37, no. 3, pp. 294–301, 2012.

[36] A. R. Sauter, K. Ullensvang, G. Niemi et al., "The Shamrock lumbar plexus block: a dose-finding study," *European Journal of Anaesthesiology*, vol. 32, no. 11, pp. 764–770, 2015.

[37] M. R. Sadean and P. S. A. Glass, "Pharmacokinetics in the elderly," *Best Practice & Research. Clinical Anaesthesiology*, vol. 17, no. 2, pp. 191–205, 2003.

Hindawi
BioMed Research International
Volume 2017, Article ID 9217145, 5 pages
https://doi.org/10.1155/2017/9217145

Review Article

Caudal Epidural Block: An Updated Review of Anatomy and Techniques

Sheng-Chin Kao and Chia-Shiang Lin

Department of Anesthesiology, Mackay Memorial Hospital, Taipei, Taiwan

Correspondence should be addressed to Chia-Shiang Lin; seancslin@gmail.com

Received 17 October 2016; Revised 17 December 2016; Accepted 7 February 2017; Published 26 February 2017

Academic Editor: Yasuyuki Shibata

Caudal epidural block is a commonly used technique for surgical anesthesia in children and chronic pain management in adults. It is performed by inserting a needle through the sacral hiatus to gain entrance into the sacral epidural space. Using conventional blind technique, the failure rate of caudal epidural block in adults is high even in experienced hands. This high failure rate could be attributed to anatomic variations that make locating sacral hiatus difficult. With the advent of fluoroscopy and ultrasound in guiding needle placement, the success rate of caudal epidural block has been markedly improved. Although fluoroscopy is still considered the gold standard when performing caudal epidural injection, ultrasonography has been demonstrated to be highly effective in accurately guiding the needle entering the caudal epidural space and produce comparative treatment outcome as fluoroscopy. Except intravascular and intrathecal injection, ultrasonography could be as effective as fluoroscopy in preventing complications during caudal epidural injection. The relevant anatomy and techniques in performing the caudal epidural block will be briefly reviewed in this article.

1. Introduction

The caudal epidural block involves placing a needle through the sacral hiatus to deliver medications into the epidural space. This approach to the epidural space is not only widely used for surgical anesthesia and analgesia in pediatric patients but also popular in managing a wide variety of chronic pain conditions in adults.

The caudal epidural block was first introduced as a landmark-based, blind technique. In children, the successful rate with the blind technique is above 96% [1, 2]. In adults, however, it was only 68–75% even in the experienced hands [3–5]. With the advent of imaging technology, fluoroscopy and ultrasonography have been increasingly used to guide caudal epidural block. In this review, we will overview recent advancement in our understanding of relevant anatomy and development of imaging guided techniques in adults.

2. Anatomy

The anatomic features and variations relevant to caudal epidural block were the focuses of several recent reports. A thorough knowledge of the relevant anatomy (Figures 1 and 2) may improve the success rate of caudal epidural needle placement while minimize the risks of complications.

2.1. Sacral Cornua. The sacral cornua are vestigial remnants of the inferior articular processes of the 5th sacral vertebra and presented as two bony prominences at the caudal end of sacrum. Palpating the bilateral sacral cornua is essential to locate the sacral hiatus in the conventional landmark-based technique. However, the sacral cornua are not always palpable. Defining a height of at least 3 mm as palpable, Sekiguchi and colleagues reported that sacral cornua were bilaterally palpable in only 19%, unilaterally palpable in 25%, and bilaterally impalpable in 54% of isolated adult sacral bone [6]. Using the same definition, Aggarwal and colleagues reported that the sacral cornua were bilaterally palpable in 55%, unilaterally palpable in 24%, and bilaterally impalpable in 21% of adult sacral bone [7]. In another report, sacral cornua were not palpable bilaterally in 14.3% and palpable unilaterally in 24.5% of cadavers [8]. In a clinical report, sacral cornua were only palpable in 59% of individuals [4]. This high percentage

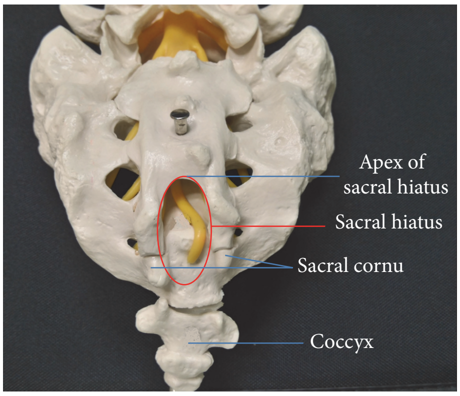

Figure 1: Posterior view of sacrum.

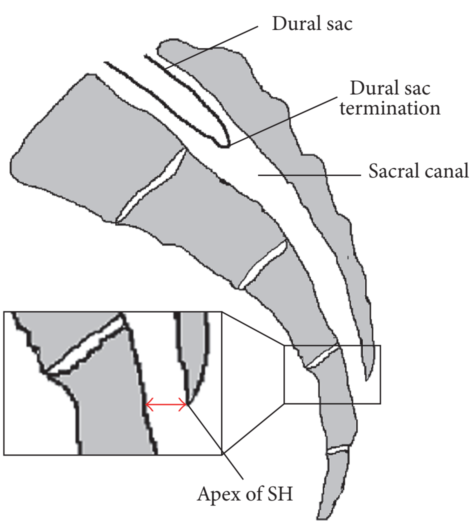

Figure 2: Sagittal view of sacrum. SH: sacral hiatus; red double-ended arrow: anterior-posterior diameter of sacral hiatus at its apex.

of impalpable sacral cornua may be partially accountable for the high failure rate of the blind technique.

2.2. Sacral Hiatus. The sacral hiatus, resulting from failure of fusion of lamina and spinous process of lower sacral vertebrae, is the caudal termination of the sacral canal. The sacral hiatus is bordered laterally by two sacral cornua and could be palpable as a dimple in between. Posteriorly, the sacral hiatus is covered by the skin, subcutaneous fat, and sacrococcygeal ligament (SCL). During caudal epidural block, inserting a needle into the sacral hiatus is essential to access the sacral canal. However, certain anatomic features and variations of sacral hiatus may make it difficult or impossible to insert a needle into the caudal epidural space or predispose this procedure to complications such as dual puncture.

The mean anterior-posterior (AP) diameter of sacral hiatus at its apex ranges from 4.6 ± 2 mm to 6.1 ± 2.1 mm [6, 7, 9–14] and decreased with age [14]. In clinical settings, an AP diameter of sacral hiatus at the apex of less than 3.7 mm was associated with difficulty in inserting a needle into the caudal epidural space by blind technique [13]. When ultrasound is used to guide needle insertion, Chen and colleagues reported that difficulty was encountered in patients with the AP diameter of sacral hiatus at apex of less than 1.6 mm [11]. Similar result has been reported in another study using ultrasound guidance. In that study, the average AP diameter of sacral hiatus at apex in patients with failed caudal epidural needle insertion was 1.61 ± 0.1 mm, significantly shorter than that (4.7 ± 1.7 mm, $P < 0.001$) in patients with successful needle insertion [12]. The incidences of short AP diameter of sacral hiatus at its apex have been reported with different definitions. In studies using dry sacral bone, the sacral AP diameter was less than 3 mm in 8.77% [7] and less than 2 mm in 1%–6.25% of cases [6, 10]. In the extreme, the sacral hiatus is completely closed, precluding inserting a needle into the caudal epidural space via the sacral hiatus. The incidence of closed sacral hiatus was 2-3% from reports studying dry human sacral bone [6, 10].

2.3. Location of the Apex of the Sacral Hiatus. The apex of sacral hiatus is most commonly located at the S4 level (65–68%), followed by the S3 and S5 level (around 15% at each level) and the S1 to S2 level in 3–5% of cases [6, 8]. Complete agenesis of posterior wall of sacral canal (failure of fusion of sacral laminae) was noted in 1% of cases [6]. The higher the apex of sacral hiatus is located, the shorter the distance between it and the dural sac termination could be. Accidental dural puncture might occur if the needle is inserted near the apex of the sacral hiatus that is located at a high level of sacrum. On the other hand, the lower the apex of sacral hiatus is located, the shorter the length of the SCL could be. A length of the SCL of less than 17.6 mm was associated with difficult caudal epidural block by blind technique [13].

2.4. Dural Sac. The dural sac usually terminates between S1 and S2 vertebra, with the majority at S2 [8, 9, 15, 16]. In 1 to 5% of patients, the dural sac terminates at S3 or below [15, 16]. In addition, 1 to 5% of patients with low back pain or sciatica have a sacral Tarlov cyst [15–17], a perineural cyst that communicates with the dural sac and is filled with cerebrospinal fluid (CSF). More than 40% of the sacral Tarlov cysts are located at or below the S3 level [15, 16]. The lower the dural sac termination or the Tarlov cyst is located, the more likely dural puncture or intrathecal injection might occur during caudal epidural block.

2.5. Distance between the Dural Sac Termination and the Apex of the Sacral Hiatus. The distance between the dural sac termination and the apex of the sacral hiatus was the interest of several studies, because the risk of dural puncture is perceived to increase as this distance decreases. The average distance varies markedly from studies conducted in different ethnics. In an Indian cadaver study, the average distance was 32 ± 12 mm, ranging from 5.8 to 60.0 mm [8]. Using magnetic resonance imaging (MRI) for measurement, this distance was 60.3 ± 13.1 mm, ranging from 34 to 80 mm in a British study [9], and 44.6 ± 11.8 mm, ranging from 10 to 80 mm in a Turkish study [16]. As shown by these reports, the distance between the dural sac termination and the apex of the sacral hiatus could be as short as less than 6 mm in some individuals.

3. Techniques of Caudal Epidural Block

3.1. Blind Caudal Epidural Block. The patient can be placed in prone or lateral decubitus position for blind caudal epidural block. A line is draw to connect the bilateral posterior superior iliac crests and used as one side of an equilateral triangle; then the location of the sacral hiatus should be approximated. By palpating the sacral cornua as 2 bony prominences, the sacral hiatus could be identified as a dimple in between. A needle is inserted at 45 degrees to the sacrum and redirected if the posterior surface of sacral bone is contacted. A subjective feeling of "give" or loss of resistance suggests piercing the SCL [18] but is associated with a miss rate up to 26% even in experienced hands [5]. The "whoosh test," performed by auscultation at the thoracolumbar region with a stethoscope while injecting 2 mL of air [19], has a sensitivity of 80% and a specificity of 60% in adults [20]. Palpating for subcutaneous bulging on rapid injection of 5 mL air or saline had a positive predictive value of 83% and a negative predictive value of 44% [4]. The inaccuracy of using blind technique for caudal epidural injection in adults, even confirmed by various tests, is clearly evident.

3.2. Fluoroscopy-Guided Caudal Epidural Block. Because of the inaccuracy of blind technique, some authors have recommended that caudal epidural injection is performed under fluoroscopic guidance [3, 5]. The patient is usually placed in prone position for fluoroscopy-guided caudal epidural block. In lateral view of fluoroscopy, the sacral hiatus could be identified as an abrupt drop off at the end of S4 lamina [21]. The block needle trajectory can be visualized and navigated accordingly into the sacral canal. By injecting contrast medium under fluoroscopy, the placement of needle tip within the sacral epidural space can be verified (Figure 3), and intravascular or intrathecal needle tip placement can be detected. During caudal epidural injection, intravascular injection was reported in 3–14% of cases by conventional fluoroscopy even after negative aspiration [3, 22, 23]. Fluoroscopy guidance has markedly improved the successful rate of caudal epidural block [3–5, 23] and is now considered as the gold standard in performing caudal block. However, routine use of fluoroscopy for caudal epidural block is limited by radiation exposure, cost, and special space requirement.

3.3. Ultrasound-Guided Caudal Epidural Block. The ultrasound-guided caudal block was first described by Klocke and colleagues in 2003 [24] and has, since then, gained increasing popularity. Several studies from various ethnic populations have repeatedly reported very high successful rates (96.9–100%) of ultrasound-guided caudal injection [11, 12, 25–27]. The patient can be placed in prone or lateral decubitus position. Usually, a 7–13 MHz, liner transducer will suffice for most caudal epidural injection; however, a 2–5 MHz, curved transducer may be needed in obese patients. The ultrasound transducer was first placed transversely at the midline to obtain the transverse view of sacral hiatus (Figure 4). The two sacral cornua appear as two hyperechoic structures. Between the sacral cornua are two band-like hyperechoic structures; the superficial one is the SCL, and the deep one is the dorsal surface of sacral bone. The sacral hiatus was the hypoechoic region between the 2 band-like hyperechoic structures [25]. At this level, the ultrasound transducer is rotated 90 degrees to obtain the longitudinal view of sacral hiatus (Figure 5). Under longitudinal view, the block needle is inserted using the "in-plane" technique. The block needle can be visualized in real time, piercing the SCL, entering the sacral hiatus, but cannot be visualized beyond the apex of sacral hiatus. Therefore, without knowledge of dural sac termination from image study in advance, it is suggested that advancement of needle tip beyond the apex of sacral hiatus be limited to 5 mm to avoid dural puncture because the distance between the apex of sacral hiatus and dural sac termination can be as short as less than 6 mm [7].

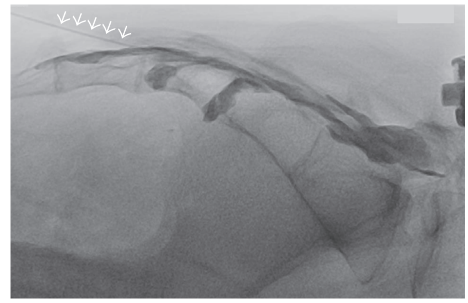

Figure 3: Fluoroscopy-guided caudal epidural block. Proper needle tip placement was verified by observing spread of contrast medium within the epidural space without intravascular uptake. Arrows: needle.

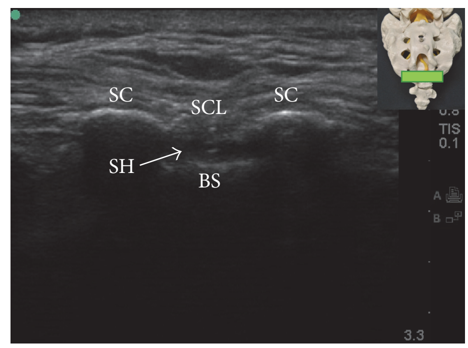

Figure 4: Transverse ultrasound view of the sacral hiatus. The inset shows the position of the ultrasound transducer. BS: base of sacrum; SC: sacral cornua; SCL: sacrococcygeal ligament; SH: sacral hiatus.

Although ultrasonography cannot provide information regarding injectate spreading during caudal epidural injection as fluoroscopy, the presence of unidirectional flow, defined as one dominant color on color Doppler image, in the longitudinal view of sacral hiatus during injection (Figure 6) was reported to be predictive of successful caudal epidural injection [27, 28] and comparable treatment outcome as fluoroscopy-guided caudal epidural injection [28]. The ultrasonography could also provide information regarding the cephalad spreading of injectate during caudal epidural injection. Using a curved-array, low frequency (2–5 MHz)

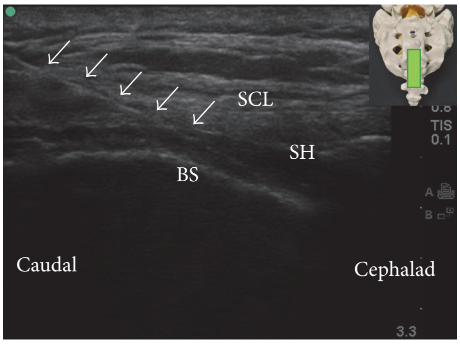

Figure 5: Longitudinal ultrasound view of sacral hiatus. The inset shows the position of the ultrasound transducer. BS: base of sacrum; SCL: sacrococcygeal ligament; SH: sacral hiatus; arrows: needle.

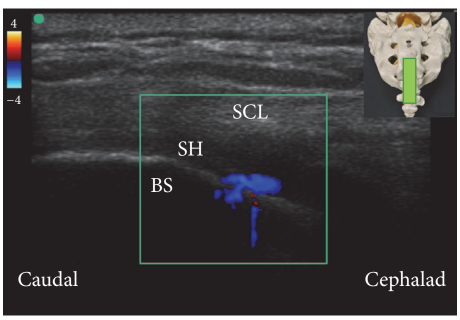

Figure 6: Color Doppler ultrasonography in longitudinal view of sacral hiatus. A predominantly one-color spectrum is observed in the sacral hiatus during caudal epidural injection. The inset shows the position of the ultrasound transducer. BS: base of sacrum; SCL: sacrococcygeal ligament; SH: sacral hiatus.

ultrasound transducer, the lumbar spinal canal could be visualized by the paramedian sagittal oblique view described by Chin and colleagues [29]. Observing color Doppler signal in the lumbar spinal canal during caudal epidural injection may indicate that the injectate has reached the lumbar epidural space (Figure 7), although this hypothesis needs to be confirmed in further studies.

While fluoroscopy with contrast medium injection is still considered the gold standard in preventing intravascular and intrathecal injection, ultrasonography could be, at least, as useful as fluoroscopy in preventing other complications during caudal epidural injection. For example, with the needle tip visualized real time going into the sacral hiatus by ultrasonography, advertently advancing the needle anteriorly into the rectum [30, 31] or a fetal skull in the birth canal [30] can be prevented. The practice of injecting air to verify needle tip position could be abandoned, because the injected air has been reported to cause portal vein air embolism [32] and motor weakness [33] after caudal epidural injection. In addition, ultrasound has some advantages over the fluoroscopy in guiding caudal epidural injection because it is easy to learn and radiation-free and can be virtually used in any clinical settings [25].

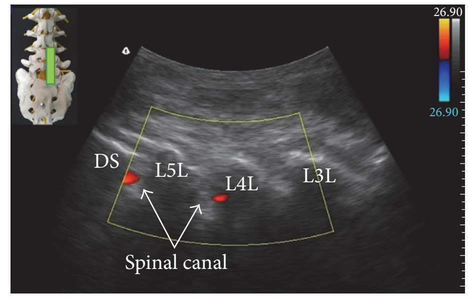

Figure 7: Color Doppler ultrasonography in paramedian sagittal oblique view of the sacral and lumbar spine. The observed color spectrum suggests the flow of injectate reaching L4-5 level. The inset shows the position of the ultrasound transducer. L3L: L3 lamina; L4L: L4 lamina; L5L: L5 lamina; DS: dorsal surface of sacrum.

4. Conclusion

There are considerable anatomic variations relevant to caudal epidural block, which may contribute to failed block by landmark-based blind technique. The advent of fluoroscopy and ultrasound has markedly improved the successful rates of caudal epidural injection. Although fluoroscopy remains the gold standard in guiding caudal epidural injection, it is not always available and radiation exposure is a concern. In addition, routine use of fluoroscopy for caudal epidural injection seems impractical in the busy operating theater and office-based clinics. Given accumulating evidence has suggested that ultrasonography is excellent in guiding caudal epidural injection with similar treatment outcome as compared with fluoroscopy-guided caudal epidural injection, ultrasound should be the preferred alternative when fluoroscopy is not available.

Competing Interests

The authors declare that there is no conflict of interests regarding the publication of this paper.

References

[1] B. Dalens and A. Hasnaoui, "Caudal anesthesia in pediatric surgery: success rate and adverse effects in 750 consecutive patients," *Anesthesia and Analgesia*, vol. 68, no. 2, pp. 83–89, 1989.

[2] R. M. Orme and S. J. Berg, "The 'swoosh' test—an evaluation of a modified 'whoosh' test in children," *British Journal of Anaesthesia*, vol. 90, pp. 62–65, 2003.

[3] D. L. Renfrew, T. E. Moore, M. H. Kathol, G. Y. El-Khoury, J. H. Lemke, and C. W. Walker, "Correct placement of epidural steroid injections: fluoroscopic guidance and contrast administration," *American Journal of Neuroradiology*, vol. 12, no. 5, pp. 1003–1007, 1991.

[4] M. Y. Stitz and H. M. Sommer, "Accuracy of blind versus fluoroscopically guided caudal epidural injection," *Spine*, vol. 24, no. 13, pp. 1371–1376, 1999.

[5] G. Barham and A. Hilton, "Caudal epidurals: the accuracy of blind needle placement and the value of a confirmatory

epidurogram," *European Spine Journal*, vol. 19, no. 9, pp. 1479–1483, 2010.

[6] M. Sekiguchi, S. Yabuki, K. Satoh, and S. Kikuchi, "An anatomic study of the sacral hiatus: a basis for successful caudal epidural block," *Clinical Journal of Pain*, vol. 20, no. 1, pp. 51–54, 2004.

[7] A. Aggarwal, A. Aggarwal, Harjeet, and D. Sahni, "Morphometry of sacral hiatus and its clinical relevance in caudal epidural block," *Surgical and Radiologic Anatomy*, vol. 31, no. 10, pp. 793–800, 2009.

[8] A. Aggarwal, H. Kaur, Y. K. Batra, A. K. Aggarwal, S. Rajeev, and D. Sahni, "Anatomic consideration of caudal epidural space: A Cadaver Study," *Clinical Anatomy*, vol. 22, no. 6, pp. 730–737, 2009.

[9] I. M. Crighton, B. P. Barry, and G. J. Hobbs, "A study of the anatomy of the caudal space using magnetic resonance imaging," *British Journal of Anaesthesia*, vol. 78, no. 4, pp. 391–395, 1997.

[10] N. Senoglu, M. Senoglu, H. Oksuz et al., "Landmarks of the sacral hiatus for caudal epidural block: an anatomical study," *British Journal of Anaesthesia*, vol. 95, no. 5, pp. 692–695, 2005.

[11] C. P. Chen, A. M. Wong, C.-C. Hsu et al., "Ultrasound as a screening tool for proceeding with caudal epidural injections," *Archives of Physical Medicine and Rehabilitation*, vol. 91, no. 3, pp. 358–363, 2010.

[12] M. Nikooseresht, M. Hashemi, S. A. Mohajerani, F. Shahandeh, and M. Agah, "Ultrasound as a screening tool for performing caudal epidural injections," *Iranian Journal of Radiology*, vol. 11, no. 2, Article ID e13262, 2014.

[13] Y. H. Kim, H. J. Park, S. Cho, and D. E. Moon, "Assessment of factors affecting the difficulty of caudal epidural injections in adults using ultrasound," *Pain Research and Management*, vol. 19, no. 5, pp. 275–279, 2014.

[14] G.-Y. Park, D. R. Kwon, and H. K. Cho, "Anatomic differences in the sacral hiatus during caudal epidural injection using ultrasound guidance," *Journal of Ultrasound in Medicine*, vol. 34, no. 12, pp. 2143–2148, 2015.

[15] J. Joo, J. Kim, and J. Lee, "The prevalence of anatomical variations that can cause inadvertent dural puncture when performing caudal block in Koreans: A Study Using Magnetic Resonance Imaging," *Anaesthesia*, vol. 65, no. 1, pp. 23–26, 2010.

[16] N. Senoglu, M. Senoglu, F. Ozkan, C. Kesilmez, B. Kizildag, and M. Celik, "The level of termination of the dural sac by MRI and its clinical relevance in caudal epidural block in adults," *Surgical and Radiologic Anatomy*, vol. 35, no. 7, pp. 579–584, 2013.

[17] R. D. Paulsen, G. A. Call, and F. R. Murtagh, "Prevalence and percutaneous drainage of cysts of the sacral nerve root sheath (Tarlov cysts)," *American Journal of Neuroradiology*, vol. 15, no. 2, pp. 293–297, 1994.

[18] R. Brull, A. J. R. MacFarlane, and V. W. S. Chan, "Spinal, epidural, and caudal anesthesia," in *Miller's Anesthesia*, R. D. Miller, Ed., pp. 1684–1720, Elsevier Health Sciences, 2015.

[19] M. P. N. Lewis, P. Thomas, L. F. Wilson, and R. C. Mulholland, "The "whoosh" test: a Clinical test to confirm correct needle placement in caudal epidural injections," *Anaesthesia*, vol. 47, no. 1, pp. 57–58, 1992.

[20] D. Eastwood, C. Williams, and I. Buchan, "Caudal epidurals: the whoosh test," *Anaesthesia*, vol. 53, no. 3, pp. 305–307, 1998.

[21] M. H. Landers and C. N. Aprill, "Epidural steroid injections," in *Pain Procedures in Clinical Practice*, T. A. Lennard, D. G. Vivian, S. D. Walkowski, and A. K. Singla, Eds., pp. 313–356, Elsevier Health Sciences, 3rd edition, 2011.

[22] W. J. Sullivan, S. E. Willick, W. Chira-Adisai et al., "Incidence of intravascular uptake in lumbar spinal injection procedures," *Spine*, vol. 25, no. 4, pp. 481–486, 2000.

[23] L. Manchikanti, K. A. Cash, V. Pampati, C. D. Mcmanus, and K. S. Damron, "Evaluation of fluoroscopically guided caudal epidural injections," *Pain Physician*, vol. 7, no. 1, pp. 81–92, 2004.

[24] R. Klocke, T. Jenkinson, and D. Glew, "Sonographically guided caudal epidural steroid injections," *Journal of Ultrasound in Medicine*, vol. 22, no. 11, pp. 1229–1232, 2003.

[25] C. P. C. Chen, S. F. T. Tang, T.-C. Hsu et al., "Ultrasound guidance in caudal epidural needle placement," *Anesthesiology*, vol. 101, no. 1, pp. 181–184, 2004.

[26] A. Blanchais, B. Le Goff, P. Guillot, J.-M. Berthelot, J. Glemarec, and Y. Maugars, "Feasibility and safety of ultrasound-guided caudal epidural glucocorticoid injections," *Joint Bone Spine*, vol. 77, no. 5, pp. 440–444, 2010.

[27] J. S. Yoon, K. H. Sim, S. J. Kim, W. S. Kim, S. B. Koh, and B. J. Kim, "The feasibility of color Doppler ultrasonography for caudal epidural steroid injection," *Pain*, vol. 118, pp. 210–214, 2005.

[28] Y. Park, J.-H. Lee, K. D. Park, J. K. Ahn, J. Park, and H. Jee, "Ultrasound-guided vs. fluoroscopy-guided caudal epidural steroid injection for the treatment of unilateral lower lumbar radicular pain: A Prospective, Randomized, Single-blind Clinical Study," *American Journal of Physical Medicine and Rehabilitation*, vol. 92, no. 7, pp. 575–586, 2013.

[29] K. J. Chin, M. K. Karmakar, and P. Peng, "Ultrasonography of the adult thoracic and lumbar spine for central neuraxial blockade," *Anesthesiology*, vol. 114, no. 6, pp. 1459–1485, 2011.

[30] C. J. Dawkins, "An analysis of the complications of extradural and caudal block," *Anaesthesia*, vol. 24, no. 4, pp. 554–563, 1969.

[31] V. Sathianathan and N. Dobby, "Rectal puncture complicating caudal blockade in a child with severe rectal distension," *Paediatric Anaesthesia*, vol. 25, no. 10, pp. 1063–1065, 2015.

[32] T. Fujikawa and S. Murai, "Portal venous gas after a caudal block," *BMJ case reports*, vol. 2014, 2014.

[33] M. H. Lee, C. S. Han, S. H. Lee et al., "Motor weakness after caudal epidural injection using the air-acceptance test," *Korean Journal of Pain*, vol. 26, no. 3, pp. 286–290, 2013.

Hindawi
BioMed Research International
Volume 2017, Article ID 7023750, 9 pages
https://doi.org/10.1155/2017/7023750

Review Article

Ultrasound-Guided Obturator Nerve Block: A Focused Review on Anatomy and Updated Techniques

Takayuki Yoshida, Tatsuo Nakamoto, and Takahiko Kamibayashi

Department of Anesthesiology, Kansai Medical University Hospital, 2-3-1 Shin-machi, Hirakata City, Osaka, Japan

Correspondence should be addressed to Takayuki Yoshida; ytaka@mac.com

Received 21 November 2016; Accepted 23 January 2017; Published 9 February 2017

Academic Editor: Ayhan Cömert

This review outlines the anatomy of the obturator nerve and the indications for obturator nerve block (ONB). Ultrasound-guided ONB techniques and unresolved issues regarding these procedures are also discussed. An ONB is performed to prevent thigh adductor jerk during transurethral resection of bladder tumor, provide analgesia for knee surgery, treat hip pain, and improve persistent hip adductor spasticity. Various ultrasound-guided ONB techniques can be used and can be classified according to whether the approach is distal or proximal. In the distal approach, a transducer is placed at the inguinal crease; the anterior and posterior branches of the nerve are then blocked by two injections of local anesthetic directed toward the interfascial planes where each branch lies. The proximal approach comprises a single injection of local anesthetic into the interfascial plane between the pectineus and obturator externus muscles. Several proximal approaches involving different patient and transducer positions are reported. The proximal approach may be superior for reducing the dose of local anesthetic and providing successful blockade of the obturator nerve, including the hip articular branch, when compared with the distal approach. This hypothesis and any differences between the proximal ONB techniques need to be explored in future studies.

1. Introduction

Obturator nerve block (ONB) is commonly performed to prevent sudden thigh adduction during transurethral resection of bladder tumor (TURBT) [1–3], to provide optimal analgesia for knee surgery [4–6], to treat chronic hip pain [7–9], and to improve persistent hip adductor spasticity in patients with paraplegia, multiple sclerosis, or cerebral palsy [10–12]. Labat first described an ONB technique based on surface landmarks in 1922 [13]. Since then, several ONB approaches using surface landmarks with or without nerve stimulation to localize the nerve have been reported [14–16]. During the last decade, ultrasound-guided ONB techniques have gained immense popularity, as have other types of peripheral nerve block. In this review, we describe the anatomy of the obturator nerve, illustrate the ultrasound-guided ONB techniques reported thus far, and identify issues that need to be addressed in the future.

2. Anatomy of the Obturator Nerve

The obturator nerve arises from the anterior rami of the second, third, and fourth lumbar nerves. The nerve descends through psoas major and emerges from the medial border of this muscle. The obturator nerve then runs along the lateral wall of the lesser pelvis and extends to the anterior thigh after passing through the obturator canal. During its course, the obturator nerve divides into anterior and posterior branches. In a cadaveric study, bifurcation of these two main branches of the obturator nerve was determined to be intrapelvic (23.22%), within the obturator canal (51.78%), or in the medial thigh (25%) [17]. The anterior and posterior branches of the obturator nerve, or the common obturator nerve, run between the pectineus and obturator externus muscles immediately after the nerve emerges from the obturator canal (Figure 1(a)). Beyond this point, the two branches are usually separated by some of the fibers of the obturator externus muscle. The anterior obturator nerve branch initially passes through

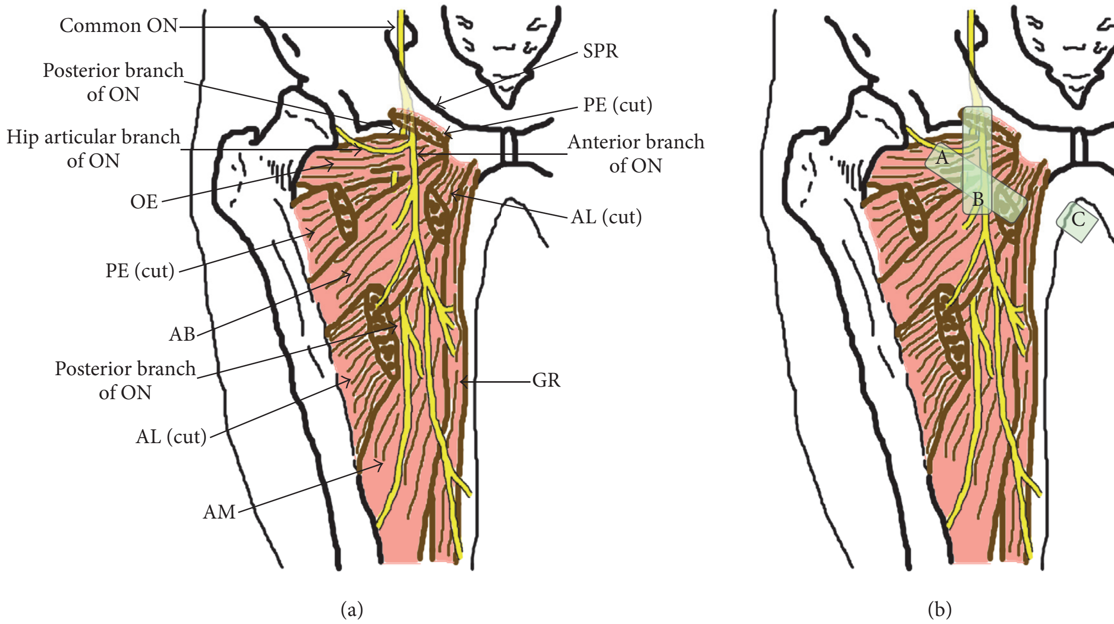

Figure 1: (a) Illustration showing the right-sided adductor muscles and the course of the obturator nerve. (b) Illustration of the positional relationship between the adductor muscles, the obturator nerve, and the transducer during each ultrasound-guided obturator nerve block technique. Large green squares with the letter A or B indicate the foot print position of the transducer. A small green square with the letter C indicates the side position of the transducer. In the distal approach, the transducer is placed at position A. In the proximal approaches reported by Anagnostopoulou et al. [17], Taha [23], and Lin et al. [42], the transducer is tilted cranially at position A to allow visualization of the plane between the pectineus and obturator externus muscles. In the approach used by Akkaya et al. [35], the transducer is placed at position B to allow visualization of the same plane in the sagittal view. Using the approach described by Yoshida et al. [31], the transducer is placed at position C in the lithotomy position to see the plane between the pectineus and obturator externus muscles. ON, obturator nerve; AL, adductor longus muscle; AB, adductor brevis muscle; AM, adductor magnus muscle; PE, pectineus muscle; OE, obturator externus muscle; SPR, superior pubic ramus; GR, gracilis muscle.

the interfascial plane between the pectineus and adductor brevis muscles. Further caudad, it runs between the adductor longus and adductor brevis muscles, innervating the adductor longus, adductor brevis, and gracilis muscles (Figure 1(a)). The anterior branch rarely innervates the pectineus muscle [17]. The posterior obturator nerve branch travels in the fascia between the adductor brevis and adductor magnus muscles (Figure 1(a)). Throughout its course, the nerve usually supplies multiple branches to the adductor magnus and adductor brevis muscles and occasionally innervates the obturator externus and adductor longus muscles as well [17]. The obturator nerve also provides articular branches for the hip and knee joints [17, 18]. The articular branch supplying the hip joint is derived from the common obturator nerve or its branches at different levels in conjunction with the obturator canal [17]. The posterior branch of the obturator nerve supplies terminal branches to the capsule of the knee joint in some individuals [17, 19, 20]. The typical cutaneous distribution of the obturator nerve is described in most textbooks to be the medial side of the thigh and above the medial side of the knee. However, the obturator nerve provides no cutaneous innervation in more than 50% of cases [21].

3. Indications

3.1. ONB for TURBT. The obturator nerve is situated directly adjacent to the lateral wall of the bladder during TURBT when the irrigation fluid used in this procedure fills the bladder. Any electrical stimulation caused by tumor resection involving the bladder may induce sudden adductor muscle contraction, which may lead to perforation of the bladder accompanied by extravesical spread of the tumor and even injury to the obturator artery [1–3, 22]. Sudden thigh movement and bladder perforation were reported to occur in 40% and 5.7% of patients, respectively, during TURBT involving the lateral wall of the bladder in the absence of ONB [3]. One retrospective study comparing recurrence rates in patients with a bladder tumor on the lateral wall and receiving TURBT with or without ONB demonstrated that an ONB could prolong the mean time to recurrence of the bladder tumor (7.8 months versus 15 months, resp.) [2]. This finding suggests that an ONB can facilitate complete resection of a tumor situated on the lateral wall of the bladder by immobilizing the surgical field. An ONB is essential for performing TURBT safely and effectively.

3.2. ONB for Knee Surgery. The knee joint capsule is partially innervated by the obturator nerve [17, 20]. In addition, an ONB is crucial for painless harvesting of the gracilis tendon in anterior cruciate ligament reconstruction because the anterior branch of the obturator nerve innervates the gracilis muscle [17, 23]. Addition of ONB to a femoral nerve block improves analgesia following both total knee replacement [4, 5] and anterior cruciate ligament reconstruction [6, 23].

3.3. ONB for Hip Surgery. The hip joint receives sensory innervation from branches of the femoral, obturator, superior gluteal, and sciatic nerves, as well as the nerve to quadratus femoris [18]. Among these, the articular branch of the obturator nerve innervates the anteromedial hip joint capsule. It remains unclear whether an ONB alone can significantly improve the management of acute pain after hip surgery, although one randomized controlled trial demonstrated that a combination of obturator and lateral femoral cutaneous nerve blockade was effective in controlling acute pain after surgery for hip fracture [24].

3.4. ONB for Pain Therapy and Hip Adductor Spasticity. Groin and thigh pain frequently arises from the articular branch of the obturator nerve, whereas trochanteric pain arises from the articular branch of the femoral nerve [8]. The nerve responsible for hip joint pain can be detected by a diagnostic nerve block using a local anesthetic. Two case series reports have suggested that percutaneous radiofrequency lesioning or pulsed radiofrequency treatment of the articular branch of the obturator nerve, performed under fluoroscopy guidance, can be an effective alternative treatment in patients with hip joint pain if a diagnostic ONB provides transient pain relief at the hip joint [8, 9].

Persistent hip adductor spasticity is a major complication of spinal cord injury, traumatic brain injury, cerebral palsy, and multiple sclerosis. Hip adductor spasticity causes hip joint deformity, pain, and scissoring of the hips, which prevents maintenance of perineal hygiene, leading to breakdown and infection of the skin in patients requiring long-term care. Some case series have reported that ONB using a neurolytic agent is effective for treatment of hip adductor spasticity in both adult and pediatric patients [10, 11, 25]. Recently, one randomized controlled trial has demonstrated that ONB guided by both ultrasound and electrical simulation using phenol as a treatment for severe hip adductor spasticity in patients requiring long-term care decreases the severity of hip adductor spasticity, improves the hygiene score, and increases the distance between the knees during passive hip abduction [12].

4. Evaluation of ONB

As described above, the obturator nerve provides no cutaneous innervation in more than half of individuals; therefore, successful ONB can be achieved despite a lack of sensory block at the medial thigh and/or knee. The success of ONB is evaluated by confirming a decrease in adductor muscle strength using a sphygmomanometer as described by Lang et al. [26]. Using this measurement method, patients are asked to extend both knees fully, dorsiflex both ankles in the supine position, and squeeze a blood pressure cuff (preinflated to 40 mmHg) between their knees by adducting the blocked hip while the nonblocked leg is restrained. The maximal pressure sustained is defined as adductor muscle strength. The adductor magnus muscle is innervated by both the posterior branch of the obturator nerve and the sciatic nerve [27]. Similarly, the femoral nerve also innervates the pectineus muscle [28]. Further, the pectineus muscle is occasionally (in 10%–30% of cases) innervated by the accessory obturator nerve, which arises from the anterior rami of the third and fourth lumbar nerves, descends along the medial border of the psoas major muscle, and passes above the superior pubic ramus [28, 29]. Thus, patients may adduct the hip joint to some extent even if ONB is successful. According to previous studies [30, 31], a decrease in adductor muscle strength of more than 40%–50% has been defined as successful ONB.

5. Ultrasound-Guided ONB Techniques

In recent times, ultrasound guidance has been used to improve the success rate and safety profile of peripheral nerve blocks, including ONB. The success rate of landmark-based nerve stimulation-guided ONB in prevention of adductor muscle contraction during TURBT has been reported to be between 84% and 96% [32, 33]. A number of studies have reported that ultrasound-guided ONB is associated with higher success rates of 93%–100% [23, 30, 31, 34–37], although there has been no direct comparison between ultrasound-guided ONB and other techniques. Inadvertent vessel puncture and nerve injury during nerve block procedures would be decreased by correct ultrasound guidance, although unintended obturator vein puncture has been reported even during an ultrasound-guided proximal level ONB [35].

Many ultrasound-guided ONB approaches have been reported and can be classified as distal or proximal.

5.1. Distal ONB Approach. The distal approach is defined as one in which the anterior and posterior branches of the obturator nerve are blocked separately by two injections of local anesthetic directed toward the interfascial planes where each branch lies. Patients are placed in the supine position with the thigh slightly abducted and externally rotated. An ultrasound transducer is placed at the inguinal crease and perpendicular to the skin (Figures 1(b) and 2(a)) to identify the pectineus, adductor longus, adductor brevis, and adductor magnus muscles (Figure 3(a)). Local anesthetics are injected into the fascia between the pectineus and adductor brevis muscles [30] or between the adductor longus and adductor brevis muscles [38, 39] using in-plane ultrasound guidance to block the anterior branch of the obturator nerve. Subsequently, local anesthetic is injected in the fascia between the adductor brevis and adductor magnus muscles to block the posterior branch of the obturator nerve [30, 38]. Concomitant use of nerve stimulation guidance is recommended when performing ONB using the distal approach because the anatomic variability in the path of the branches of the obturator nerve would be greater at the more distal thigh [30]. The interfascial plane between the adductor brevis and magnus muscles is located relatively

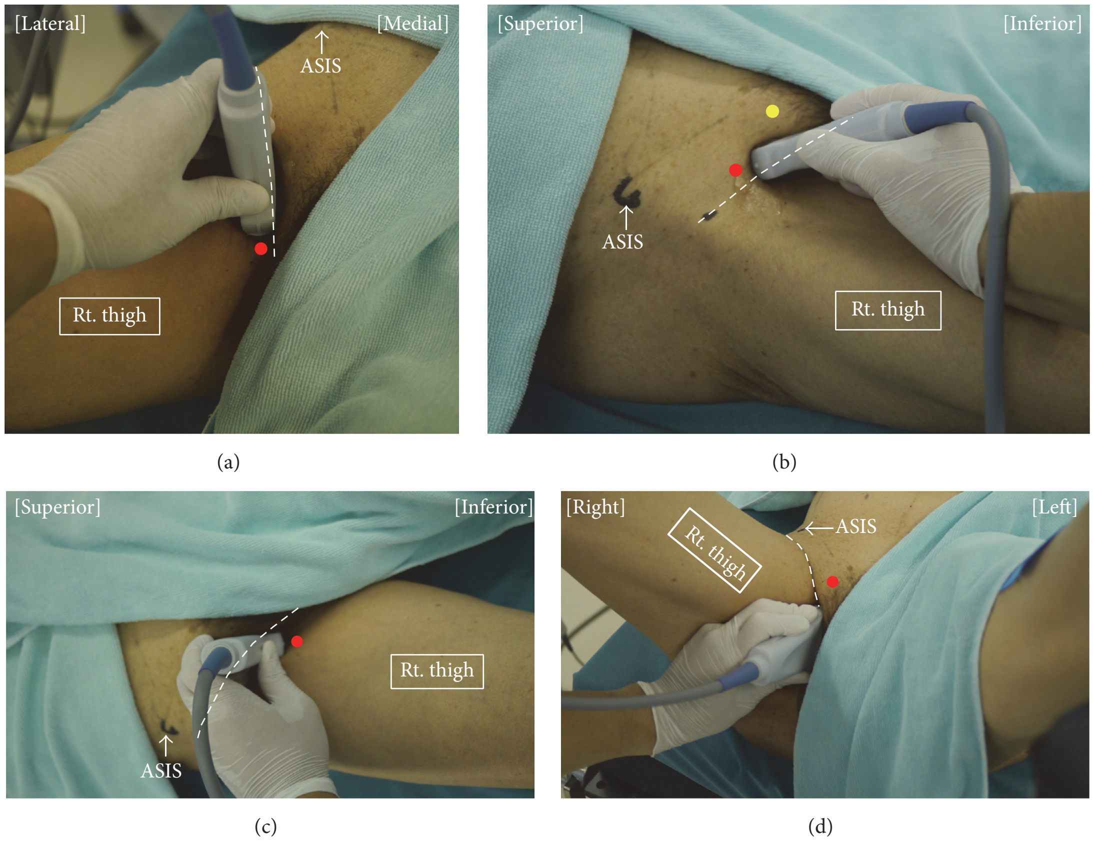

Figure 2: Patient and transducer positions for performance of each ultrasound-guided right-sided obturator nerve block technique. The dotted lines indicate the inguinal crease. (a) The patient is placed in the supine position with his hip slightly abducted and externally rotated. In the distal approach for obturator nerve block, the transducer is placed medial to the femoral vein, along the inguinal crease, perpendicularly to the skin. A needle is inserted from the point indicated by the red circle, in-plane with the transducer, in a medial-to-lateral direction. (b) The transducer is tilted cranially from the position shown in Figure 2(a) to obtain an ultrasound image similar to that in Figure 3(b). A needle is inserted from the point indicated by the yellow circle in an anterior-to-posterior direction using out-of-plane ultrasound guidance in the approach devised by Taha [23]. In the approach used by Lin et al. [42], a needle is inserted from the point indicated by the red circle, in a lateral-to-medial direction, using in-plane ultrasound guidance. (c) The technique described by Akkaya et al. [35] can be performed with the patient in a supine position and his/her leg straight. The transducer is placed in the sagittal plane on the inguinal crease between the femoral vein and the pubic tubercle. A needle is inserted from the point indicated by the red circle, in-plane with the transducer, in an inferior-to-superior direction. (d) In the approach devised by Yoshida et al. [31], the patient is placed in the lithotomy position. The transducer is placed immediately lateral to the perineum on the medial aspect of the thigh along the extended line of the inguinal crease and orientated cephalad. A needle is inserted 2-3 cm cephalad from the anterior side of the transducer (red circle) and advanced in-plane with the transducer in an anterior-to-posterior direction. ASIS, anterior superior iliac spine.

deeper. Thus, blockade of the posterior branch requires a steeper angle of needle insertion, which compromises visibility of the needle under ultrasound [40, 41]. ONB at the distal level requires at least two interfascial injections of local anesthetic, so it involves use of a larger volume of local anesthetic than that provided by the single interfascial injection used in the proximal approach, although there has been no research comparing the two approaches in this respect.

Sudden adductor muscle contraction during TURBT might occur even if an ONB using the distal approach is correctly performed because of various patterns of ramification of the obturator nerve when it terminates in the adductor muscles [17]. In other words, an obturator nerve branch, which diverges proximal to the inguinal crease, might not be blocked by the distal ONB approach. Using the distal approach, the local anesthetic injection points are also further away from the bifurcation of the hip joint branch of the obturator nerve when compared with the proximal approach, resulting in less possibility of blockade of the hip joint branch.

5.2. Proximal ONB Approach. Taha reported that ultrasound-guided injection of local anesthetic into the interfascial plane between the pectineus and obturator externus muscles successfully produces blockade of both the anterior and posterior branches of the obturator nerve [23]. Yoshida et al. reported that a dye injected into the plane between the pectineus and obturator externus muscles of a cadaver spread into the pelvic cavity through the obturator canal, staining the anterior and posterior branches of the obturator nerve and the common obturator nerve within the obturator canal [31]. Both the

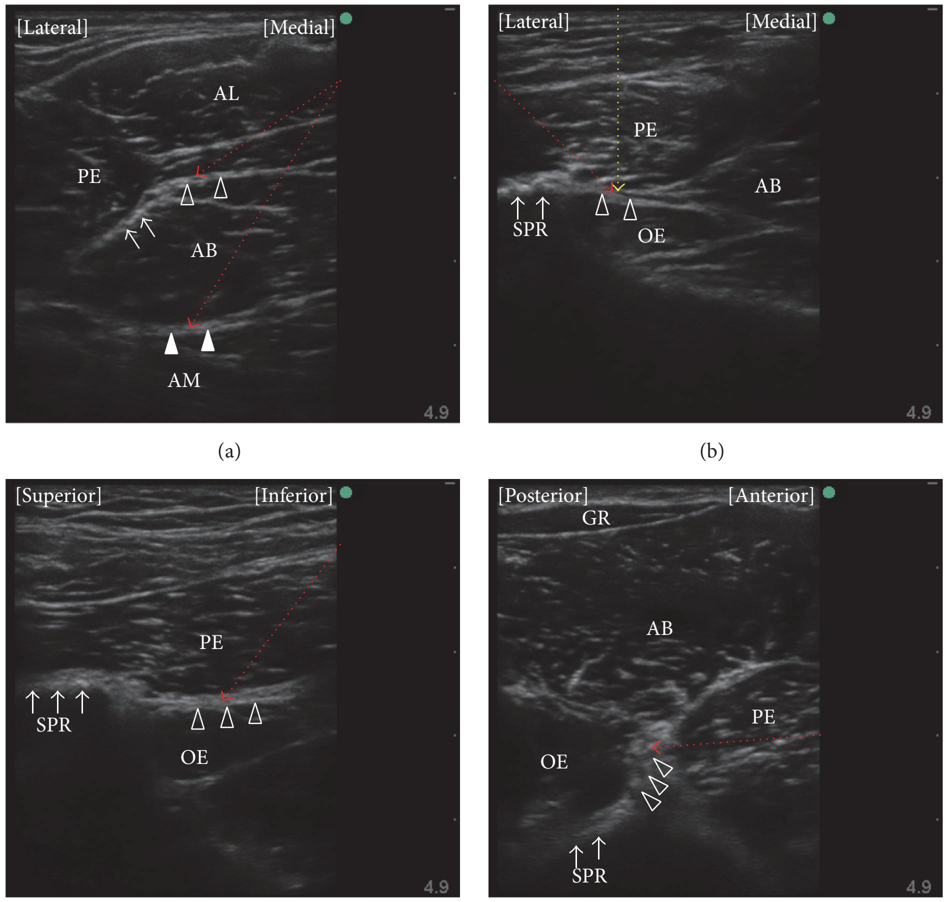

(a) (b) (c) (d)

Figure 3: Ultrasound images obtained during obturator nerve block. (a) A preprocedure view of the distal approach, which is obtained with the transducer located as in Figure 2(a). The anterior branch of the obturator nerve is located at the hyperechoic thick fascia between the adductor brevis muscle and the pectineus (arrows) or adductor longus (open triangles) muscles. The posterior branch of the obturator nerve lies within the fascia between the adductor brevis and adductor magnus muscles (closed triangles). A needle is introduced into these fasciae in a medial-to-lateral (red dotted lines) or lateral-to-medial direction under in-plane ultrasound guidance. (b) A preprocedure view obtained with the transducer located as in Figure 2(b). A hyperechoic structure with an acoustic shadow (arrows) represents the superior pubic ramus. The target for injection of local anesthetic is the fascia, which is seen as contiguous with the superior pubic ramus and located between the pectineus and obturator externus muscles (open triangles). In the approach used by Taha [23], a needle is introduced into this plane under out-of-plane ultrasound guidance (yellow dotted line). In the approach used by Lin et al. [42], a needle is inserted into this plane under in-plane ultrasound guidance in a lateral-to-medial direction (red dotted line). (c) A preprocedure view obtained with the transducer located as in Figure 2(c). Hyperechoic thick fascia between the pectineus and obturator externus muscles (open triangles) is seen inferior to a hyperechoic structure with an acoustic shadow, which represents the superior pubic ramus (arrows). A needle is inserted into this fascia under in-plane ultrasound guidance in an inferior-to-superior direction (red dotted line). (d) A preprocedure view obtained with the transducer located as in Figure 2(d). The obturator externus muscle is seen superficial to the superior pubic ramus (arrows) and the pectineus muscle is seen anterior to the obturator externus muscle. A hyperechoic thick fascia between the pectineus and obturator externus muscles (open triangles) is the target plane. As a needle is inserted 3 cm cephalad from the anterior side of the transducer and advanced in-plane with the transducer toward this fascia in this case (red dotted line), the needle-ultrasound beam angles come to be almost perpendicular. AL, adductor longus muscle; AB, adductor brevis muscle; AM, adductor magnus muscle; PE, pectineus muscle; OE, obturator externus muscle; SPR, superior pubic ramus; GR, gracilis muscle.

anterior and posterior branches of the obturator nerve may run over the obturator externus muscle whereas the posterior branch passes through some fibers of the obturator externus muscle immediately after its emergence from the obturator canal in some cases [17]. Even in these cases, local anesthetics injected into the plane between the pectineus and obturator externus muscles can block both the anterior and posterior branches of the obturator nerve by spreading around these branches and/or the common obturator nerve along the obturator canal, as reported by Yoshida et al. [31]. This retrograde spread of liquid through the obturator canal is key to understanding why the ultrasound-guided proximal

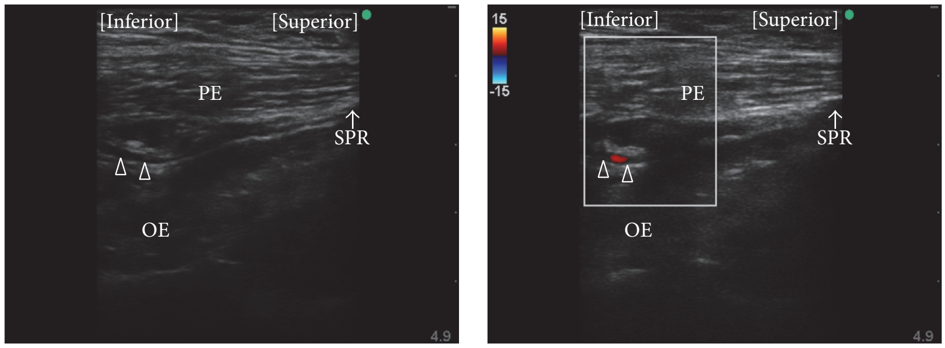

(a) (b)

Figure 4: Observation of the obturator artery. (a) Long axis view of a luminal structure (open triangles) is seen at the plane between the pectineus and obturator externus muscles during preprocedure observation using the approach described by Akkaya et al. [35]. (b) The luminal structure was confirmed to be the obturator artery using color flow Doppler. PE, pectineus muscle; OE, obturator externus muscle; SPR, superior pubic ramus.

approach for ONB, which is provided by a single interfascial injection of local anesthetic, works successfully. Several proximal approaches for ONB have been reported [17, 23, 31, 35, 42], all of which target the plane between the pectineus and obturator externus muscles as the site for injection of local anesthetic but use different patient positions (i.e., supine or lithotomy), transducer locations (i.e., the inguinal crease or medial thigh), modes of needle insertion (i.e., out-of-plane or in-plane), and needle trajectories (i.e., anterior-to-posterior, inferior-to-superior, or lateral-to-medial).

The same patient and transducer positions were used in the reports published by Anagnostopoulou et al. [17], Taha [23], and Lin et al. [42]. These proximal approaches are performed with the patient in the supine position and the hip slightly abducted and externally rotated. The lack of need to change the position of the patient would be the greatest advantage of these techniques when the surgery is also performed in the supine position. A linear ultrasound transducer is first placed at the inguinal crease perpendicular to the skin. Subsequently, the transducer is tilted 40–50 degrees cranially (Figures 1(b) and 2(b)) until a hyperechoic structure deep and lateral to the pectineus muscle, which represents the inferior margin of the superior pubic ramus, is seen (Figure 3(b)). In this view, the target interfascial plane is seen deep in relation to the pectineus muscle separating it from the obturator externus muscle (Figure 3(b)). Using the approach described by Anagnostopoulou et al. [17] and Taha [23], the needle is inserted using out-of-plane ultrasound guidance without nerve stimulation. Out-of-plane ultrasound-guided needle insertion is essentially inferior to an in-plane technique in terms of being able to observe the position of the needle tip in real time [43], although Taha reported a 100% success rate without complication using his approach in 60 patients [23]. The approach devised by Lin et al. [42] entails in-plane lateral-to-medial needle insertion with the same transducer position. In-plane ultrasound guidance allows visualization of the needle tip in real time, which may help to decrease the risk of inadvertent vessel or nerve injury. On the other hand, if the transducer is tilted to a significant degree, it can be difficult to align the needle insertion point with the transducer position and see the needle and target simultaneously under in-plane ultrasound guidance [40].

Akkaya et al. evaluated a further proximal approach in both cadaveric and clinical studies [35]. Using that approach, the patient is placed in the supine position and an ultrasound transducer is introduced in the sagittal plane at the pubic region between the femoral vein and the pubic tubercle (Figures 1(b) and 2(c)) to visualize the superior pubic ramus, the pectineus muscle, and the obturator externus muscle (Figure 3(c)). A block needle is inserted in an inferior-to-superior direction toward the plane between the pectineus and obturator externus muscles under in-plane ultrasound guidance using peripheral nerve stimulation. This approach has a potential advantage contributed by in-plane ultrasound guidance, that is, real-time visualization of the needle tip. However, the relatively steep angle of needle insertion required because of the deep location of the target did not allow good visualization of the needle under in-plane ultrasound guidance. Further, obturator vein puncture occurred in one patient during the clinical application portion of this study [35]. The obturator artery and vein usually descend through the obturator canal from the pelvic cavity; thus, using the approach of Akkaya et al., the long axis of the transducer can be placed parallel to these vessels just as they emerge from the obturator canal [44, 45] (Figure 4). Even slight sliding or tilting of transducer may result in failure to capture an object that exists parallel to the long axis of the transducer under in-plane ultrasound guidance because the width of ultrasound beam is less than 1 mm. We speculate that the inadvertent puncture of an obturator vein in this study occurred because of the positional relationship between the transducer and vessels when this approach is used.

Most recently, Yoshida et al. have described a new approach for proximal level ONB [31]. This approach differs from other ultrasound-guided proximal level approaches in that the interfascial plane between the pectineus and

Table 1: Technical differences in ultrasound-guided obturator nerve block techniques.

	Soong et al. [38] Fujiwara et al. [39] Sinha et al. [30]	Akkaya et al. [35]	Anagnostopoulou et al. [17] Taha [23]	Lin et al. [42]	Yoshida et al. [31]
Ultrasound probe orientation	In-plane	In-plane	Out-of-plane	In-plane	In-plane
Transducer position	Inguinal crease	Pubic region	Inguinal crease	Inguinal crease	Medial thigh
Transducer tilt	Not required	Not required	Required	Required	Not required
Needle-ultrasound beam angle	Small (posterior branch)	Small	NA	Small	Large
Nerve stimulation guidance	Recommended	Recommended	Not needed	Not needed	Not needed
Patient position	Supine	Supine	Supine	Supine	Lithotomy

NA, not applicable.

obturator externus muscles is seen from the medial side of the proximal thigh (Figure 1(b)). The transducer cannot be placed at the medial side of the proximal thigh when the patient is in the supine position with the leg straight, so patients are placed either in the lithotomy position or in the supine position with the hip fully flexed and externally rotated. A linear transducer is placed immediately lateral to the perineum on the medial aspect of the thigh along the extended line of the inguinal crease and orientated cephalad (Figure 2(d)). The superior pubic ramus should be identified first, after which the obturator externus muscle can be seen lying superficial to the superior pubic ramus (Figure 3(d)). The pectineus muscle is identified anterior (i.e., on the right hand side of an ultrasound monitor screen) to the obturator externus muscle and the superior pubic ramus (Figure 3(d)). A hyperechoic thick fascia between the pectineus and obturator externus muscles contains the obturator nerve. A needle is inserted a few centimeters (depending on the depth of the target fascia) cephalad from the anterior side of the transducer and advanced in-plane with the transducer toward this fascia. With the patient and transducer positions used in this approach, the needle can be directed almost perpendicularly to the ultrasound beam. Hence, this technique would be theoretically superior for achieving real-time needle visualization when compared with other proximal approaches. A potential disadvantage of this technique is the requirement for the lithotomy position. However, this is not a concern in TURBT because the surgery is performed in the same position.

Nerve stimulation guidance is not always used to perform proximal level ONB procedures because injection of local anesthetic into the interfascial plane between the pectineus and obturator externus muscles, which can be easily identified using ultrasound, provides successful ONB. This interfascial plane is seen as a hyperechoic thick fascia under ultrasound guidance, while the obturator nerve itself can also be seen as a hyperechoic thick structure within this fascia. Therefore, it may be difficult to distinguish the nerve from the interfascial plane under ultrasound guidance alone in some cases. Because an intraneural injection within the perineurium requires a higher injection force than one outside the perineurium, it would be helpful to monitor the injection pressure during ONB, especially in cases without peripheral nerve stimulation, to avoid intrafascicular injection of local anesthetic and the concomitant risk of neurologic complications [46–48].

Technical differences between the above-mentioned ultrasound-guided ONB approaches are summarized in Table 1. Potential advantages and disadvantages of these techniques should be validated in comparative studies in the future.

6. Issues to Be Addressed

The superiority of ultrasound-guided ONB techniques over landmark-based ONB techniques has not yet been validated by a prospective comparative trial, although theoretically ultrasound guidance would improve the success rates and safety profiles of peripheral nerve blocks. Various approaches for ultrasound-guided ONB have been reported; however, there has been no study comparing the advantages or disadvantages of these approaches in any respect (e.g., block performance time, success rates, needle visibility under ultrasound, and incidence of complications). The proximal approaches for ONB would be superior to a distal approach for reducing the minimum local anesthetic dose required to achieve blockade and for providing successful blockade of the hip articular branch of the obturator nerve. Nevertheless, this is still a hypothesis that needs to be tested. Further study in a large population would be required to assess the safety of these techniques.

Fluoroscopy guidance was used to perform percutaneous radiofrequency lesioning and pulsed radiofrequency treatment of the obturator nerve for hip joint pain in previous case series reports [8, 9]. These interventions could be performed under ultrasound guidance using a more recent high-performance ultrasound machine with a high-frequency linear transducer, thereby avoiding exposure to radiation.

7. Conclusions

Various ultrasound-guided ONB techniques have been reported and can be classified according to whether the approach is distal or proximal. The proximal approach, which comprises a single injection of local anesthetic into the interfascial plane between the pectineus and obturator externus muscles, would be superior for reducing the minimum dose of local anesthetic required and for achieving successful blockade of the obturator nerve, including the hip articular branch, when compared with the distal approach. Nevertheless, this hypothesis should be validated in future studies. The pros and cons of each proximal ONB technique also need to be evaluated in a randomized controlled trial.

Competing Interests

The authors declare that there is no conflict of interests regarding the publication of this paper.

Acknowledgments

The authors thank Editage for providing editorial assistance.

References

[1] V. Venkatramani, A. Panda, R. Manojkumar, and N. S. Kekre, "Monopolar versus bipolar transurethral resection of bladder tumors: a single center, parallel arm, randomized, controlled trial," *Journal of Urology*, vol. 191, no. 6, pp. 1703–1707, 2014.

[2] Z. T. Tekgül, R. T. Divrik, M. Turan, E. Konyalioglu, E. Simsek, and M. Gönüllü, "Impact of obturator nerve block on the short-term recurrence of superficial bladder tumors on the lateral wall," *Urology Journal*, vol. 11, no. 1, pp. 1248–1252, 2014.

[3] D. Bolat, O. Aydogdu, Z. T. Tekgul et al., "Impact of nerve stimulator-guided obturator nerve block on the short-term outcomes and complications of transurethral resection of bladder tumour: a prospective randomized controlled study," *Canadian Urological Association Journal*, vol. 9, no. 11-12, pp. E780–E784, 2015.

[4] D. A. McNamee, L. Parks, and K. R. Milligan, "Post-operative analgesia following total knee replacement: an evaluation of the addition of an obturator nerve block to combined femoral and sciatic nerve block," *Acta Anaesthesiologica Scandinavica*, vol. 46, no. 1, pp. 95–99, 2002.

[5] D. Macalou, S. Trueck, P. Meuret et al., "Postoperative analgesia after total knee replacement: the effect of an obturator nerve block added to the femoral 3-in-1 nerve block," *Anesthesia and Analgesia*, vol. 99, no. 1, pp. 251–254, 2004.

[6] S. Sakura, K. Hara, J. Ota, and S. Tadenuma, "Ultrasound-guided peripheral nerve blocks for anterior cruciate ligament reconstruction: effect of obturator nerve block during and after surgery," *Journal of Anesthesia*, vol. 24, no. 3, pp. 411–417, 2010.

[7] S. H. Heywang-Köbrunner, B. Amaya, M. Okoniewski, D. Pickuth, and R.-P. Spielmann, "CT-guided obturator nerve block for diagnosis and treatment of painful conditions of the hip," *European Radiology*, vol. 11, no. 6, pp. 1047–1053, 2001.

[8] M. Kawaguchi, K. Hashizume, T. Iwata, and H. Furuya, "Percutaneous radiofrequency lesioning of sensory branches of the obturator and femoral nerves for the treatment of hip joint pain," *Regional Anesthesia and Pain Medicine*, vol. 26, no. 6, pp. 576–581, 2001.

[9] H. Wu and J. Groner, "Pulsed radiofrequency treatment of articular branches of the obturator and femoral nerves for management of hip joint pain," *Pain Practice*, vol. 7, no. 4, pp. 341–344, 2007.

[10] J.-Y. Kwon and J.-S. Kim, "Selective blocking of the anterior branch of the obturator nerve in children with cerebral palsy," *American Journal of Physical Medicine and Rehabilitation*, vol. 88, no. 1, pp. 7–13, 2009.

[11] T. Akkaya, E. Unlu, A. Alptekin, H. I. Gumus, E. Umay, and A. Cakci, "Neurolytic phenol blockade of the obturator nerve for severe adductor spasticity," *Acta Anaesthesiologica Scandinavica*, vol. 54, no. 1, pp. 79–85, 2010.

[12] K. Lam, D. Wong, C. K. Tam et al., "Ultrasound and electrical stimulator-guided obturator nerve block with phenol in the treatment of hip adductor spasticity in long-term care patients: a randomized, triple blind, placebo controlled study," *Journal of the American Medical Directors Association*, vol. 16, no. 3, pp. 238–246, 2015.

[13] G. Labat, *Regional Anesthesia, Its Technic and Clinical Application*, WB Saunders, Philadelphia, Pa, USA, 1st edition, 1922.

[14] M. R. Wassef, "Interadductor approach to obturator nerve blockade for spastic conditions of adductor thigh muscles," *Regional Anesthesia*, vol. 18, no. 1, pp. 13–17, 1993.

[15] O. Choquet, X. Capdevila, K. Bennourine, J.-L. Feugeas, S. Bringuier-Branchereau, and J.-C. Manelli, "A new inguinal approach for the obturator nerve block: anatomical and randomized clinical studies," *Anesthesiology*, vol. 103, no. 6, pp. 1238–1245, 2005.

[16] K. Pladzyk, L. Jureczko, and T. Łazowski, "Over 500 obturator nerve blocks in the lithotomy position during transurethral resection of bladder tumor," *Central European Journal of Urology*, vol. 65, no. 2, pp. 67–70, 2012.

[17] S. Anagnostopoulou, G. Kostopanagiotou, T. Paraskeuopoulos, C. Chantzi, E. Lolis, and T. Saranteas, "Anatomic variations of the obturator nerve in the inguinal region: implications in conventional and ultrasound regional anesthesia techniques," *Regional Anesthesia and Pain Medicine*, vol. 34, no. 1, pp. 33–39, 2009.

[18] K. Birnbaum, A. Prescher, S. Heßler, and K.-D. Heller, "The sensory innervation of the hip joint—an anatomical study," *Surgical and Radiologic Anatomy*, vol. 19, no. 6, pp. 371–375, 1997.

[19] D. Burckett-St Laurant, P. Peng, L. Girón Arango et al., "The nerves of the adductor canal and the innervation of the knee: an anatomic study," *Regional Anesthesia and Pain Medicine*, vol. 41, no. 3, pp. 321–327, 2016.

[20] T. F. Bendtsen, B. Moriggl, V. Chan, and J. Børglum, "The optimal analgesic block for total knee arthroplasty," *Regional Anesthesia and Pain Medicine*, vol. 41, no. 6, pp. 711–719, 2016.

[21] H. Bouaziz, F. Vial, D. Jochum et al., "An evaluation of the cutaneous distribution after obturator nerve block," *Anesthesia and Analgesia*, vol. 94, no. 2, pp. 445–449, 2002.

[22] T. Akata, J. Murakami, and A. Yoshinaga, "Life-threatening haemorrhage following obturator artery injury during transurethral bladder surgery: a sequel of an unsuccessful obturator nerve block," *Acta Anaesthesiologica Scandinavica*, vol. 43, no. 7, pp. 784–788, 1999.

[23] A. M. Taha, "Ultrasound-guided obturator nerve block: a proximal interfascial technique," *Anesthesia and Analgesia*, vol. 114, no. 1, pp. 236–239, 2012.

[24] S. Rashiq, B. Vandermeer, A. M. Abou-Setta, L. A. Beaupre, C. A. Jones, and D. M. Dryden, "Efficacy of supplemental peripheral nerve blockade for hip fracture surgery: multiple treatment comparison," *Canadian Journal of Anesthesia*, vol. 60, no. 3, pp. 230–243, 2013.

[25] A. Ghai, S. S. Sangwan, S. Hooda, S. Kiran, and N. Garg, "Obturator neurolysis using 65% alcohol for adductor muscle spasticity," *Saudi Journal of Anaesthesia*, vol. 6, no. 3, pp. 282–284, 2012.

[26] S. A. Lang, R. W. Yip, P. C. Chang, and M. A. Gerard, "The femoral 3-in-1 block revisited," *Journal of Clinical Anesthesia*, vol. 5, no. 4, pp. 292–296, 1993.

[27] D. Jochum, G. Iohom, O. Choquet et al., "Adding a selective obturator nerve block to the parasacral sciatic nerve block: an evaluation," *Anesthesia and Analgesia*, vol. 99, no. 5, pp. 1544–1549, 2004.

[28] R. T. Woodburne, "The accessory obturator nerve and the innervation of the pectineus muscle," *The Anatomical Record*, vol. 136, no. 3, pp. 367–369, 1960.

[29] T. Akkaya, A. Comert, S. Kendir et al., "Detailed anatomy of accessory obturator nerve blockade," *Minerva Anestesiologica*, vol. 74, no. 4, pp. 119–122, 2008.

[30] S. K. Sinha, J. H. Abrams, T. T. Houle, and R. S. Weller, "Ultrasound-guided obturator nerve block an interfascial injection approach without nerve stimulation," *Regional Anesthesia and Pain Medicine*, vol. 34, no. 3, pp. 261–264, 2009.

[31] T. Yoshida, T. Onishi, K. Furutani, and H. Baba, "A new ultrasound-guided pubic approach for proximal obturator nerve block: clinical study and cadaver evaluation," *Anaesthesia*, vol. 71, no. 3, pp. 291–297, 2016.

[32] M. Kakinohana, Y. Taira, T. Saitoh, A. Hasegawa, M. Gakiya, and K. Sugahara, "Interadductor approach to obturator nerve block for transurethal resection procedure: comparison with traditional approach," *Journal of Anesthesia*, vol. 16, no. 2, pp. 123–126, 2002.

[33] Y. Y. Jo, E. Choi, and H. K. Kil, "Comparison of the success rate of inguinal approach with classical pubic approach for obturator nerve block in patients undergoing TURB," *Korean Journal of Anesthesiology*, vol. 61, no. 2, pp. 143–147, 2011.

[34] P. E. Helayel, D. B. da Conceição, P. Pavei, J. A. Knaesel, and G. R. de Oliveira Filho, "Ultrasound-guided obturator nerve block: a preliminary report of a case series," *Regional Anesthesia and Pain Medicine*, vol. 32, no. 3, pp. 221–226, 2007.

[35] T. Akkaya, E. Ozturk, A. Comert et al., "Ultrasound-guided obturator nerve block: a sonoanatomic study of a new methodologic approach," *Anesthesia and Analgesia*, vol. 108, no. 3, pp. 1037–1041, 2009.

[36] S. H. Lee, C. W. Jeong, H. J. Lee, M. H. Yoon, and W. M. Kim, "Ultrasound guided obturator nerve block: a single interfascial injection technique," *Journal of Anesthesia*, vol. 25, no. 6, pp. 923–926, 2011.

[37] A. Thallaj and D. Rabah, "Efficacy of ultrasound-guided obturator nerve block in transurethral surgery," *Saudi Journal of Anaesthesia*, vol. 5, no. 1, pp. 42–44, 2011.

[38] J. Soong, I. Schafhalter-Zoppoth, and A. T. Gray, "Sonographic imaging of the obturator nerve for regional block," *Regional Anesthesia and Pain Medicine*, vol. 32, no. 2, pp. 146–151, 2007.

[39] Y. Fujiwara, Y. Sato, M. Kitayama, Y. Shibata, T. Komatsu, and K. Hirota, "Obturator nerve block using ultrasound guidance," *Anesthesia and Analgesia*, vol. 105, no. 3, pp. 888–889, 2007.

[40] A. T. Gray, "Ultrasound-guided regional anesthesia: current state of the art," *Anesthesiology*, vol. 104, no. 2, pp. 368–373, 2006.

[41] K. J. Chin, A. Perlas, V. W. S. Chan, and R. Brull, "Needle visualization in ultrasound-guided regional anesthesia: challenges and solutions," *Regional Anesthesia and Pain Medicine*, vol. 33, no. 6, pp. 532–544, 2008.

[42] J.-A. Lin, T. Nakamoto, and S.-D. Yeh, "Ultrasound standard for obturator nerve block: the modified Taha's approach," *British Journal of Anaesthesia*, vol. 114, no. 2, pp. 337–339, 2015.

[43] A. Ruiz, X. Sala-Blanch, J. Martinez-Ocón, M. J. Carretero, G. Sánchez-Etayo, and A. Hadzic, "Incidence of intraneural needle insertion in ultrasound-guided femoral nerve block: a comparison between the out-of-plane versus the in-plane approaches," *Revista Española de Anestesiología y Reanimación*, vol. 61, no. 2, pp. 73–77, 2014.

[44] S. Kendir, T. Akkaya, A. Comert et al., "The location of the obturator nerve: a three-dimensional description of the obturator canal," *Surgical and Radiologic Anatomy*, vol. 30, no. 6, pp. 495–501, 2008.

[45] H.-S. Won, J.-H. Kim, U.-Y. Lee, K. H. Rha, and D. K. Kim, "Topographical relationships between the obturator nerve, artery, and vein in the lateral pelvic wall," *International Urogynecology Journal and Pelvic Floor Dysfunction*, vol. 27, no. 2, pp. 213–218, 2016.

[46] B. C. H. Tsui, L. X. Y. Li, and J. J. Pillay, "Compressed air injection technique to standardize block injection pressures," *Canadian Journal of Anesthesia*, vol. 53, no. 11, pp. 1098–1102, 2006.

[47] J. Gadsden, C. McCally, and A. Hadzic, "Monitoring during peripheral nerve blockade," *Current Opinion in Anaesthesiology*, vol. 23, no. 5, pp. 656–661, 2010.

[48] J.-A. Lin and H.-T. Lu, "A convenient alternative for monitoring opening pressure during multiple needle redirection," *British Journal of Anaesthesia*, vol. 112, no. 4, pp. 771–772, 2014.

Hindawi
BioMed Research International
Volume 2017, Article ID 2752876, 7 pages
https://doi.org/10.1155/2017/2752876

Review Article

Ultrasound-Guided Quadratus Lumborum Block: An Updated Review of Anatomy and Techniques

Hironobu Ueshima,[1] Hiroshi Otake,[1] and Jui-An Lin[2]

[1] *Department of Anesthesiology, Showa University Hospital, Tokyo, Japan*
[2] *Department of Anesthesiology, Wan Fang Hospital, Taipei Medical University and Department of Anesthesiology, School of Medicine, College of Medicine, Taipei Medical University, Taipei, Taiwan*

Correspondence should be addressed to Hironobu Ueshima; ueshimhi@yahoo.co.jp

Received 31 October 2016; Accepted 24 November 2016; Published 3 January 2017

Academic Editor: Eberval G. Figueiredo

Purpose of Review. Since the original publication on the quadratus lumborum (QL) block, the technique has evolved significantly during the last decade. This review highlights recent advances in various approaches for administering the QL block and proposes directions for future research. *Recent Findings*. The QL block findings continue to become clearer. We now understand that the QL block has several approach methods (anterior, lateral, posterior, and intramuscular) and the spread of local anesthetic varies with each approach. In particular, dye injected using the anterior QL block approach spread to the L1, L2, and L3 nerve roots and within psoas major and QL muscles. *Summary*. The QL block is an effective analgesic tool for abdominal surgery. However, the best approach is yet to be determined. Therefore, the anesthetic spread of the several QL blocks must be made clear.

1. Introduction

The quadratus lumborum (QL) block was first described by Blanco [1]. Currently, the QL block is performed as one of the perioperative pain management procedures for all generations (pediatrics, pregnant, and adult) undergoing abdominal surgery [2–4]. However, disagreement regarding the best approach for administering the block prevails because of unclear mechanisms responsible for the effects and complicated nomenclature system.

2. Ultrasound Identification of QL

After recognizing three layers of abdominal wall muscles, transversus abdominis is traced more posteriorly until the transversus aponeurosis appears. At this region, usually we can find the peritoneum curves away from the muscles from anterior to posterior and the retroperitoneal fat lies behind the peritoneum and deep to the transversalis fascia. The retroperitoneal fat is generally scanty above the iliac crest and more prominent closer to the iliac crest. Tilting the probe slightly caudal into the pelvis thus improves the view of the retroperitoneal fat and the tapered end of transversus aponeurosis. QL is usually identified medial to the aponeurosis of transversus abdominis muscle [5].

3. Nomenclature (Figure 1)

Current literature on the QL block reports 4 different approaches, with authors using varying nomenclature for describing each block. The QL block was first described as an ultrasound-guide "posterior" transversus abdominis plane (TAP) block by Blanco in 2007, approximating the double-pop TAP technique at the lumbar triangle of Petit [1, 6]. However, QL and TAP blocks are essentially different because a posterior TAP block is, by definition, superficial to the TAP and its aponeurosis. In a recent open forum discussion by Blanco, the QL1 block is actually deep to the transversus abdominis aponeurosis [7]. For QL2 block, the injection is posterior to the QL muscle. Furthermore, the QL block described by Børglum et al. was a transmuscular QL block [8], where the local anesthetic is injected anteriorly between the psoas major (PM) muscle and the QL muscle. Finally, for

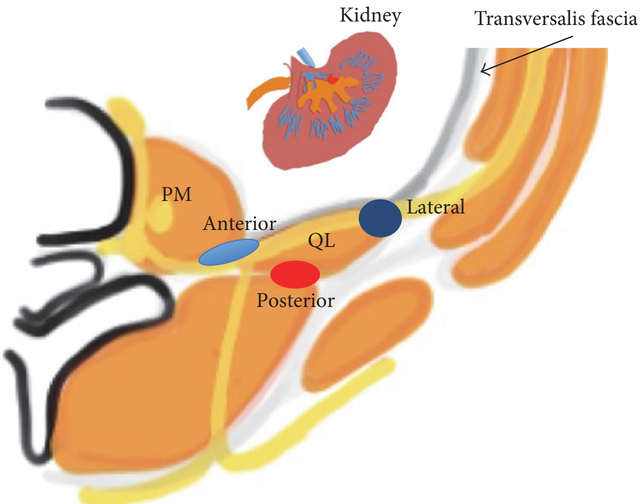

Figure 1: Anatomic view of quadratus lumborum (QL) block (anterior, lateral, and posterior). The lateral QL block injects the local anesthetic at the lateral to the QL muscle. The posterior QL block injects the local anesthetic at the posterior to the QL muscle. The anterior QL block injected the local anesthetic between the PM muscle and the QL muscle. QL: quadratus lumborum muscle, PM: psoas major muscle, and gray line: transversalis fascia.

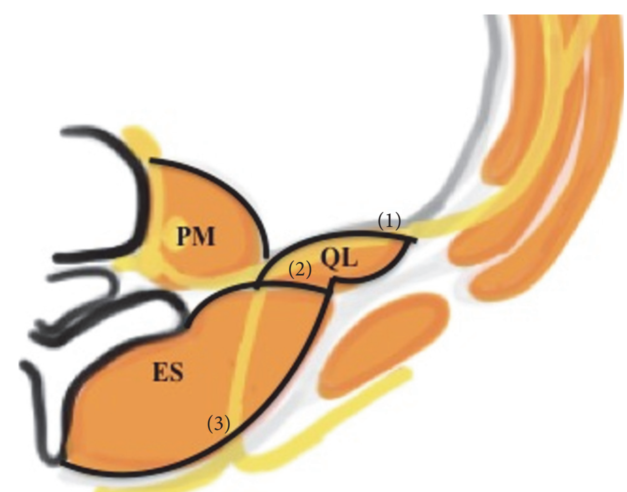

Figure 2: Anatomic view of the thoracolumbar fascia (TLF). The TLF is divided into 3 layers (anterior (1), middle (2), and posterior (3)). QL: quadratus lumborum, ES: erector spinae, LD: latissimus dorsi, and PM: psoas major.

the intramuscular QL block, the local anesthetic is injected directly into the QL muscle [9, 10].

We need to know the anatomy of the tissue layers surrounding the QL muscle, particularly the thoracolumbar fascia (TLF, Figure 2), to understand these QL blocks [11]. The TLF is a sheet of fused aponeuroses and fascial layers that encases the muscles of the back extending from the thoracic to the lumbar spine and affects the spread of local anesthetic [12]. The TLF is divided into 3 layers (anterior, middle, and posterior) around the muscles of the back. The anterior layer is anterior to the QL muscle. The middle layer

Figure 3: Probe position for anterior QLB. The convex probe was vertically attached above the iliac crest.

is located between the erector spinae and the QL muscle. The posterior layer of thoracolumbar fascia encloses the erector spinae instead of the QL muscle. The anterior layer also blends medially with the fascia of the PM and blends laterally with the transversalis fascia. Injection between the anterior layer and QL can spread cranially under the lateral arcuate ligament to the endothoracic fascia and reach the lower thoracic paravertebral space posterior to the endothoracic fascia [13]. As for QL2 block, recently it was disclosed that in the area where the middle lumbar fascia joins the deep lamina of the posterior layer (paraspinal retinacular sheath) on the lateral border of the erector spinae, a triangular structure named the lumbar interfascial triangle (LIFT) was targeted as the optimal point of injection for QL2 block [14]. Not only serving as the conduit for local anesthetic spread into the thoracic paravertebral space, TLF per se with a high-density network of sympathetic fibers as well as mechanoreceptors was also believed to be another main component responsible for the effects of QL block.

It is logically and communicationally easier to name QL blocks based on the needle tip position in relation to QL than the publication sequence or needle trajectory [12]. Accordingly, the QL 1 block is referred to as the lateral QL block because it involves injecting local anesthetic lateral to the QL muscle with the spread at the junction of QL with transversalis fascia, similar to the pattern of transversalis fascia plane block [5]. By the same rule, the QL 2 block is considered a posterior QL block. The transmuscular QL block is named the anterior QL block because it involves injecting the local anesthetic at the anterior aspect of the QL muscle. Finally, the intramuscular QL block is referred to as the intramuscular QL block.

4. Techniques of QL Block

4.1. Anterior QL Block. The patient was in the lateral position. A low-frequency convex probe was vertically attached above the iliac crest (Figure 3), and a needle was inserted in the

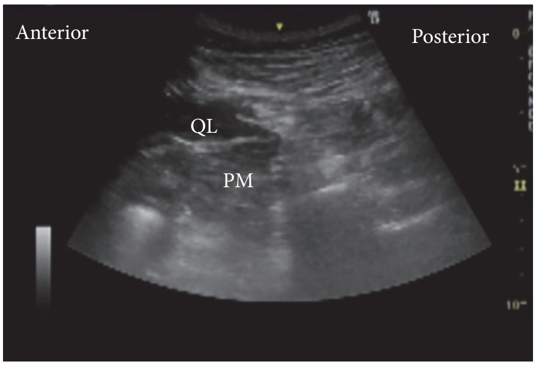

(a)

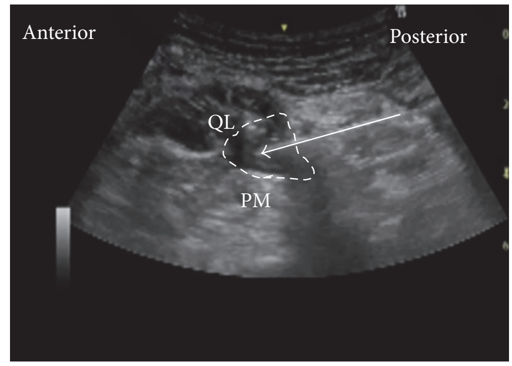

(b)

Figure 4: Ultrasound images of anterior QLB. (a) Preinjection and (b) postinjection. QL: quadratus lumborum, PM: psoas muscle, white arrow: needle trajectory, and white dotted line: spread of local anesthetic.

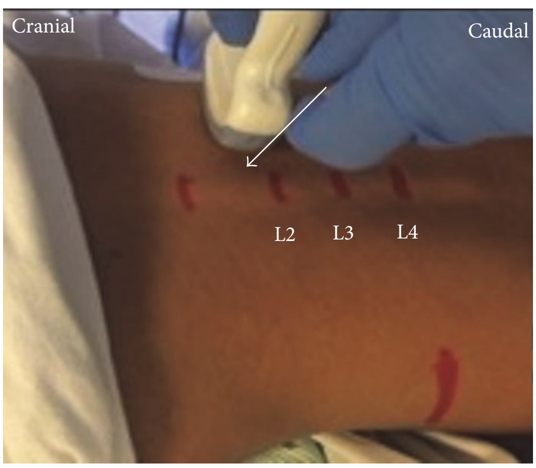

Figure 5: Probe position for subcostal QL block. A low-frequency convex probe is placed with a transverse, oblique, and paramedian orientation approximately 3 cm lateral to the L2 spinous process.

plane from the posterior edge of the convex probe through the QL in an anteromedial direction (Figure 4(a)). The needle tip was placed between the PM muscle and the QL muscle and the local anesthetic was injected into the fascial plane. We confirmed that the local anesthetic appeared to press down the PM in the ultrasound image (Figure 4(b)).

Also, there is an another anterior QL block with paramedian sagittal oblique (subcostal) approach (subcostal QL block) [13]. The patient was in the lateral position. A low-frequency convex probe is placed with a transverse, oblique, and paramedian orientation approximately 3 cm lateral to the L2 spinous process (Figure 5). The needle is then inserted in-plane from the medial side of the transducer and advanced laterally to enter the interfascial plane between the quadratus lumborum and psoas major muscles (Figure 6). With this approach, we think that the psoas major muscle provides a better protective barrier against accidental needle entry into the peritoneal cavity than the thin transversalis fascial layer.

4.2. Lateral QL Block. The patient was in the supine position. A high-frequency linear probe was attached in the area of the triangle of Petit (Figure 7) until the QL was confirmed (Figure 8(a)). The needle tip was placed at the anterolateral border of the QL at its junction of QL with transversalis fascia, and the local anesthetic was injected. We confirmed via ultrasound that the local anesthetic is deep to the transversus abdominis aponeurosis (Figure 8(b)).

4.3. Posterior QL Block. The patient was in the same supine position as the lateral QL block (Figure 7). The patient was occasionally supported on a pillow to create space under the patient's back to be able to move a low-frequency convex probe freely. The posterior aspect of the QL muscle was confirmed, and the needle tip was inserted into this aspect of the QL muscle (Figure 9(a)). The local anesthetic was then injected into the LIFT behind the QL muscle (Figure 9(b)).

4.4. Intramuscular QL Block. The patient was also in the same supine position as the lateral QL block (Figure 7), and a high-frequency linear probe was placed slightly cephalad to the iliac crest. The needle tip was advanced until it penetrated the fascia and was inserted into the QL muscle (Figure 10(a)). Test injection was initially administered to verify that the local anesthetic spreads within the QL muscle (Figure 10(b)). Finally, the local anesthetic spread reaching any area between the fascia and the muscle will predict a successful block [10] (Figure 10(c)).

We also recommend adding pressure monitors to avoid possible intrafascicular spread during administration of these blocks [15]. This is especially important for anterior and lateral QL blocks, because nerves are located anterior to the QL where the needle tip will be placed (Figure 1). Another reason for adding the half-the-air pressure monitor is to reduce the risk of local anesthetic systemic toxicity (LAST) and at the same time save the local anesthetic when the block site is deep with rich vascularity [16] and needs test injection to confirm the correct spread in the interfascial plane [17], such as the deep anterior QL block involving the thoracolumbar fascia through which vessels exit from the paravertebral space [14].

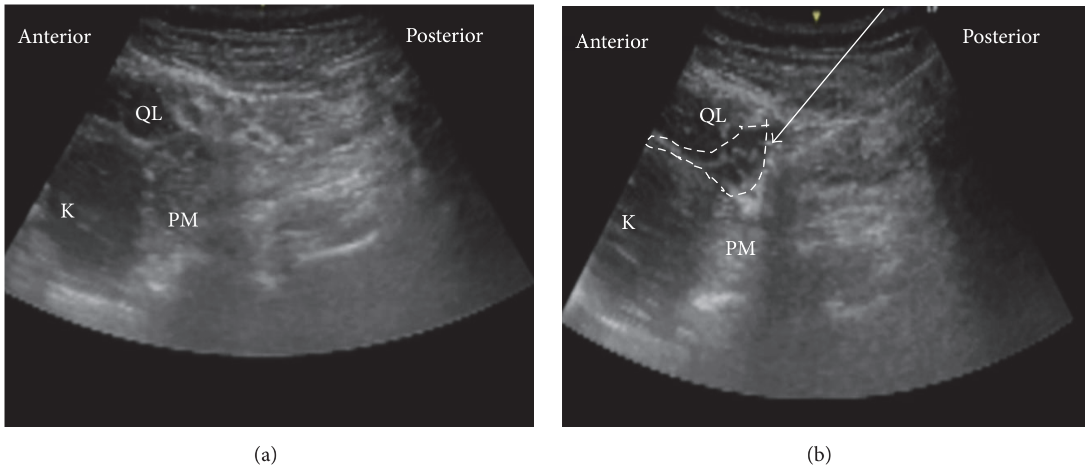

Figure 6: Ultrasound images of subcostal QL block. (a) Preinjection and (b) postinjection. QL: quadratus lumborum, PM: psoas muscle, white arrow: needle trajectory, and white dotted line: spread of local anesthetic.

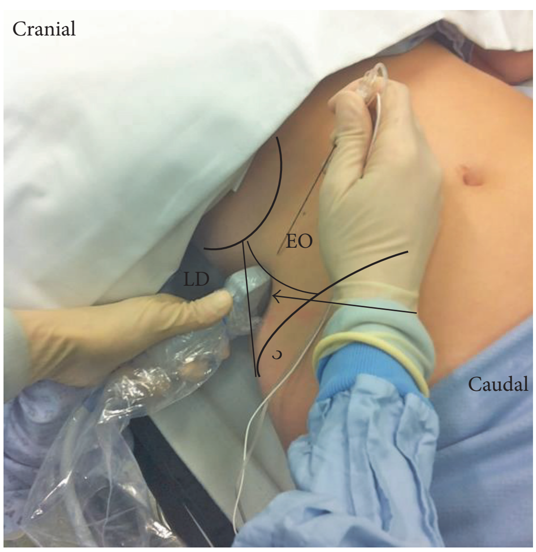

Figure 7: Lateral QL block. A high-frequency linear probe was attached in the area of the triangle of Petit. EO: external abdominal oblique; LD: latissimus dorsi; black arrow: the triangle of Petit.

5. Spread of QL Block

A MRI investigation comparing the posterior QL block and the lateral QL block showed that the posterior QL block had spread more than the lateral QL block. Further, the posterior QL block provided a more predictable spread of the local anesthetic into the paravertebral space [3]. However, the calculated volume reaching the paravertebral space was still too small for QL2 block; thus the role of spread into the thoracolumbar plane was considered another synergistic pathway to achieve the effect [14].

Carline et al. investigated the spread of the dye and nerve involvement after 4 anterior, 3 lateral, and 3 posterior QL blocks using an ultrasound-guided technique in soft embalmed cadavers [18]. They injected 20 ml of dye solution for each QL block. The anterior QL block consistently dyed lumbar nerve roots and sometimes nerves within the TAP. The posterior and lateral QL blocks nearly dyed within the TAP, the subcutaneous tissue surrounding the abdominal flank, and into the deep muscles of the back. However the results (especially from the posterior and lateral QL blocks) lack credibility because they were only performed on a few soft embalmed cadavers.

There is no study reporting the dye spread in the intramuscular QL block. Because the injection is intramuscular, the local anesthetic may stay within the QL muscle. Watanabe et al. reported a case undergoing the intramuscular QL block where the spread of the local anesthetic was confirmed by using a fluoroscopy. According to this case, 15 mL of the total radiocontrast injected into the QL muscle remained within the QL muscle [19].

To better assess the mechanism of the several QL blocks, we must simultaneously perform the dye spread study of the 4 different approaches in many soft embalmed cadavers.

6. Analgesia (Table 1)

Both the needle trajectory and needle tip position are deemed relevant regarding the spread of local anesthetic after different approaches of QL blocks [12]; thus it is of paramount importance to compare and analyze their analgesic levels, respectively.

The lateral and posterior QL blocks may play a role in conventional perioperative pain management for abdominal surgery [3, 18]. Because the local anesthetic injected via the approach of the posterior QL block can more easily extend beyond the TAP to the thoracic paravertebral space or the thoracolumbar plane [3, 14], the posterior QL block entails a broader sensory-level analgesic than the lateral QL block. Some clinical case studies of patients with caesarean section, gastrostomy, laparoscopy, colostomy, pyeloplasty, and myocutaneous flap surgery showed that the lateral and posterior QL blocks may generate analgesia from T7 to L1 [2–4, 9, 10, 19–22].

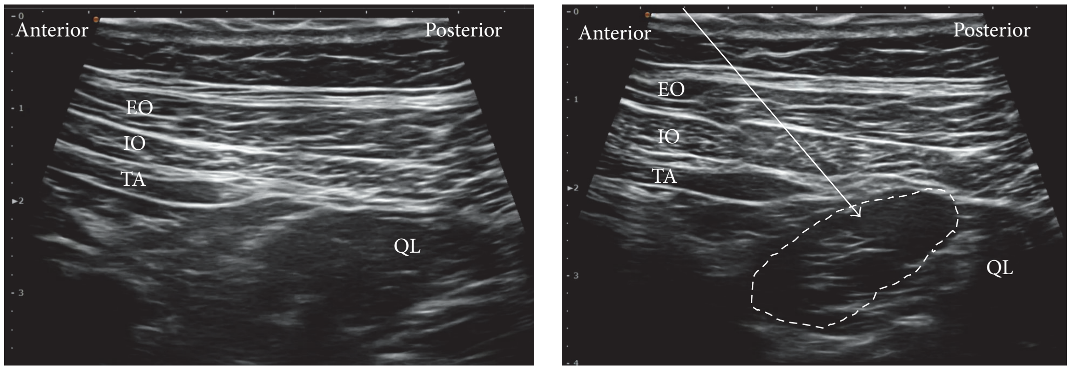

(a) (b)

Figure 8: Ultrasound images of lateral QLB. (a) Preinjection and (b) postinjection. EO: external oblique muscle, IO: internal oblique muscle, TA: transversus abdominis, QL: quadratus lumborum, white arrow: needle trajectory, and white dotted line: spread of local anesthetic.

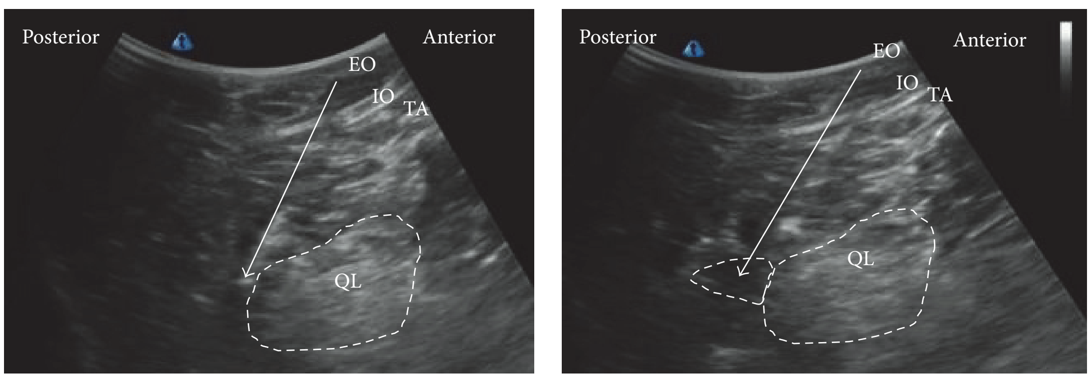

(a) (b)

Figure 9: Ultrasound images of posterior QLB. (a) Preinjection and (b) postinjection. EO: external oblique muscle, IO: internal oblique muscle, TA: transversus abdominis, QL: quadratus lumborum, white arrow: needle trajectory, and white dotted line: spread of local anesthetic.

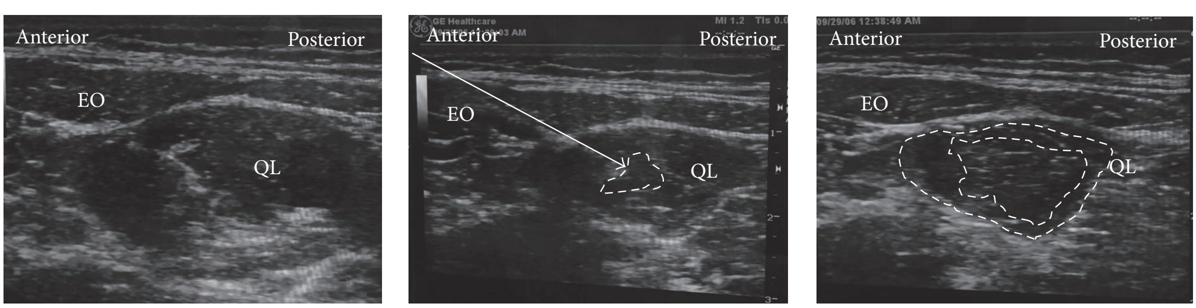

(a) (b) (c)

Figure 10: Ultrasound images of intramuscular QLB. (a) Preinjection, (b) test injection, and (c) postinjection. EO: external oblique muscle, QL: quadratus lumborum, white arrow: needle trajectory, and white dotted line: spread of local anesthetic within (b) or in between (c).

Table 1: Multidimensional comparison regarding different approaches.

Approach	Analgesia	Technique	Safety	Reference
Anterior (subcostal)	T10 to L4 (T6-7 to L1-2)	Difficult	Not dangerous	Børglum et al. [8] (Elsharkawy [13])
Posterior	T7 to L1	Not easy	Safe	Blanco et al. [3]
Lateral	T7 to L1	Not easy	Not dangerous	Blanco et al. [3]
Intramuscular	T7 to T12	Easy	Safe	Murouchi et al. [8, 9]

For the anterior QL block, the local anesthetic is injected between the PM muscle and the QL muscle. Considering the branches of lumbar plexus nerves run between the PM and the QL, the anterior QLB may play a role in analgesia not only for the trunk but for the lower extremities as well [23]. A dye injection study showed that the anterior QL block consistently dyed lumbar nerve roots and sometimes nerves within the TAP. Therefore, the anterior QL block may generate analgesia from T10 to L4 [18]. For the subcostal QL block (subtype of anterior QL block), the local anesthetic injected anterior to the QL between the QL muscle and the anterior layer of the thoracolumbar fascia observed the spread in cephalad direction close to the T12 rib with anterior displacement of the anterior layer of thoracolumbar fascia. This produces reliable dermatomal coverage from T6-T7 to L1-2 [13].

The intramuscular QL block [9, 10], which involves injection of the local anesthetic directly into the QL muscle, has recently been disclosed. Murouchi et al. reported that, after the lateral QL block, the sensory effects evaluated using a cold test may demonstrate analgesia from T7 to T12 [9]. We consider that the intramuscular QL block is an effective block for lower abdominal surgery such as laparoscopy and femoral-femoral bypass [19].

7. Discussion

Since the first description of the QL block about 10 years ago [1], several QL blocks have been reported [1, 7–10, 13, 14]. The QL block cannot generate anesthesia without additional procedures. We do not know whether each QL block relieves complete somatic and visceral pain; hence we recommended QL block as an add-on block to reduce the requirement of general anesthetic intraoperatively or it could be used as the main component of multimodal analgesia postoperatively. Though the anterior and posterior QL blocks may spread the local anesthetic into the paravertebral space, the full scope of spread from each of the four blocks is not clear [3, 18]. To further understand the mechanisms of the several QL blocks, we must perform dye injection study simultaneously using each approach in many soft embalmed cadavers and assess the spread using multiple modalities.

Variable volumes of local anesthetic in regard to each QL block were reported. We are unsure regarding the adequate volume needed to accomplish the block. However, considering previous reports [9, 18], at least 20 mL of the local anesthetic at one site may be required. Because of the large volume, it is important to confirm the safety of the block to avoid LAST. Murouchi et al. measured the local anesthetic concentration after the intramuscular QL block [9]. A total of 150 mg of ropivacaine (0.375%, 20 mL per side) was administered bilaterally. After administration, arterial ropivacaine levels were measured using high-performance liquid chromatography with carbamazepine [9]. The ropivacaine concentration was less than 2.2 μg/mL, which represented the arterial and venous threshold values of systemic toxicity [24]. Therefore, the injection of the QL block with 150 mg of ropivacaine may be safe. However, immediate transfer to the ward after QL block should be avoided, because the ropivacaine peak was observed around 30 to 60 minutes after the QL block [9].

There were a few randomized trials for the QL block. Murouchi et al. compared the intramuscular QL block with the lateral TAP block for laparoscopic surgery. Compared with the TAP block, QL block resulted in a widespread and long-lasting analgesic effect after laparoscopic ovarian surgery [9]. Blanco et al. compared the spinal anesthesia in addition to either the anterior or posterior QL block versus using only spinal anesthesia for caesarean sections [3]. The QL block after caesarean section was effective and provided satisfactory analgesia in combination with a typical postoperative analgesic regimen. In addition, Blanco et al. also compared the posterior QL block with the TAP block, where the posterior QL block was found more effective in reducing morphine consumption and demands than TAP block up to 48 hours postoperatively [14]. The QL block needs to be compared with other modalities to further prove its superiority and safety against others, such as epidural analgesia or the rectus sheath block.

In the present circumstances, the posterior, lateral, and intramuscular QL blocks are an effective analgesic method for abdominal surgery, particularly effective for lower abdominal surgery [3, 18]. From the viewpoint of safety and technique (Table 1), the intramuscular QL block may be an easier QL block for novice. Compared with these QL blocks, the anterior QL block may be an effective analgesia for the lower extremity surgery as well as the abdominal surgery.

There were no studies reporting complications after the QL block. Compared with the TAP block, some QL blocks are deep nerve blocks. Therefore, we must watch sites for infection, blood hematoma, and organ injuries [25, 26]. In particular, the anterior QL block is a deeper nerve block compared with the lateral and posterior QL block. From described above, consensus for the indications regarding each QL block should be achieved as soon as possible and our review could provide a comprehensive suggestion ready on the way.

8. Conclusion

The QL block is an effective analgesic tool for abdominal surgery and perhaps lower extremity. However, the best approach needs further validation and should be tailored to fit specific surgery whenever possible. Therefore, this review aims to make clear criteria to assess the performance of each QL block in comprehensive aspects, which facilitates future study design, provides the most updated knowledge, and contributes to the advances of techniques in deep regional blocks.

Competing Interests

The authors declare that there is no conflict of interests.

Acknowledgments

The authors would like to thank the assistance of Dr. Blanco from the Anaesthetic Department, Corniche Hospital, who provided the images with Figure 8 and Dr. Murouchi from the Department of Anesthesia, Kitami Red Cross Hospital, who provided the images with Figure 10.

References

[1] R. Blanco, "TAP block under ultrasound guidance: the description of a 'non pops technique'," *Regional Anesthesia and Pain Medicine*, vol. 32, supplement 1, p. 130, 2007.

[2] V. R. Kadam, "Ultrasound-guided quadratus lumborum block as a postoperative analgesic technique for laparotomy," *Journal of Anaesthesiology Clinical Pharmacology*, vol. 29, no. 4, pp. 550–552, 2013.

[3] R. Blanco, T. Ansari, and E. Girgis, "Quadratus lumborum block for postoperative pain after caesarean section: a randomised controlled trial," *European Journal of Anaesthesiology*, vol. 32, no. 11, pp. 812–818, 2015.

[4] A. Chakraborty, J. Goswami, and V. Patro, "Ultrasound-guided continuous quadratus lumborum block for postoperative analgesia in a pediatric patient," *A & A Case Reports*, vol. 4, no. 3, pp. 34–36, 2015.

[5] P. D. Hebbard, "Transversalis fascia plane block, a novel ultrasound-guided abdominal wall nerve block," *Canadian Journal of Anesthesia*, vol. 56, no. 8, pp. 618–620, 2009.

[6] M. Abrahams, R. Derby, and J.-L. Horn, "Update on ultrasound for truncal blocks: a review of the evidence," *Regional Anesthesia and Pain Medicine*, vol. 41, no. 2, pp. 275–288, 2016.

[7] R. Blanco and J. G. McDonnell, Optimal point of injection: the quadratus lumborum type I and II blocks. 2013, http://www.respond2articles.com/ANA/forums/post/1550.aspx.

[8] J. Børglum, K. Jensen, B. Moriggl et al., "Ultrasound-guided transmuscular quadratus lumborum blockade," *BJA—Out of the blue E-letters*, 2013.

[9] T. Murouchi, S. Iwasaki, and M. Yamakage, "Quadratus lumborum block: analgesic effects and chronological ropivacaine concentrations after laparoscopic surgery," *Regional Anesthesia and Pain Medicine*, vol. 41, no. 2, pp. 146–150, 2016.

[10] T. Murouchi, "Quadratus lumborum block intramuscular approach for pediatric surgery," *Acta Anaesthesiologica Taiwanica*, 2016.

[11] F. H. Willard, A. Vleeming, M. D. Schuenke, L. Danneels, and R. Schleip, "The thoracolumbar fascia: anatomy, function and clinical considerations," *Journal of Anatomy*, vol. 221, no. 6, pp. 507–536, 2012.

[12] K. El-Boghdadly, H. Elsharkawy, A. Short, and K. J. Chin, "Quadratus lumborum block nomenclature and anatomical considerations," *Regional Anesthesia and Pain Medicine*, vol. 41, no. 4, pp. 548–549, 2016.

[13] H. Elsharkawy, "Quadratus lumborum block with paramedian sagittal oblique (subcostal) approach," *Anaesthesia*, vol. 71, no. 2, pp. 241–242, 2016.

[14] R. Blanco, T. Ansari, W. Riad, and N. Shetty, "Quadratus lumborum block versus transversus abdominis plane block for postoperative pain after cesarean delivery," *Regional Anesthesia and Pain Medicine*, vol. 41, no. 6, pp. 757–762, 2016.

[15] J.-A. Lin and H.-T. Lu, "A convenient alternative for monitoring opening pressure during multiple needle redirection," *British Journal of Anaesthesia*, vol. 112, no. 4, pp. 771–772, 2014.

[16] J. A. Lin, "Importance of half-the-air pressure test in Shamrock lumbar plexus block," *European Journal of Anaesthesiology*, vol. 33, no. 10, p. 784, 2016.

[17] J.-A. Lin, T.-Y. Chuang, H.-Y. Yao, S.-F. Yang, and Y.-T. Tai, "Ultrasound standard of peripheral nerve block for shoulder arthroscopy: a single-penetration double-injection approach targeting the superior trunk and supraclavicular nerve in the lateral decubitus position," *British Journal of Anaesthesia*, vol. 115, no. 6, pp. 932–934, 2015.

[18] L. Carline, G. A. McLeod, C. Lamb, and L. Colvin, "A cadaver study comparing spread of dye and nerve involvement after three different quadratus lumborum blocks," *British Journal of Anaesthesia*, vol. 117, no. 3, pp. 387–394, 2016.

[19] K. Watanabe, S. Mitsuda, J. Tokumine, A. K. Lefor, K. Moriyama, and T. Yorozu, "Quadratus lumborum block for femoral–femoral bypass graft placement," *Medicine*, vol. 95, no. 35, p. e4437, 2016.

[20] J. M. Cardoso, M. Sá, H. Reis et al., "Type II Quadratus Lumborum block for a sub-total gastrectomy in a septic patient," *Brazilian Journal of Anesthesiology*, vol. 16, pp. 30155–30156, 2016.

[21] D. K. Baidya, S. Maitra, M. K. Arora, and A. Agarwal, "Quadratus lumborum block: an effective method of perioperative analgesia in children undergoing pyeloplasty," *Journal of Clinical Anesthesia*, vol. 27, no. 8, pp. 694–696, 2015.

[22] N. Z. Spence, P. Olszynski, A. Lehan, J.-L. Horn, and C. A. J. Webb, "Quadratus lumborum catheters for breast reconstruction requiring transverse rectus abdominis myocutaneous flaps," *Journal of Anesthesia*, vol. 30, no. 3, pp. 506–509, 2016.

[23] H. Ueshima, S. Yoshiyama, and H. Otake, "The ultrasound-guided continuous transmuscular quadratus lumborum block is an effective analgesia for total hip arthroplasty," *Journal of Clinical Anesthesia*, vol. 31, p. 35, 2016.

[24] W.-W. Qin, Z. Jiao, M.-K. Zhong et al., "Simultaneous determination of procaine, lidocaine, ropivacaine, tetracaine and bupivacaine in human plasma by high-performance liquid chromatography," *Journal of Chromatography B: Analytical Technologies in the Biomedical and Life Sciences*, vol. 878, no. 15-16, pp. 1185–1189, 2010.

[25] P. Lancaster and M. Chadwick, "Liver trauma secondary to ultrasound-guided transversus abdominis plane block," *British Journal of Anaesthesia*, vol. 104, no. 4, pp. 509–510, 2010.

[26] J. B. Long, P. K. Birmingham, G. S. De Oliveira Jr., K. M. Schaldenbrand, and S. Suresh, "Transversus Abdominis plane block in children: a multicenter safety analysis of 1994 cases from the PRAN (Pediatric Regional Anesthesia Network) database," *Anesthesia and Analgesia*, vol. 119, no. 2, pp. 395–399, 2014.